



SKRIFTER NR. 180

Geo-scientific investigations
in the Barents and
Greenland-Norwegian Seas



NORSK POLARINSTITUTT
OSLO 1984

DET KONGELIGE MILJØVERNDEPARTEMENT

NORSK POLARINSTITUTT

Rolfstangveien 12, Snarøya, 1330 Oslo Lufthavn, *Norway*

SALG

Bøkene selges gjennom
bokhandlere eller
bestilles direkte fra:

Universitetsforlaget
Boks 2977, Tøyen
Oslo 6
Norway

Global Book Resources Ltd.
109 Great Russell Street
London WC 1B 3NA
England

ORDERS

may be placed at your
bookstore or you may
order direct from:

Columbia University Press
136 South Broadway
Irvington-on-Hudson
NY 10533, U.S.A.



SKRIFTER NR. 180

Geo-scientific investigations in the Barents and Greenland–Norwegian Seas



NORSK POLARINSTITUTT
OSLO 1984

ISBN 82-90307-27-6
Trykt september 1984

Contents

Elverhøi, Anders & Lauritzen, Ørnulf: Bedrock geology of the northern Barents Sea (west of 35 °E) as inferred from the overlying Quaternary deposits	5
Eldholm, Olav, Sundvor, Erik & Crane, Kathleen: Sonobuoy measurements during the «Ymer» Expedition	17
Kristoffersen, Yngve, Milliman, J.D. & Ellis, J.P.: Unconsolidated sediments and shallow structure of the northern Barents Sea	25
Myhre, Annik: Compilation of seismic velocity measurements along the margins of the Norwegian-Greenland Sea	41
Faleide, Jan I., Gudlaugsson, Steinar T., Johansen, Bård, Myhre, Annik M. & Eldholm, Olav: Free-air gravity anomaly maps of the Greenland Sea and the Barents Sea	63

Bedrock geology of the northern Barents Sea (west of 35° E) as inferred from the overlying Quaternary deposits

Elverhøi, Anders & Lauritzen, Ørnulf 1984: Bedrock geology of the northern Barents Sea (west of 35°E) as inferred from the overlying Quaternary deposits. *Nor Polarinst. Skr.* 180: 5–16. ISBN 82-90307-26-6.

Assuming that Quaternary sediments reflect the lithology and age of underlying bedrock, a southeastwards stratigraphical younging is demonstrated in the northern Barents Sea (W of 35°E): 1. Precambrian and Lower Palaeozoic rocks (Hecla Hoek) are exposed east of Nordaustlandet and around Kvitøya. 2. Upper Permian rocks extend east and southeast of Nordaustlandet and also east of Edgeøya in a narrow window. 3. Triassic and Lower Jurassic rocks are present north, east and south of Kong Karls Land and also north of Hopen. 4. Jurassic – Lower Cretaceous rocks are probably exposed at Storbanken and south to Sentralbanken and have a western boundary along the 30°E longitude. The sequence in the Barents Sea seems more coarse-grained than the Mesozoic exposures of onland Svalbard. The exposure of successively older rocks to the northwest may reflect the northeastern part of the Svalbard archipelago's development as a predominantly positive area through much of the Mesozoic and Cenozoic.

Anders Elverhøi and Ørnulf Lauritzen, Norsk Polarinstitutt, P.O. Boks 158, 1330 Oslo Lufthavn, Norway. Received April 1983 (revised June 1983).

Introduction

The northern Barents Sea forms a shallow platform of 150–250 m water depth bounded to the west by the Svalbard archipelago, to the east by Frans Josef Land and to the north by the shelf edge (Fig. 1). Our knowledge of the submarine geology of the area is poor and largely based on geophysical investigations and correlation with the geology of the surrounding islands. To the northwest, a basement with metamorphic rocks of Precambrian and Lower Palaeozoic age is assumed to be present, while Triassic – Lower Jurassic rocks probably extend southwards to 74°–75°N (Dibner 1978; Rønnevik & Motland 1979; Dibner et al. 1981). North of Kong Karls Land the Mesozoic rocks are characterized by a gentle southwest dip, while the structure is more complex south of the islands (Kristoffersen et al. 1984). A general southward younging of the Mesozoic rocks has been suggested by the probable presence of Cretaceous rocks on Sentralbanken and in the northern part of Bjørnøyrenna (Hinz & Schlüter 1978; Rønnevik & Motland 1979; Bjærke 1979).

Recent years' shallow geological and geophysical investigations in the northern Barents Sea

have shown the presence of only a thin (< 5 m) veneer of Quaternary sediments above the bedrock in most of the area (Elverhøi & Solheim 1983; Kristoffersen et al. 1984). The sediments, till overlain by glaciomarine and postglacial (Holocene) deposits, are thought to be of rather local origin (Elverhøi et al. 1983; Pfirman pers. comm. 1983). The main objective of this paper is to identify lithological and stratigraphical provinces of the Quaternary sediments and relate the results to the geology of the underlying bedrock, based on studies of gravel and coarser sized clasts.

Data acquisition and analyses

The material used in this investigation is rock fragments (> 5 cm) from 93 dredge hauls in the northern Barents Sea (Fig. 1) obtained in 1980 (Kristoffersen & Elverhøi 1980). The samples were classified in eight lithological classes or types, of which all but two are of sedimentary origin. Material from 19 stations (1 to 7 samples) were selected for thin section analyses.

Additional palynological analyses were carried out on 71 rock fragments from 41 stations (Fig. 1) (Bjærke 1980). The palynological studies also

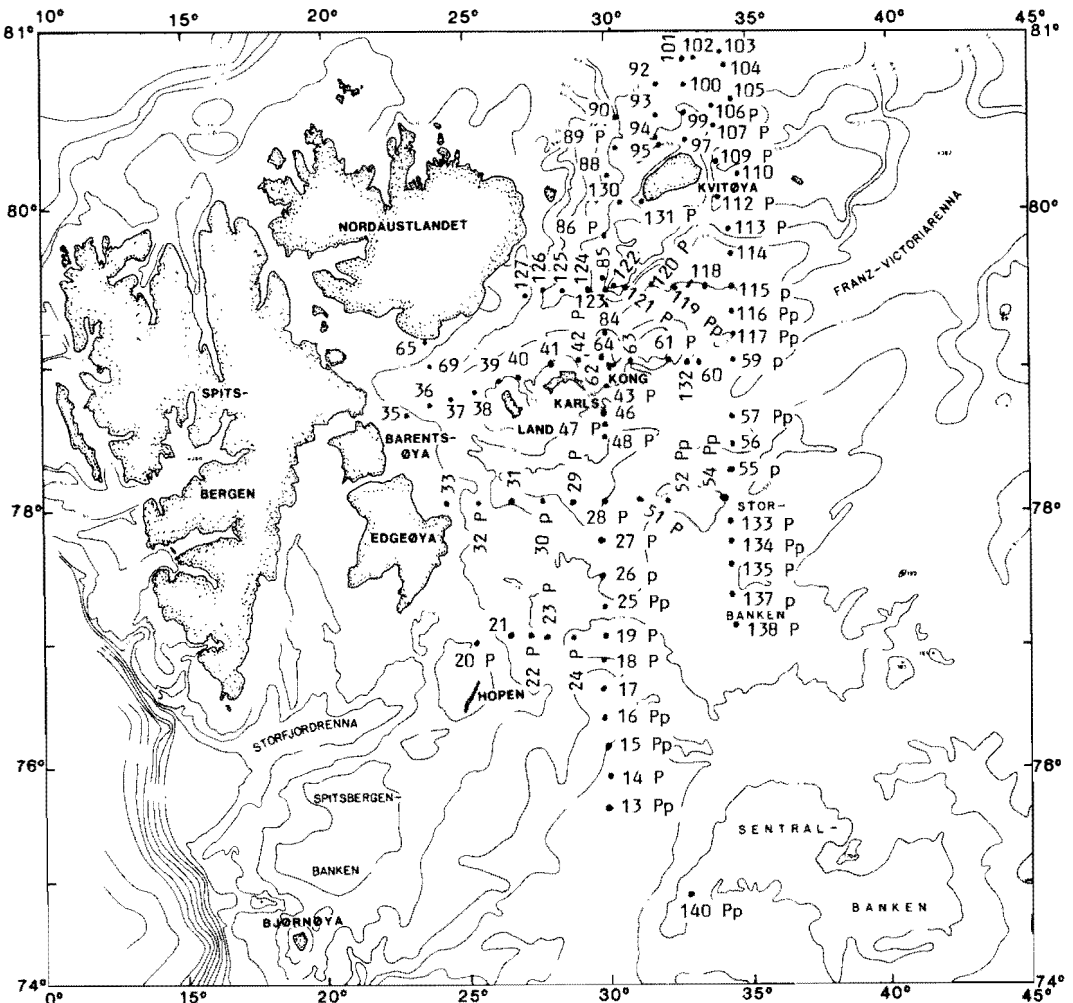


Fig. 1 Locations of dredge samples listed in Figs. 2 and 3, showing stations for palynological analyses.

P: rock fragments.

p: mud and sand sized material.

included investigations on the finer fractions and mud (< 75 μm) and sand (75 μm –1mm) (Fig. 1) (Bjærke 1982). (The results of Bjærkes' studies are incorporated in this paper.)

Lithology

General description.

The lithology of the samples and their distribution are shown in Fig. 2. In general one rock type predominates in any single station (Fig. 3), but the large differences in lithology between adjacent stations are often striking.

The eight lithological classes used as base for this study are as follows:

1. *Sandstone*: Usually fine- to medium-grained, but with some coarser grains up to pebble size. The colours vary from grey to greenish and brownish with occasional darker brown weathered rims. Clay/quartz cement dominates but calcareous cement is also common. (Quartz sand included in ironstone is here classified as sandstone).
2. *Siltstone*: Often with grains of fine sand. Varying greyish and greenish colours. Clay present as thin laminae.
3. *Mudstone*: Massive clay rich, mostly grey – often with carbonate lime.
4. *Shale*: Laminated clay rich, often dark grey to black. Contains silt/sand beds or nodules.

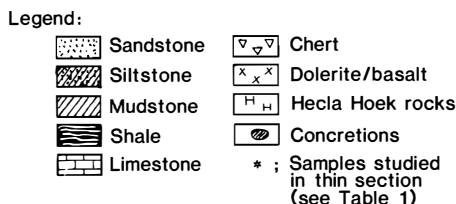
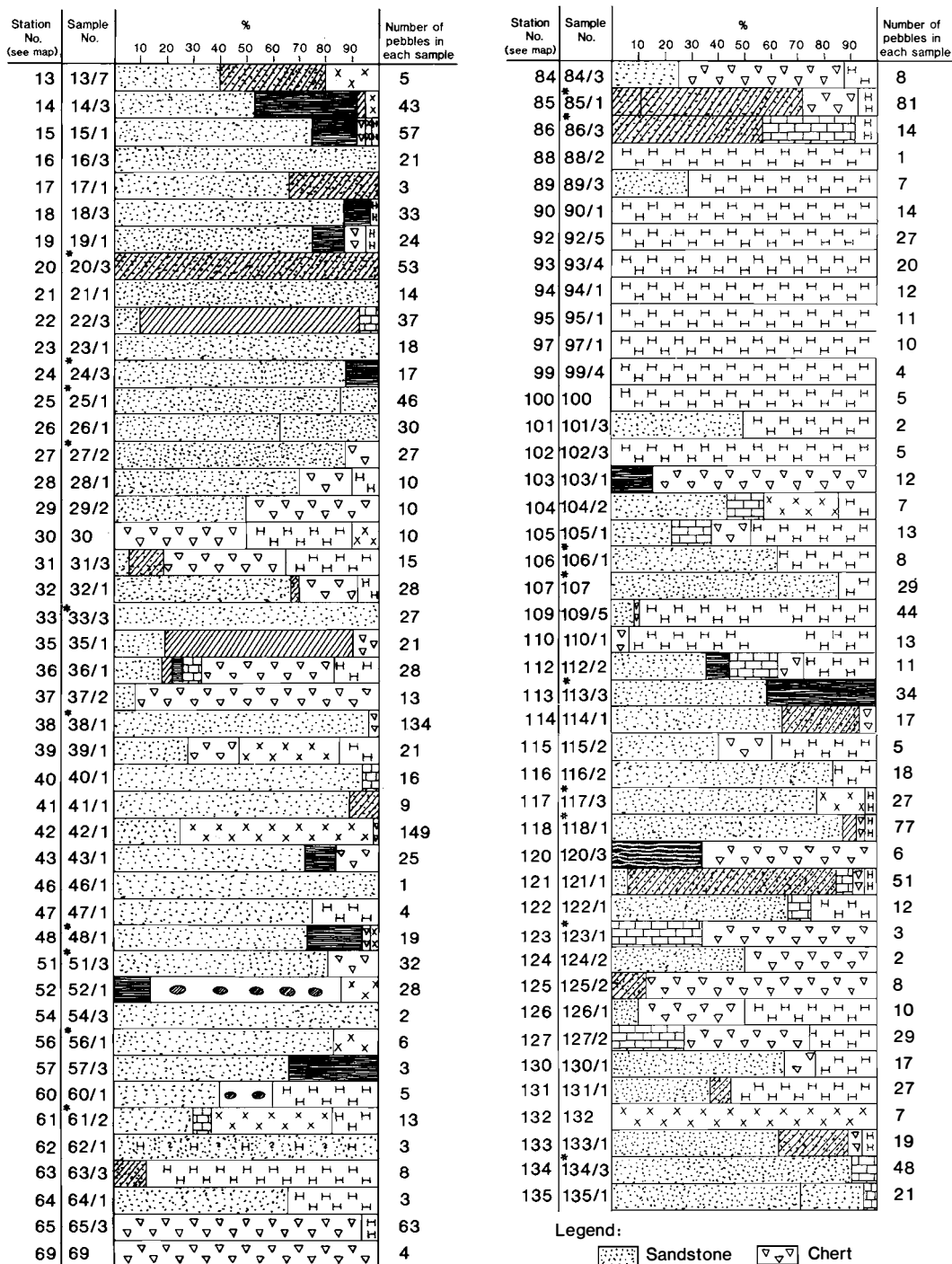


Fig. 2 Distribution of rock types.

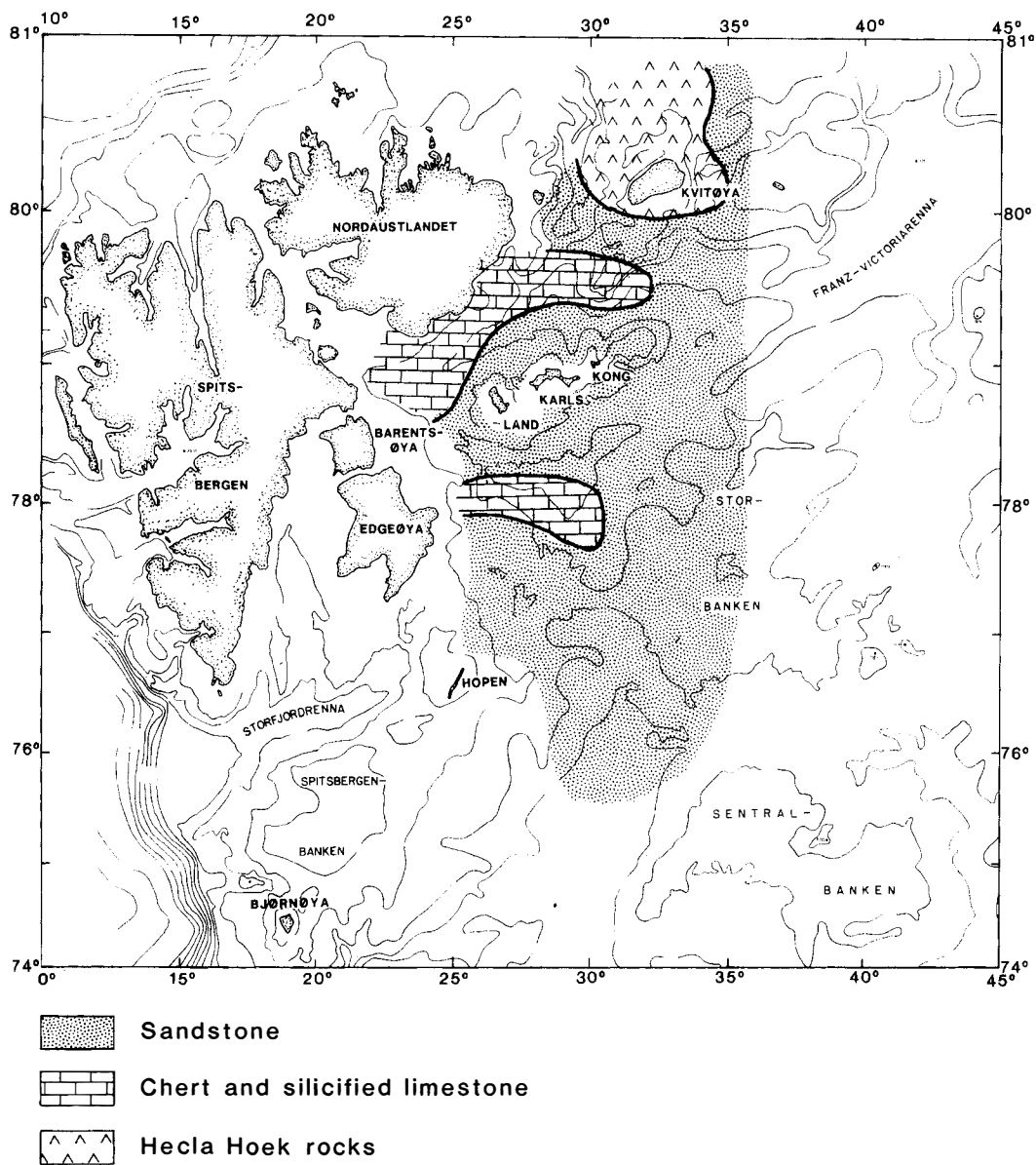


Fig. 3 Map showing distribution of predominant lithologies (> 50%) based on rock fragments in the Quaternary deposits.

5. *Limestone*: Mainly biogenic, both micritic and sparitic. Mostly light coloured and fossiliferous.
6. *Chert*: Dense fine-grained silicified limestones, shales and sandstones. Colours varying from light to dark. Often fossiliferous. (Mainly related to the Kapp Starostin Formation in Svalbard.)
7. *Basalt (dolerite)*: Crystalline, dark to greenish volcanics/intrusives. (Probably associated with sills and dykes of late Jurassic/early Cretaceous age.)
8. *Hecla Hoek*: Crystalline and metamorphic rocks. Granites, gneisses and sediments. (Belongs to the Pre-Devonian.)

Table 1. Samples from stations chosen for thin sections studies, showing dominant grain size, type of cement and texture.

Sample (station number)	Rock type	Dominating grain-size (Wentworth)	Cement			bitumen	Texture	Comments
			clay ●○○	carb. ●●○	quartz ●○○			
20 a	sandy siltstone	silt	x	x	x		faint bedding	
b	siltstone	silt	x	x	x	x	thinly laminated	bioturbation (?)
c	calcareous siltstone	silt	x	x	x	x	thinly laminated	
d	sandy siltstone	silt	x	x	x		bedded	cross-bedding
e	sandy siltstone	silt	x	x	x		bedded	clay on bedding planes
f	sandy siltstone	silt	x	x	x		bedded	chattered feldspar
g	siltstone	silt	x				bedded	clastic mica
24 a	concretion	sand						pyrite
b	silty sandstone	fine sand	x		x	x	faint bedding	partly porous
c	concretion	sand						iron oxides
d	sandstone	medium sand	x	x	x		bedded	chert common
27 a	sandstone	medium sand	x		x		homogeneous	iron oxides
33 a	sandstone	medium sand	x	x	x		homogen./faint bed.	
b	sandstone	medium sand	x	x	x		homogeneous	
c	calcareous sandstone	fine sand	x	x	x		homogen./faint bed.	
d	sandstone	medium sand	x	x	x		homogen./faint bed.	chert common
e	sandstone	medium sand	x	x			homogen./faint bed.	
38 a	sandstone	fine sand	x		x	x	bedded	
b	sandstone	fine sand	x	x	x	x	bedded	cross-bedding
c	calcareous sandstone	fine sand		x			homogeneous	grains rounded
d	calcareous sandstone	fine sand		x			homogeneous	
38/1	sandstone	fine sand	x				bedded	iron oxides
45	sandstone	fine sand	x				homogen./faint bed.	
51	silty micrite	clay					homogeneous	
56 a	calcareous sandstone	fine sand		x			homogeneous	cross-bedded (?)
b	calcareous sandstone	fine sand		x			homogeneous	
61 a	silty micrite	clay					bedded	
b	calcareous sandstone	fine sand		x			homogeneous	
c	sandstone	fine sand	x		x		homogen./faint bed.	
d	calcareous siltstone	silt		x			bedded	
86/3	biosparite			x				bivalves
a	biosparite			x				bivalves
b	calcareous siltstone	silt		x			homogen./faint bed.	
106	sandstone	fine sand	x	x	x		homogen./faint bed.	
106/1c	conglomerate	gravel		x				partly dolomite
107	sandstone	fine sand	x		x		bedded	
113	sandstone	fine sand	x	x	x		bedded	
117 a	sandstone	fine sand	x				homogeneous	
b	sandstone	fine sand	x	x	x		homogeneous	
c	sandstone	medium sand	x	x		x	homogeneous	
116/1	calcareous sandstone	medium sand		x			homogeneous	
123/1	biosparite			x			thinly laminated	bivalves
134	dolomicrite	clay					bedded, lithoclasts	

● abundant ○ less abundant ○ traces

Thin section studies

Thin sections were made to describe the rock types most characteristic for the stations, mostly with regard to the clastics, but carbonate rocks were also chosen from five stations. The results from these studies are listed in Table 1, but the following additional features should be noted:

The sandstones are all fine- to medium-grained and well cemented by either quartz/clay or carbonate cement. Only sample 24b has some porosity left. Even samples with iron oxides, which normally exhibit porosity, are shown to be dense.

The quartz grains normally have a rim of clay minerals (mainly illite) which give them a «dirty» appearance. Clastic mica grains in the rocks are

common, while grains of feldspar are rare. Quartz overgrowth is seen in most samples.

Carbonate cemented sandstones are less abundant even though carbonate occurs in most samples, usually scattered throughout the rock. The size of the calcite grains is closely related to the size of the detrital grains. In samples where the cement is dominated by calcite, parts of the rocks with poikilitic cement can be recognized.

Siltstones are the second major group of clastics studied, even though they occur in minor quantities. Quartz/clay cements dominate. Grains of fine sand are found within most siltstones, and clay is also an important constituent. This content of different grain size often gives a thin laminated bedding, with detrital micas parallel to bedding.

Table 2. Palynological analyses of rock fragments and of mud and sand sized sediment fractions.

STATION NO.	ROCK TYPE	SED. TY.	GRAIN SIZE		STRATIGR. INTERVALS	PROBABLE EQUIV. STRATIGR. UNIT IN SVALBARD	COMMENTS
			S	M			
13	siltst sst	GM GM	*	*	H G,D G,D	Wilhelmøya Fm	Barren
14	shale shale sst sst				F F E g	Agardhfj. Mb Agardhfj. Mb Rurikfj. Mb DeGeerdalen Fm	
15	shale siltst sst	GM GM	*	*	g E F E,g	DeGeerdalen Fm Helvetiafj. Fm Rurikfj. Mb	Barren
16	siltst sst	GM GM	*	*	E e F E	Rurikfj. Mb	
18	shale sst sst mudst				F E	Agardhfj. Mb	NDA NDA
19	siltst sst sst				G E E	DeGeerdalen Fm Rurikfj. Mb Rurikfj. Mb	
20	shale				G	Wilhelmøya Fm	
22	sst						Barren
23	sst sst				e E	Helvetiafj. Fm	
24	sst sst shale				E	Rurikfj. Mb	Barren Barren
25	sst	GM	*	*	e e	Rurikfj. Mb Rurikfj. Mb	
26		GM	*	*	E	Helvetiafj. Fm	
27	shale sst				E E	Rurikfj. Mb Rurikfj. Mb	
28	shale						Barren
29	sst				g		
30		PG PG	*	*	G,f,e		NDA
32	sst				g	DeGeerdalen Fm	
42	sst sst				d		NDA
43	shale siltst				g g	DeGeerdalen Fm	
47	sst				g	Wilhelmøya Fm	
48	shale						Barren
	shale				f	Agardhfj. Mb	
	sst						Barren
51	sst						Barren
52	mudst shale	PG PG	*	*	E E e E	Rurikfj. Mb Rurikfj. Mb Rurikfj. Mb Rurikfj. Mb	
54	shale	GM GM	*	*	G G,F,e	Wilhelmøya Fm	Barren

→

STATION NO.	ROCK TYPE	SED. TY.	GRAIN SIZE S M	STRATIGR. INTERVALS	PROBABLE EQUIV. STRATIGR. UNIT IN SVALBARD	COMMENTS
55		GM GM	* *	D		NDA
57	siltst siltst	GM GM	* *	F G G,E	Agardhfj. Mb	
59		GM GM	* *	G, F		NDA
61	sst			G		
86	shale					Barren
89	shale					NDA
106	sst					Barren
107	sst					Barren
109	sst					Barren
112	sst					Barren
113	shale shale					Barren NDA
115		PG GM GM	* * *	g g		NDA
116	shale sst	GM GM	* *	g G	Wilhelmøya Fm	NDA NDA
117	shale mudst	PC	*			NDA Barren Barren
119	shale	GM GM	* *	G		NDA NDA
120		GM GM	* *	G		NDA
121		GM GM	* *	G		NDA
131	shale					NDA
133	sst mudst			D		Barren
134	shale	PG GM GM	* * *	G g,d	Wilhelmøya Fm	NDA NDA
135	sst sst			E E	Helvetiafj. Fm Helvetiafj. Fm	
137		GM GM	* *	E		NDA
138	sst sst			G g	DeGeerdalen Fm	
140	sst	GM GM GM GM	* * * *	G E,g G,f,E I,D I,D	Wilhelmøya Fm Agardhfj. Mb Rurikfj. Mb	

ROCK TYPE : siltst: siltstone, sst: sandstone, mudst: mudstone
 SED. TY. : Type of Quaternary sediment, GM: glaciomarine deposits, PG: postglacial deposits.
 GRAIN SIZE: S: sand 75 µm - 1 mm, M: < 75 µm
 STRATIGR. See Fig.5
 INTERVALS : Small letters indicate tentative dating
 COMMENTS : NDA: no diagnostic assemblage present

Palynological analyses

The dated samples were referred to five broadly defined stratigraphical intervals and compared with equivalent palynofloras found in lithostratigraphical units in onshore areas (Table 2, Fig. 4). Of the 71 samples of rock fragments studied, the ages of 41 were determined with different levels of confidence. Age diagnostic species were found in 21 samples. Twenty samples were only tentatively dated based on comparison with onshore sequences with respect to kerogen composition, preservation and presence of characteristic, but more long-range species. Thirty samples were barren or produced none-diagnostic assemblages.

Sand-sized sediments always produced a poorer palynological assemblage than the finest fraction. This indicates that individual palynomorphs are present in the sediment, but concentrated in the clay and silt fraction. The age range found in the sediments are in general agreement with that found in the rock fragments (Table 2).

The dated samples can be grouped into three provinces (Fig. 5):

1. A Mesozoic mixed province with predominance of palynoflora suggesting an equivalence to the Helvetiafjellet Formation and Rurikfjellet Member of the Janusfjellet Formation (Lower Cretaceous) of Svalbard. This province is confined to Storbanken and northern part of Bjørnøyrenna, including Sentralbanken.
2. A province with samples dated to the equivalent of the Wilhelmøya and DeGeerdalen Formations (Upper Triassic/Lower Jurassic) of Svalbard. This province forms a SW-NE trending belt around Kong Karls Land.
3. The northernmost area is characterized by barren samples.

The poor representation of Jurassic rocks has been explained in terms of the difficulties in recognizing this unit (Bjærke 1980). Alternatively, it may also be due to a possible thinning or erosion of this interval. On Kong Karls Land, the Middle and Upper Jurassic part of the sequence reaches a maximum of 70 m but is considerably thinner in most localities (Smith et al. 1976). Reworked Jurassic palynomorphs are present in some Lower Cretaceous assemblages, indicating erosion of Jurassic sediments during the Lower

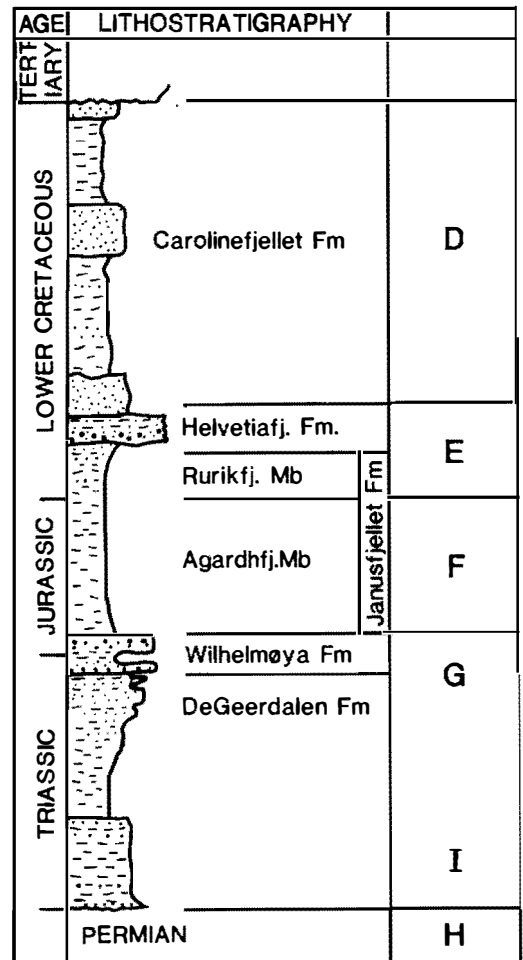


Fig. 4. Generalized lithological scheme of the Mesozoic succession in Svalbard. Stratigraphical intervals D-H shown.

Cretaceous. The distribution of Jurassic sediments in the area is therefore highly uncertain.

Discussion

Provenance of the dredged sediments

Knowledge of the origin of the recovered sediments is essential for a meaningful discussion of the underlying bedrock geology. Most of the samples are from glaciomarine sediments, likely to have been deposited during the withdrawal of the Late Weichselian ice sheet in the area (Elverhøi & Solheim 1983). Investigations of ongoing sedimentary processes outside calving glaciers on Svalbard indicate that the major part

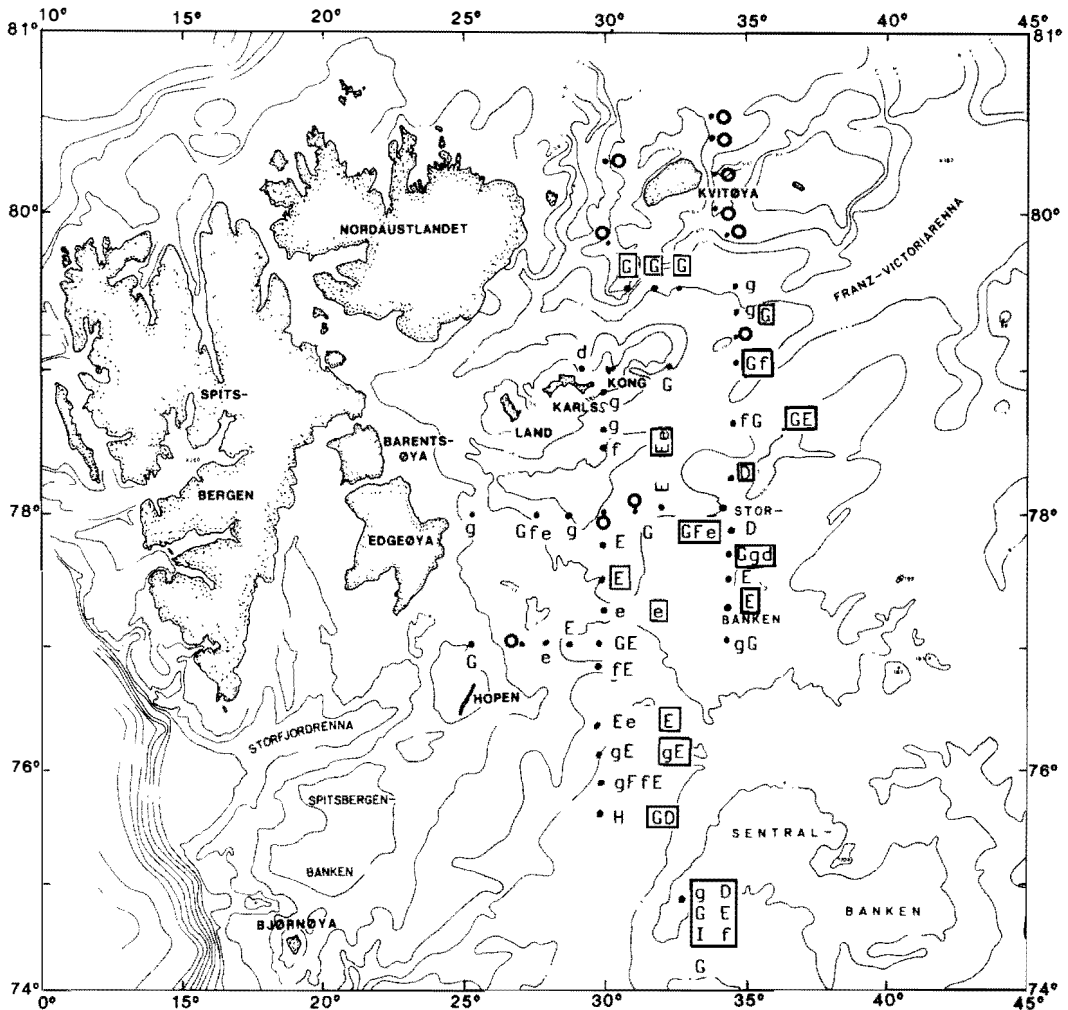


Fig. 5. Distribution of dated samples within the study area. Capital letters refer to Fig. 4. Small letters indicate tentative dated samples. □ mud and sand sized material ○ barren or no diagnostic assemblages.

of both the ice rafted material and the meltwater transported material is deposited relatively close (< 10–15 km) to the ice front (Elverhøi et al. 1980; Elverhøi et al. 1983; S. Pfirman pers. comm. 1983). The part of the ice rafted material deposited close to the ice front is in general localized at the sole of the ice, i.e. basal till. Numerous investigations have shown that such sediments are normally deposited/comminuted within 10 to 50 km (e.g. Gross & Moran 1971; Lindquist 1977; Haldorsen 1977; Vorren 1979). These results mainly account for till deposited during the ice recession, which may also be the case in the northern and central Barents Sea. A working hypothesis is therefore that the main

part of glaciomarine sediments in the study area has a high probability of reflecting the bedrock geology in its vicinity.

The shale/sandstone ratio

The recovered lithologies are more coarse-grained than equivalent Mesozoic exposures in Svalbard. The depletion of shale could be explained in terms of more intensive glacial comminution of such fine-grained strata. However, shale fragments are predominant in till and glaciomarine sediments on the slope south of Hopen (Bjørlykke et al. 1978). Also, the same age range is found in the clay and silt sized

sediments as in the rock fragments, indicating the ice rafted component and the finer grade materials to have been derived from a common source.

Stratigraphical provinces

Crystalline or highly metamorphosed rocks from the Hecla Hoek basement is overlain by younger sedimentary sequences in Svalbard. Dominance of Hecla Hoek rocks is so prominent in the northern parts of the investigated area, that a well defined Hecla Hoek province can be established around Kvitøya (Fig. 6).

The cherts and silicified sandstones of limestones of the Upper Permian Kapp Starostin Formation are normally easily distinguishable, partly because of their characteristic lithologies and partly because of their rich fossil content. This Upper Permian unit is an excellent stratigraphical and seismic marker horizon, which can be traced over large areas. Samples with Upper Permian clasts form the predominant lithology east and south of Nordaustlandet, indicating that such rocks may be present in the underlying strata (Fig. 6). Permian and Triassic clasts were recovered from east of Edgeøya; the predominance of cherts suggests that Upper Permian rocks may be present in this area. Samples dated to be equivalent to the DeGeerdalen and Wilhelmøya Formations, except for one (uncertain) late Lower Cretaceous dating, characterize the regions south, east and northeast of Kong Karls Land. No younger rocks seem to be present in the underlying strata in this area.

The relatively few samples dated from the area north of Hopen, suggest an equivalence to the DeGeerdalen and Wilhelmøya Formations.

These formations are exposed on the island, and we suggest that these rocks extend to the north. This is also in agreement with recent results of Dibner et al. (1981).

Even though material dated as equivalent to the Helvetiafjellet Formation and Rurikfjellet Member are predominant in the northern part of Bjørnøyrenna, Sentralbanken and Storbanken, Triassic and Jurassic assemblages have also been identified. However, the presence of pre-Cretaceous material in the area is not necessarily indicative for exposure of these strata in the underlying rocks. The center of the Late

Weichselian ice sheet is believed to have been located in the central, northern Barents Sea (Salvigsen 1981; Boulton et al. 1982; Elverhøi & Solheim 1983), with a successive northward deglaciation. Material from the northern regions may then have been transported southwards, while the reverse situation is less likely. Accordingly, Sentralbanken is included in the Jurassic – Lower Cretaceous province.

The western boundary in the inner part of Bjørnøyrenna is drawn based on previously published data (Bjærke 1979; Dibner et al. 1981).

Geological implications

Assuming that surficial deposits reflect the geology of the substratum in the vicinity, the following summary can be made of the subsurface geology in the northern Barents Sea:

In the northernmost regions, east of Nordaustlandet and around Kvitøya, our data support previous suggestions of exposure of Lower Palaeozoic and older rocks belonging to the Hecla Hoek basement (Dibner 1978).

Permian rocks (mostly Upper Permian) are found to extend off-shore south and southeast of Nordaustlandet as previously suggested (Orvin 1940). Permian rocks are also exposed in a narrow window east of Edgeøya.

Triassic and Lower Jurassic deposits are found north, east and south of Kong Karls Land. The gentle dip north of Kong Karls Land and exposure of Permian rocks halfway between the island and Nordaustlandet indicate a limited thickness. To the northeast, sonobuoy measurements show a 3.45 km/s refractor at about 1 km depth (Eldholm pers. comm. 1983). Refraction measurements on Triassic rocks on Edgeøya have shown velocities of 4 km/s (Elverhøi & Grønlie 1981), and Triassic rocks may extend to a depth of about 1.5 km, where a 4.63 km/s refractor is present (Eldholm pers. comm.). However, sedimentological investigations on onland Svalbard indicate a maximum possible thickness of the whole Triassic succession on Edgeøya of about 850 m (Worsley pers. comm. 1983). The base of the Triassic rocks is therefore most likely defined by the former refractor.

The northward extent of Jurassic – Lower

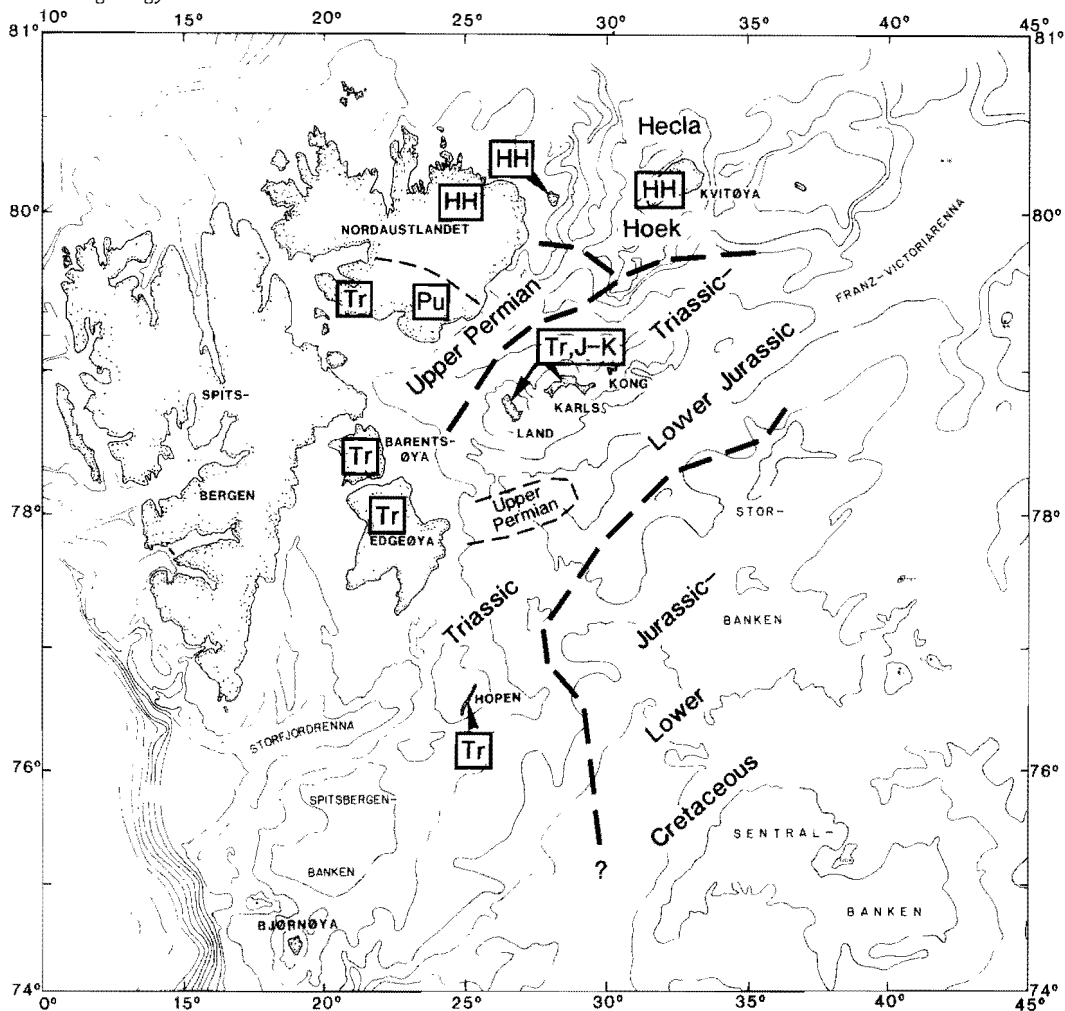


Fig. 6. Map showing stratigraphical provinces for the Quaternary sediments, which are suggested to reflect the underlying bedrock. ● land geology in adjacent areas is indicated in squares.

Cretaceous rocks has been suggested to be as far north as 74°–75°N (Rønnevik & Motland 1979). The rocks of Sentralbanken were first believed to be Mesozoic by Spjeldnæs (1971) and vary from Triassic (Dibner et al. 1981) to Jurassic – Lower Cretaceous (Rønnevik & Motland 1979; Bjærke 1979) to Tertiary (Manum pers. comm. 1983). The data presented here indicate that the complex of Jurassic – Lower Cretaceous rocks extends northward to Storbanken and has a western boundary along the 30°E longitude. The Jurassic – Lower Cretaceous rocks on Kong Karls Land have not been identified offshore, except for an uncertain sample, very close to the shoreline of the easternmost island.

Although coarser-grained sandstone compositions and cements in samples from the shelf seem to be similar to those of equivalent units on land we note especially the frequency of carbonate cement in Triassic rocks (Table 1, stations 33, 38 and 61). A similar cement is also typical for Triassic rocks on Edgeøya and eastern Spitsbergen (Elverhøi & Grønlie 1981).

The distribution of the stratigraphical provinces demonstrates successively younger rocks to the southeast, which may be due to non-deposition or erosion of Mesozoic – Tertiary strata in the northern Barents Sea. The rocks on Edgeøya and Barentsøya have apparently been subjected to relatively little overburden (< 1.5

km, Trondsen 1979), which implies the north-eastern part of the Svalbard archipelago to have been a predominantly positive area at least since the Triassic. The more coarse-grained Mesozoic rocks in the Barents Sea may then be explained in terms of a more marginal facies development as a response to uplift of this area.

Acknowledgements

We are very grateful for the financial support from the Norwegian Petroleum Directorate. We also want to thank Tor Bjærke, Henning Dypvik and Dr. David Worsley for their critical reading of the manuscript, and Dr. Worsley for his improving of the English text. Thanks are also due to E. Kopperud for the final drafting of the figures for this paper and to Dr. Yngve Kristoffersen, chief scientist on board the M/V NORVARG 1980 cruise, for providing the samples and making useful comments on the manuscript.

References

- Bjørlykke, K., Bue, B. & Elverhøi, A. 1978: Quaternary sediments in the northwestern part of the Barents Sea and their relation to the underlying Mesozoic bedrock. *Sedimentology* 25, 227–246.
- Bjærke, T. 1979: Geology of the Barents Sea Shelf; Evidences from palynological studies of drift materials. NPF–Norwegian Sea Symp., Tromsø 1979. NSS 17.
- Bjærke, T. 1980: Palynological analysis of rock fragments from the Barents Sea. Unpubl. report, Norsk Polarinstitut. 18 pp.
- Bjærke, T. 1982: Palynological analysis of sediments and rock fragments from the Barents Sea. Unpubl. report, Norsk Polarinstitut, 14 pp.
- Boulton, G.S., Baldwin, C.T., Peacock, J.D., McCabe, A.M., Miller, G., Jarvis, J., Horsefield, B., Worsley, P., Eyles, N., Chroston, P.N., Day, T.E., Gibbard, P., Hare, P.E. & von Brunn, V. 1982: A glacio-isostatic facies model and amino acid stratigraphy for late Quaternary events in Spitsbergen and the Arctic. *Nature* 298: 437–441.
- Dibner, V.D. 1978: Morfostruktura sel'fa Barenceva morja. Nedra, Leningrad, 211 pp. *NIIGA, Trudy 185* (in Russian).
- Dibner, V.D., Korotkevic, V.D. & Lodkina, L.B. 1981: Carboniferous, Permian, and Triassic Palynocomplexes of the Barents Shelf and their geological significance (On materials of ground sampling). Pp. 49–63 in : Geologija i mineragenija Arkticeskoj oblasti SSSR. Sbornik nauchnyh trudov. (Geology and Mineralogy of the Arctic Area of the USSR. Collection of scientific papers).
- Dibner, V.D. 1978: Morfostruktura sel'fa Barenceva morja. Nedra, Leningrad, 211 pp. *NIIGA, Trudy 185* (in Russian).
- Elverhøi, A., Liestøl, Ø. & Nagy, J. 1980: Glacial erosion, sedimentation and microfauna in the inner part of Kongsfjorden, Spitsbergen. *Norsk Polarinstitut Skrifter* 172: 33–58.
- Elverhøi, A. & Grønlie, G. 1981: Diagenetic and Sedimentologic Explanation for High Seismic Velocity and Low Porosity in Mesozoic-Tertiary Sediments, Svalbard Region. *Am. Ass. Petrol. Geol. Bull.* 65: 145–153.
- Elverhøi, A. & Solheim, A. 1983: The Barents Sea ice sheet – a sedimentological discussion. *Polar Research* 1(1) n.s.: 23–42.
- Elverhøi, A., Lønne, Ø. & Seland, R. 1983: Glaciomarine sedimentation in a modern fjord environment, Spitsbergen. *Polar Research* 1(2) n.s.:127–149.
- Gross, D.L. & Moran, S.R. 1971: Grain-size and mineralogical gradations within tills of the Allegheny Plateau. In: Goldthwait, R.P. (ed) *Till: A Symposium*: 251–274. Ohio State Univ. Press, Columbus. 402 pp.
- Haldorsen, S. 1977: The petrography of tills – A study from Kingsaker, south-eastern Norway. *Norges geol. Unders.* 336: 1–36.
- Hinz, K. & Schlüter, H.–U. 1978: The geological structure of the western Barents Sea. *Marine Geology* 26: 199–230.
- Kristoffersen, Y. & Elverhøy, A. 1980: Maringeologiske og geofysiske undersøkelser, Svalbardekspedisjonen 1980. *Tokt-rapport* 80pp.
- Kristoffersen, Y., Milliman, J.P. & Ellis, J.D. 1984: Unconsolidated sediments and shallow structure of the northern Barents Sea. *Norsk Polarinstitut Skrifter* 180: 25–39 (this volume).
- Lundquist, J. 1977: Till in Sweden. *Boreas* 6: 73–85.
- Orvin A.K. 1940: Outline of the geological history of Spitsbergen. *Skr. om Svalbard og Ishavet* 78: 1–57.
- Rønnevik, H. & Motland, K. 1979: Geology of the Barents Sea. *NPF–Norwegian Sea Symp., Tromsø 1979. NSS* 15.
- Salvigsen, O. 1981: Radiocarbon dated raised beaches in Kong Karls Land, Svalbard, and their consequences for the glacial history of the Barents Sea Area. *Geogr. Ann.* 63A: 283–291.
- Smith, D.G., Harland, W.B., Hughes, N.F. & Pickton, C.A.G. 1976: The Geology of Kong Karls Land, Svalbard. *Geol. Mag.* 113: 193–232.
- Spjeldnæs, N. 1971: Mesozoic (?) bedrock exposed on the bottom of the Barents Sea. *Marine Geology* 11:47–50.
- Thronsen, T. 1979: Kerogen maturation of Triassic deposits in Svalbard. *NPF–Norwegian Sea Symp., Tromsø 1979. NSS* 28.
- Vorren, T.O. 1979: Weichselian ice movements, sediments and stratigraphy on Hardangervidda, South Norway, *Norges geol. Unders.* 350: 1–117

Sonobuoy measurements during the «Ymer» Expedition

Eldholm, Olav, Sundvor, Eirik & Crane, Kathleen 1984: Sonobuoy measurements during the «Ymer» Expedition. *Nor. Polarinst. Skr.* 180: 17–23 ISBN 82-90307-26-6.

Results of sonobuoys recorded during the «Ymer» expedition supports the idea that the Wandel Sea Basin sediments extend onto the continental shelf. A seismic refraction traverse northeast of Kong Karls Land has yielded layers of average velocities 3.10, 3.45, 4.00, 4.63, and 5.29 km/s. The section is interpreted to consist of a series of Mesozoic sediments overlying Permian clastics with velocity 5.29 km/s.

Olav Eldholm, Department of Geology, University of Oslo, Blindern, Oslo 3, Norway; Eirik Sundvor, Seismological Observatory, University of Bergen, 5014 Bergen, Norway; Kathleen Crane, Lamont-Doherty Geological Observatory, Palisades, N.Y., U.S.A. Received April 1983 (revised October 1983).

Introduction

In the summer of 1980 a multidisciplinary Arctic research expedition was carried out onboard the Swedish ice-breaker «Ymer». The scientific program extended from Frans Josef Land westward to Northeast Greenland. The geological program (Schytt et al. 1981) also included geophysical measurements such as PDR-echosoundings (Eldholm et al. 1982), single channel seismic profiling, ship- and helicopter-borne magnetics, gravity, heatflow (Crane et. al. 1982), and seismic refraction measurements using expendable sonobuoys.

As a part of the geological program five sonobuoy refraction profiles were measured on the inner continental shelf off Kronprins Christians Land, Northeast Greenland (Fig. 1) and nine sonobuoys were recorded along a traverse northeast of Kong Karls Land (Figs. 2 and 3). The sonobuoys, model SSQ 41A, received signals from a 120 cu. inch Bolt airgun and the data were recorded on an EPC analog recorder.

In this note we present the results of the surveys and a brief geologic interpretation.

Northeast Greenland shelf

The sonobuoys were recorded in partly open water 15–25 km off the coastline. Technical problems and ice conditions resulted in two profiles of moderate quality (Y3, Y5), whereas the other three are relatively poor. The data have

been reduced by the slope-intercept method and corrected for seafloor dip. Only a few refractors have been mapped but the velocities are relatively consistent. The results are shown in Table 1 and Fig. 4.

The rocks exposed onshore belong to the Wandel Sea Basin containing slightly deformed sedimentary rocks, Carboniferous to Tertiary in age (Dawes 1976). Our results exhibit average velocities of 2.2, 3.5, and 5.0 km/s. We do not

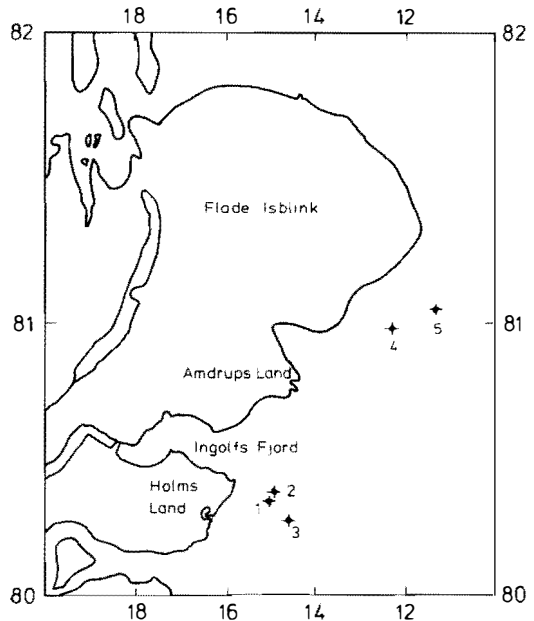


Fig. 1. Location of sonobuoy profiles on the inner continental shelf, Northeast Greenland.

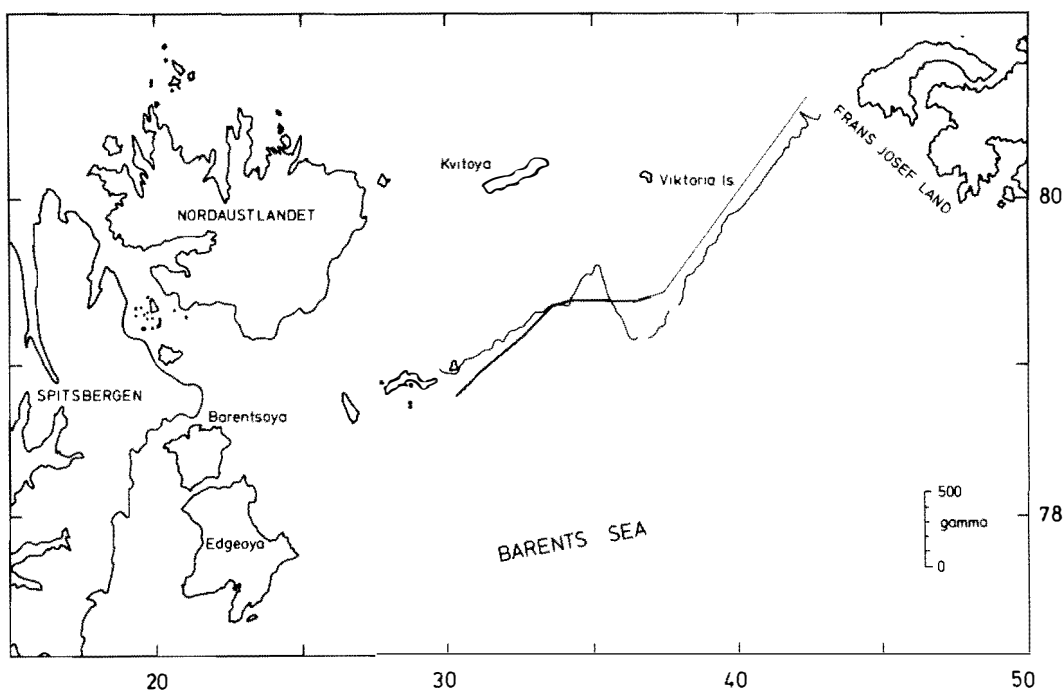


Fig. 2. «Ymer» track and the magnetic anomaly field plotted along the ship's track in the northern Barents Sea. The location of the sonobuoy traverse is shown by a thicker track line.

feel the few refractors observed allow much of a geologic interpretation. However, the data do support the suggestion of Dawes & Soper (1973) that the Wandel Sea Basin rocks continue underneath the continental shelf.

Traverse northeast of Kong Karls Land

On the return trip towards Tromsø «Ymer» sailed between Kvitøya and Frans Josef Land turning southwestward toward Kong Karls Land with a stop at Kongsøya (Figs. 2 and 3).

Along the southwestern leg toward Kongsøya we recorded a sonobuoy traverse as well as bathymetric and magnetic measurements. This part of the Barents Sea is geophysically relatively unexplored.

The bathymetry along the ship's track shows a gentle relief with a system of shoals and depressions. Closer to Kong Karls Land, however, the sea floor shallows as the traverse runs along a north-northeast trending ridgelike feature of which the islands are the emerged part (Fig. 3). A detailed discussion of the bathymetry is present

in the accompanying paper by Kristoffersen et al. (1984) who have included the «Ymer» soundings in their maps. The seafloor geology as reflected by shallow seismic reflection studies and bottom samples is described by Kristoffersen et al. (1984) and Elverhøi & Lauritzen (1984).

In Kong Karls Land the rocks have been dated as spanning the period from Late Triassic to Early Cretaceous changing from continental facies in the Late Triassic/Early Jurassic to a marine environment in the Late and Middle Jurassic, returning to continental facies with volcanics in the Early Cretaceous. Moderate syn-depositional tectonic movements occurred and a minimum of six volcanic events has been suggested in the Late Jurassic/Early Cretaceous (Smith et al. 1976).

On Kvitøya to the north only crystalline and metamorphic assemblages are observed (Hjelle 1980), whereas the Frans Josef Land archipelago exhibits sequences similar to those in Kong Karls Land (Smith et al. 1976). This may indicate a possible geologic continuity eastward across the northernmost Barents Sea.

The sonobuoy traverse was shot between 37° E and Kongsøya (Fig. 3). The objective was to

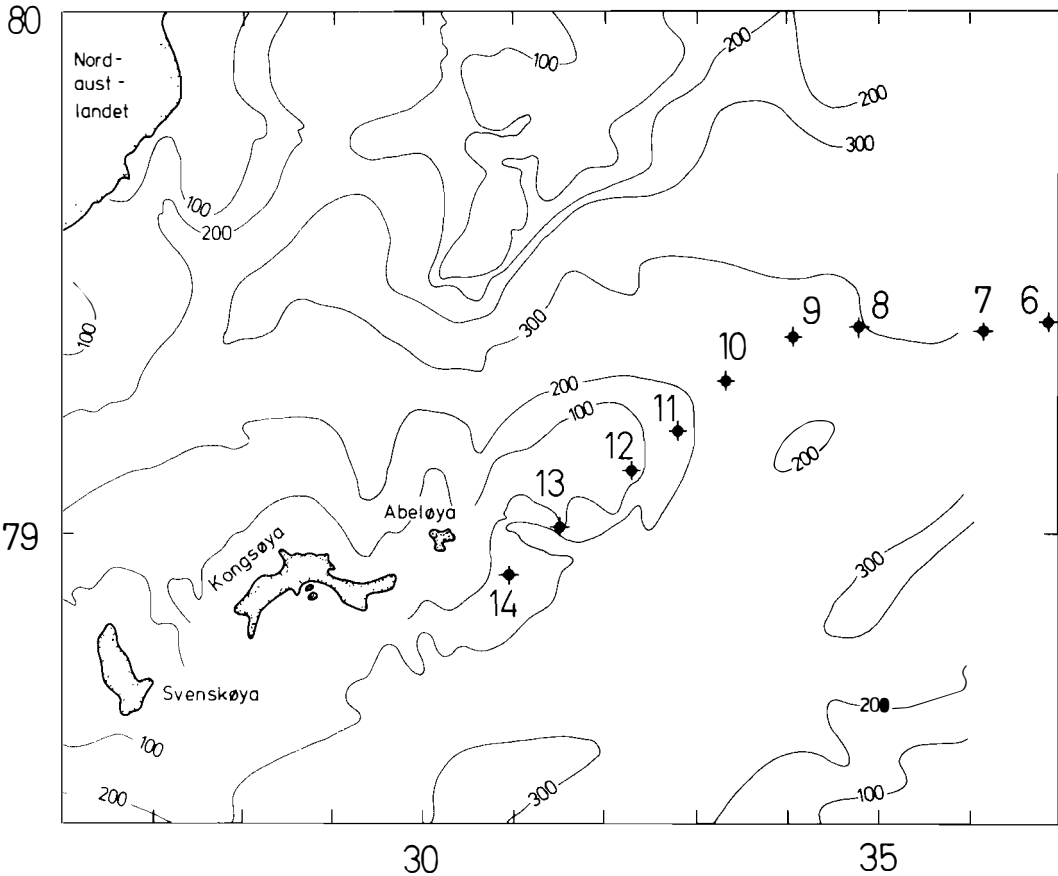


Fig. 3. Location of sonobuoy traverse northeast of Kong Karls Land. Bathymetry from Kristoffersen et al. (1984).

obtain an end-to-end configuration, starting a new profile when no identifiable refracted arrivals could be obtained from the preceding buoy. With the exception of an about 12 km gap between profiles Y7 and Y8 all of the buoys were recorded end-to-end.

As no obvious curvature was observed in the first arrival curve, the sonobuoys have been reduced by picking straight line refracted arrivals using a conventional slope-intercept approach to determine depth to the refracting interfaces. For profiles recorded end-to-end, we constructed artificial reversed profiles by connecting intercept times and reversed points (Fig. 5). If the refractors have a constant dip, one may calculate true velocities. All solutions have been corrected for sea floor topography. In some profiles it was not possible to identify refracted arrivals from the sediments at the sea floor; therefore an assumed

sea floor velocity based on adjacent profiles, has been used.

The results are listed in Table 1 and plotted as a seismic structure section in Fig. 6. The velocities in the various profiles are quite consistent and typical refractors have been correlated. Average velocities of 3.1, 3.5, 4.0, 4.6, and 5.3 km/s have been computed for the section. The 3.5 km/s layer thins towards the northeast and the uppermost part of the sequences has only been identified in profiles Y12 and Y14, where the waterdepth is quite shallow, yielding values of 2.55 and 2.83 km/s, respectively. Profile Y14 lies about 14 km southeast of a sparker refraction line of Kristoffersen et al. (1984) who measured a sea floor velocity of 2.3 km/s.

The limited geophysical and geological information in this region makes a geological interpretation of Fig. 6 difficult. However, we

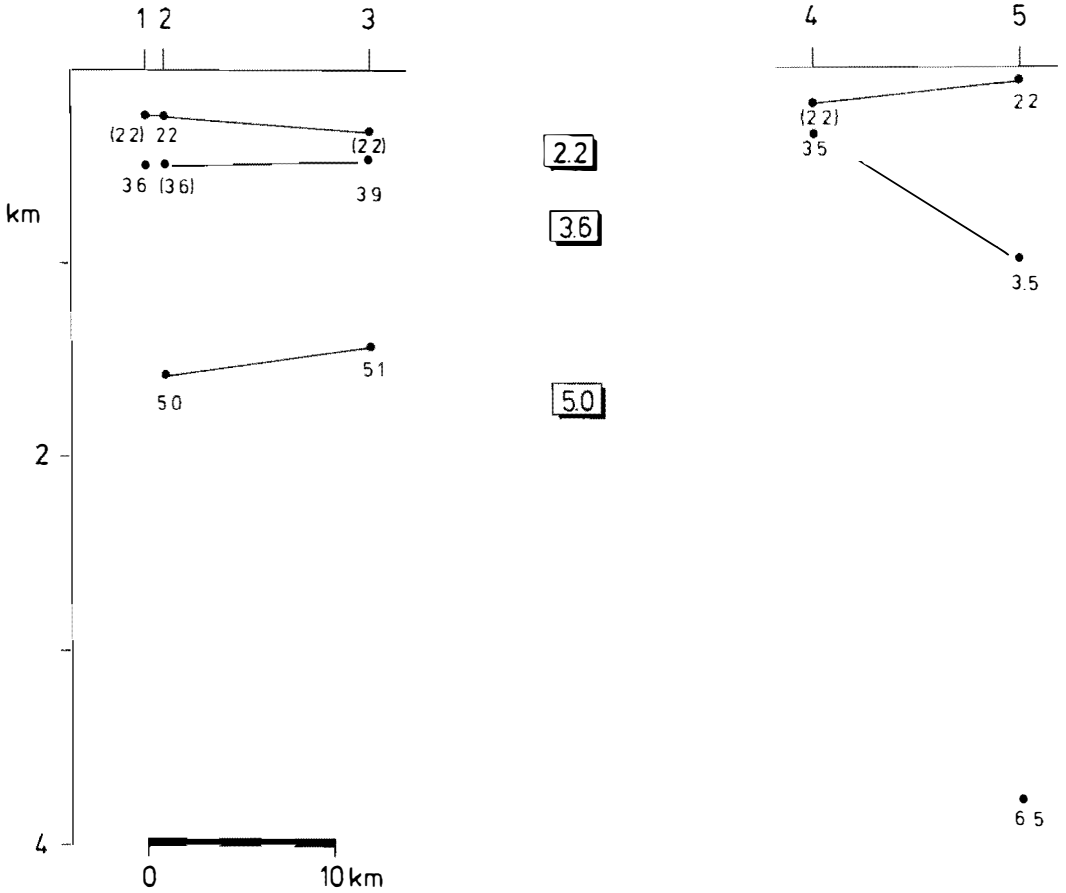


Fig. 4. Sonobuoy results off Northeast Greenland.

feel that our profile reveals a sequence of layered sedimentary rocks with a minimum thickness of 2–2.5 km.

In a study of bottom samples, assuming that the Quaternary deposits reflect the lithology and age of the underlying bedrock, Elverhøi & Lauritzen (1984) have predicted a change in stratigraphy southeastward from Nordaustlandet. Upper Permian ages are indicated just offshore Nordaustlandet; Kong Karls Land is centered in a zone of Triassic/Lower Jurassic changing to Jurassic/Lower Cretaceous south of the broad topographic high on which the islands are located. The sonobuoy section lies in the central area of Triassic/Lower Jurassic subcrop. Similar inferences have been made for the southern Barents Sea by Bjærke (1979). On the other hand, Faleide & Gudlaugsson (1981) have sug-

gested from multichannel reflection data that there often are differences in the subcrop configuration and the composition of the bottom samples.

Kristoffersen et al. (1984) recorded seven sonobuoys in the nearshore areas north of Kong Karls Land, and one profile just south of Abeløya. The sparker energy source only gave refracted arrivals from the uppermost sediments. The velocities obtained were all in the range 2.0–2.5 km/s, averaging 2.3 km/s. In some profiles a thin veneer of low velocity, 1.7–1.8 km/s, surficial sediments was recorded. Triassic sandstones exist in bottom samples in this region (Elverhøi & Lauritzen 1984), but Kristoffersen et al. (1984) note that seafloor velocities are significantly lower than what is observed in comparable sediments on Edgeøya and eastern Spitsbergen.

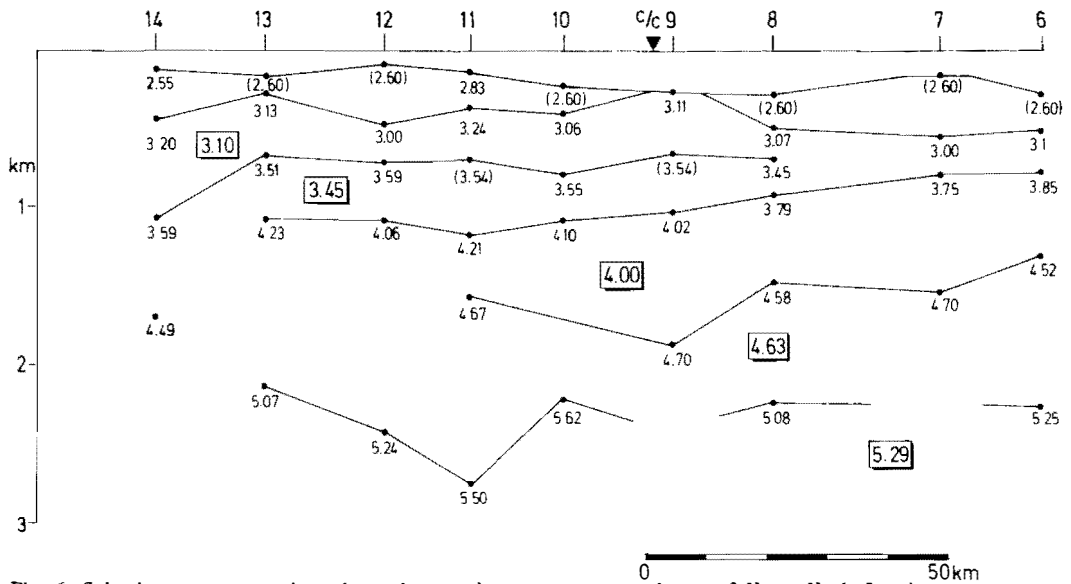


Fig. 6. Seismic structure section along the sonobuoy traverse northeast of Kong Karls Land.

They suggest that higher porosities at Kong Karls Land and a regional change due to diagenetic influences, may imply a lowered velocity eastward.

Although local occurrences of Tertiary sediments may exist, regional studies seem to indicate an absence of such sediments on the Svalbard Platform and offshore the eastern Svalbard islands (Faleide & Gudlaugsson 1981; Rønnevik et al. 1982). Keeping in mind that considerable regional velocity differences can occur within rock units of comparable lithology and age, we have compared our results with those of Faleide (pers. comm.). They have related seismic velocities to subsurface geology and made general inferences which may prove useful. Although their analysis is mainly based on data from the western Barents Sea and does not cover the area as far north as Kong Karls Land the results are considered important. Velocities in the range 2.5–3.5 km/s are representative of the Paleocene and Upper Cretaceous section, 2.7–3.8 km/s in the Lower Cretaceous, 3.7–5.4 km/s in the Jurassic and Triassic section, and 5.0–6.4 km/s in the Permo-Carboniferous sediments. On the Svalbard Platform where the Cenozoic and upper Mesozoic sections are absent the velocities are slightly higher than those in the same sequences farther south (Faleide pers. comm.) For example, Triassic sediments range from 4.3 to 5.5 km/s

with sea floor velocities of 4.3–4.4 km/s close to Hopen.

Rønnevik et al. (1982) indicate schematically pre middle-Jurassic sediments to the east of Kong Karls Land. Furthermore, they have presented an isochrone map to seismic reflector F_1 . This horizon is dated as Lower Permian by Rønnevik et al. (1982) but Faleide & Gudlaugsson (1981) have suggested it marks the top of silicified clastics of Upper Permian age. The 5.29 km/s refractor in Fig. 6 corresponds quite well with the F_1 reflector.

These arguments indicate either dramatic lateral velocity changes in the Lower Jurassic/Triassic sections compared with the adjacent islands and the offshore region to the south and southwest, or the existence of post-middle Jurassic rocks along the sonobuoy traverse. The refraction velocities could of course be in error, but correspond reasonably well with interval velocities from an adjacent multichannel line. Although lateral changes cannot be ruled out, we tentatively propose that our results indicate that the layers shown in the seismic section are composed of predominantly Mesozoic rocks, including also Upper Jurassic and possibly Cretaceous sediments. According to Faleide & Gudlaugsson (1981) this sequence is predominantly of clastic origin.

In Fig. 2 we have plotted the magnetic anomaly

along the ship's track. The field is in general quiet except for a local excursion at about 80.4° N and a prominent peak to peak anomaly of 500 gamma over sonobuoys Y6–Y8. The seismic section does not appear to reflect structural changes associated with the anomaly, consequently we interpret the top of the anomaly source to be located at least 2.5 km below the seafloor. We note, however, that Rønnevik et al. (1982) have mapped a narrow north-northeast trending graben-like feature which intersects our profile at the location of the magnetic anomaly. This feature is observed at the level of the F₁ horizon. It is probable that the faulting marks relief in the underlying magnetic basement which is responsible for the anomaly.

Acknowledgements

This work was carried out as a part of the Swedish Ymer-80 expedition. We thank the scientific staff, officers and crew for their helpful assistance. Most of the equipment was made available by the Seismological Observatory, University of Bergen. We are greatly indebted to Dr. G. Leonard Johnson for providing the sonobuoys.

The project was supported by the Norwegian Research Council for Science and the Humanities (Grant D 40.31–25) and by the Office of Naval Research Arctic Research Grant N-00014-80-C-0260.

References

- Bjørke, T. 1979: Geology of the Barents Sea shelf: Evidence from palynological studies of drift material. *Norw. Petrol. Soc., NSS-17*. 15 pp.
- Crane, K., Eldholm, O., Myhre, A.M. & Sundvor, E. 1982: Thermal implications for the evolution of the Spitsbergen transform fault. *Tectonophysics* **89**: 1–32.
- Dawes, P.R. 1976: Precambrian to Tertiary of northern Greenland. In: Escher, A. & Watt, W.S. (eds.) *Geology of Greenland. Grøn. Geol. Unders.*: 248–303.
- Dawes, P.R. & Soper, N.J. 1973: Pre-Quaternary history of North Greenland. In: Pitcher, M.G. (ed.) *Arctic Geology, Mem. Amer. Assoc. Petrol. Geol.* 19: 117–134.
- Eldholm, O., Sundvor, E., Sand, M. & Crane, K. 1982: YMER-80: Navigation and bathymetry. *Inst. Geol. Oslo, Intern. Skr. ser. nr. 36*, 47 pp.
- Elverhøi, A. & Lauritzen, Ø. 1984: Bedrock geology of the northern Barents Sea (west of 35° E) as inferred from the overlying Quaternary deposits. *Nor. Polarinst. Skr.* **180**: 5–16 (this volume).
- Faleide, J.I. & Gudlaugsson, S.T. 1981: *Geology of the Western Barents Sea – A regional study based on marine geophysical data*. Cand. real. thesis, Univ. of Oslo, 160 pp.
- Hjelle, A. 1980: An outline of the Pre-Carboniferous geology of Nordaustlandet. *Polarforschung* **48**: 62–77.
- Kristoffersen, Y., Milliman, J.D. & Ellis, J.P. 1984: Distribution of unconsolidated sediments and the shallow geologic structure of the northern Barents Sea. *Nor. Polarinst. Skr.* **180**: 25–39 (this volume).
- Rønnevik, H.C., Beskow, B. & Jacobsen, H.P. 1982: Structural and stratigraphic evolution of the Barents Sea. *Norw. Petrol. Soc., ONS* **82**, 29 pp.
- Schytt, V., Bostrøm, K. & Hjort, C. 1981: Geoscience during the YMER-80 expedition to the Arctic. *Geol. För. Stockholm Förh.* **103**: 109–119.
- Smith, D.G., Harland, W.B., Hughes, N.F. & Pickton, C.A.G. 1976: The geology of Kong Karls Land, Svalbard. *Geol. Mag.* **113**: 193–232.

Unconsolidated sediments and shallow structure of the northern Barents Sea*

Kristoffersen, Y., Milliman, J.D. & Ellis J.P.: Unconsolidated sediments and shallow structure of the northern Barents Sea. *Norsk Polarinstitutt Skrifter Nr. 180*: 25–39 ISBN 82-90307-26-6.

The northern Barents Sea is dominated by NE-SW trending ridges and intervening basins. Except for moraine/till deposits on the bank area at 77°30'N 34°E and piles of acoustically transparent sediment seaward of the melting glaciers on southern Nordaustlandet, generally less than 10–15 meters of unconsolidated sediment occurs on the ridges and in shallow water areas. Basins locally contain more than 40 m of unconsolidated sediment. Only the top meter of this unit appears to be modern. The rest was glacially deposited during the late Weichselian.

Seismic profiles show southward dipping rocks south of the Nordaustlandet – Kvitøya high. Correlation with land geology and dredged rocks suggest the strata to be Permo-Carboniferous cherts and sandstones. Structurally, the eastern part of Kong Karls Land forms the core of a syncline trending along the island chain which marks the transition between gentle southward dipping strata to the north and structurally more complex strata to the south. The more complex structures represent more intensive regional deformation, possibly induced by salt movement or block faulting at depth. Seismic velocity of Triassic sandstone at the sea floor around Kong Karls Land is 2.3 km/s.

Yngve Kristoffersen, Norsk Polarinstitutt, P.O. Box 158, 1330 Oslo Lufthavn, Norway; J.D. Milliman and J.P. Ellis, Woods Hole Oceanographic Institution, Woods Hole, Ma, U.S.A. Received May 1982 (revised November 1983).

Introduction

Knowledge of the bathymetry and submarine geology of the northeastern Barents Sea (north of 77°N) has been sparse because the area is often covered with ice during the summer months. Nansen's chart (1904) of the North Polar Seas showed only a few available soundings north of 77°N, mostly near islands. Later Russian bathymetric maps (Klenova 1960) appear to conform reasonably well with the most recent information. Eggvin's (1963) map also displays the major features, but with significant discrepancies south of Kvitøya. The present navigational chart of the area (Chart 507 issued in 1969) only shows depth soundings along a dozen lines north of the latitude of Kong Karls Land (79°N).

Published data on the northern Barents Sea are also few. The first regional summary of geological sampling in the Barents Sea, in the 1920's by the Academy of Sciences in Moscow (Klenova 1960), dealt extensively with the distribution and character of bottom sediments. More recently, workers at the Polar Scientific Research Institute

of Marine Fisheries and Oceanography (PINRO) in Murmansk and (NIIGA) in Leningrad directed their attention to pre-Quaternary deposits of the Barents Sea (Dibner et al. 1970; Dibner 1978).

This paper deals with some of the results of a 1980 reconnaissance geophysical/geological survey by Norsk Polarinstitutt (Norwegian Polar Research Institute) and Oljedirektoratet (Petroleum Directorate) in cooperation with Woods Hole Oceanographic Institution. The scientific program included bathymetry, shallow seismic reflection and sonobuoy measurements, suspended matter sampling, and bottom photography. In this paper the bathymetry and seismic results are emphasized.

Data acquisition

A chartered 155 foot sealer/ice-breaker, M/V NORVARG, was used to collect 1900 line kilometers of shallow seismic reflection measurements and sediment samples at 146 stations during a 34-day cruise in the northern Barents Sea – 10 August – 12 September 1980 (Fig. 1). Positioning was by a Magnavox MX-1105 integrated satellite/Omega receiver. As log and gyro-

* Contribution No. 5145 from the Woods Hole Oceanographic Institution.

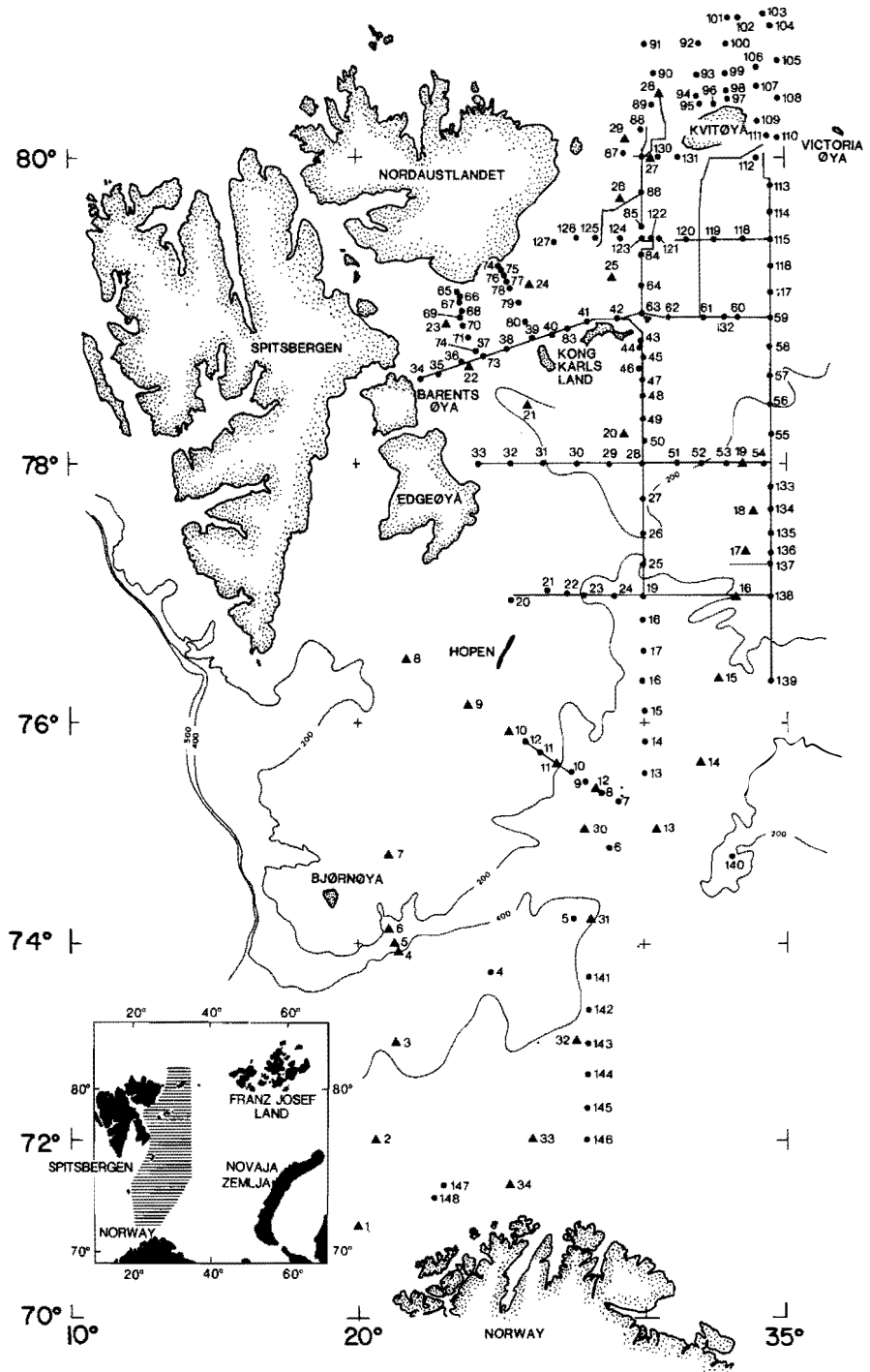


Fig. 1. Shallow seismic reflection profiles (solid lines) and geologic sampling locations (dots) of the Norsk Polarinstittutt Svalbard Expedition 1980.

information had to be entered manually, navigational accuracy is estimated to be 500 to 1000 meters.

An EG&G sparker (Max. 4.3 kJoules) system was used as energy source. Signals were received by a 200 element 50 meter-long streamer and displayed on an EPC graphic recorder after band pass filtering (50-500 Hz) and also recorded on analog tape. Short range seismic refraction measurements were made in shallow water with AN/SSQ-41A sonobuoys and 1 kJ sparker as energy source. Depth soundings were made with a Simrad 38 kHz (Skipperlodd) echosounder recording on wet paper. Sediment cores were obtained with a 3 meter long 110 mm diameter gravity corer; a pipe dredge was used for dredging.

Bathymetry

A bathymetric map of the northern Barents Sea (Fig. 2) has been compiled based on the 1900 km of echo-sounding data collected by NORVARG augmented by data from the YMER-80 Expedition and a subsequent 1981 cruise in the Nordaustlandet area. The YMER data (navigation and bathymetry) were kindly made available by Dr. O. Eldholm (Univ. of Oslo). The area south of Kong Karls Land and west of 30°E was surveyed by Norsk Polarinstitut in 1972 with 5 km line-spacing using Decca Hi-Fix navigation. Data from the area east of 30°E and south of 79°N were provided by Fiskeridirektoratets Havforskningsinstitut, Bergen (The Oceanographic Research Institute of the Fisheries Directorate). North of about 80°30'N, however, the map is based primarily on scattered soundings given on Nautical Chart No. 507, and as such the bathymetry in this northernmost area should be considered only schematic.

The southern and middle portions of the study area are dominated by a number of ENE-WSW lineaments that suggest a regional structural trend. South of Kong Karls Land (the Svenskøya-Kongsøya-Abeløya island chain) is the Hinlopen Basin; maximum water depths reach 350 m, but the basin is best defined by the 300 m contour. The basin shoals slightly to the east, before deepening to greater than 300 m in the eastern-

most part of the study area. The south-eastern portion of the basin shoals to less than 100 m, while in the south depths are less than 200 m.

The structural high of the Kong Karls Land islands continues towards the east as a series of shallow banks, the largest one being more than 20 km across. North of the island chain is the Kongsøya Basin, also trending in a ENE-WSW direction. Again, the deepest parts of the basin exceed 350 m, thereby dividing the basin into two parts, one in the east and the other in the west. The 300 m contour is open to the east, but probably closed to the north. On the other hand, the 250 m contour clearly opens to the north and connects with the basin north of the Kvitøya-Nordaustlandet Straits.

Kvitøya has several banks off its northwestern and southwestern corners, with water depths shoaling to less than 50 m on the south side. Because of the sparse soundings north of the straits, the basin west of Kvitøya is difficult to define. However, depths locally exceed 500 m (the greatest depths noted in the entire area) and are generally greater than 350 m. The available data are not conclusive as to whether the basin is open or closed to the north. We feel that it is closed, based on the very few soundings which show depths generally less than 200 m north of the basin and also because hydrographic data indicate that North Atlantic water enters the Barents Sea from the eastern side of Kvitøya; if the western side were open to the north, it also would transport North Atlantic deep water.

Bathymetry on the north side of Nordaustlandet is also poorly defined. Nevertheless, YMER transects in the area show a trend of deeply cut narrow basins (one in excess of 300 m) that apparently cut perpendicularly to the shoreline. Presumably these basins represent offshore continuations of the fjords on the north shore of Nordaustlandet. Although data are few, these basins presumably close to the north. Depths on the northern shelf range from 100 to 150 m, with local shallows associated with small islands.

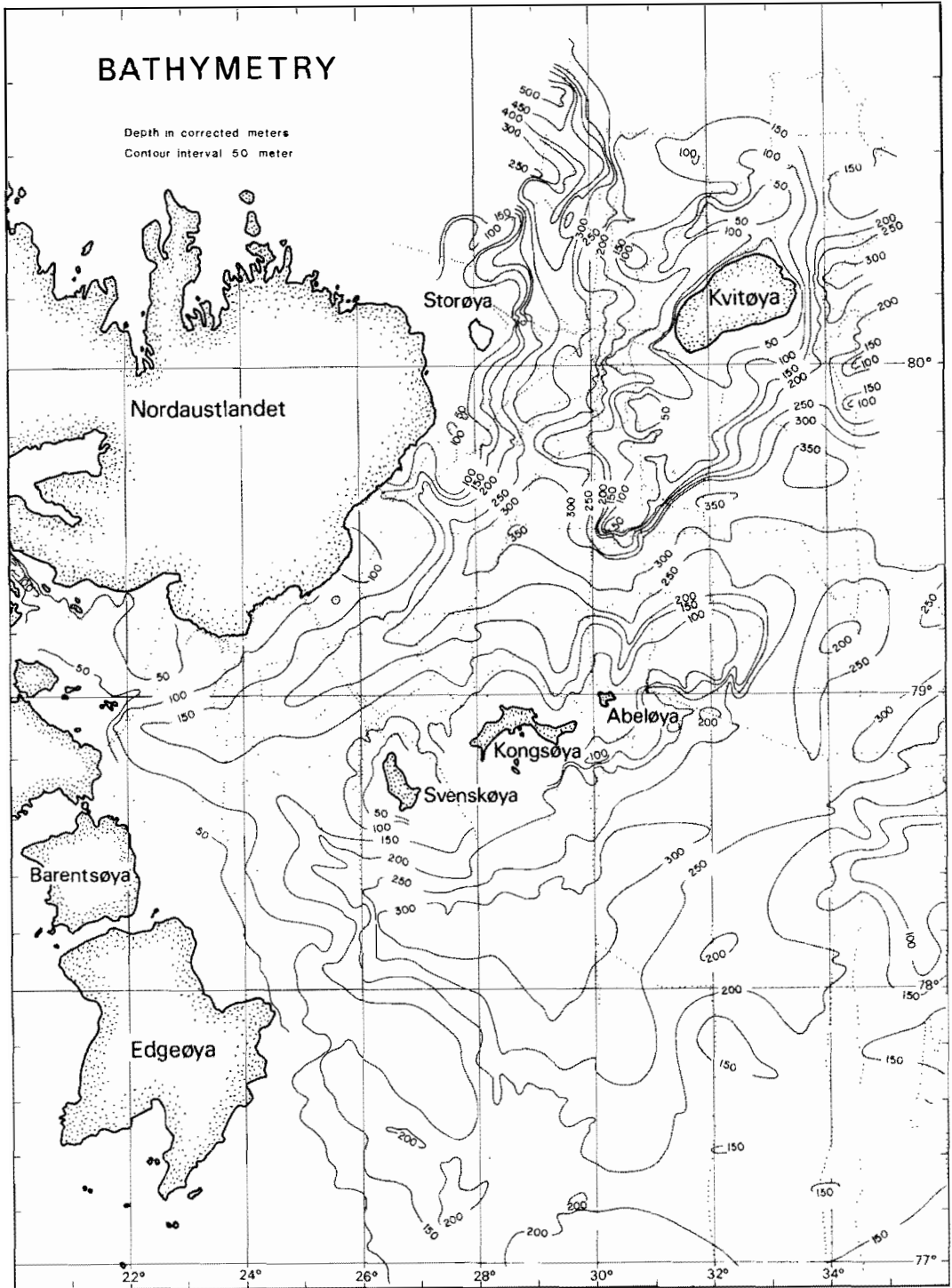


Fig. 2. Bathymetric map of the northern Barents Sea compiled from soundings collected by vessels using satellite navigation or more precise electronic positioning systems (Decca Hi-Fix). Data sources north of Kong Karls Land: the Norsk Polarinstittutt Svalbard Expedition 1980 and 1981, the Swedish YMER-expedition 1980, and the Norwegian Petroleum Directorate Survey 1980. Data sources south of Kong Karls Land: Nautical chart (Decca Hi-Fix navigation) and Fiskeridirektoratets Havforskningsinstitutt (area east of 31°E). Depth in corrected meters. Eastern and southern coastline of Nordaustlandet updated from Landsat imagery by K. Svendsen (pers. comm.).

Geological outline of islands adjacent to the northern Barents Sea and hypothesis on the glacial history

Geology

The Barents Sea is bounded to the north and west by islands forming the sub-arctic part of the Barents shelf. The geologic and glacial history of these islands provide a first overview of the major geologic and glacial events which must be reflected in the submarine geology of the northern Barents Sea.

The Frans Josefs Land archipelago to the northeast (Fig. 1) encompasses a total of 132 islands within a 360 km × 230 km area, with 87% of the archipelago presently covered by glaciers. The exposed sedimentary section (total thickness of 2300 meters) is mainly continental sandstones, siltstones, clays and sometimes brown coal ranging in age from Late Triassic to Early Cretaceous interrupted by a section of Late/Middle Jurassic marine shales and thinly bedded siltstones (Dibner 1957, 1961, 1970; Pirozhnikov 1958). The presence of older lower Carboniferous coal-bearing rocks has been inferred from boulders found at several localities (Dibner 1970).

Victoria Island, located at 80°08' N, 36°45' E, is the westernmost part of the Soviet Arctic (Fig. 1). The island covers an area of 2 km × 4 km and is capped by a glacier except for a 50-80 m wide and 400 meter long beach on the NNW side. Boulders and gravels on the beach are dominantly Middle Carboniferous (Moscovian) limestones and silicified limestones with occasional gneiss boulders (Horn 1932; Klenova 1960; Klubov & Soloveva 1972). Horn (1932) speculated that the crystalline boulders may have been brought to the island by ice; all authors consider Carboniferous rocks to be present beneath the glacier.

Kvitøya, the easternmost island in the Svalbard archipelago (Fig. 5), is covered by the Kvitsjøkulen glacier except for two small areas: Kræmerpynten and Hornodden in the east where gabbros and diorites outcrop, and Andréeneset to the west where gneisses, migmatites and granites are exposed (Hjelle 1978).

The eastern and southern part of Nordaustlandet is covered by an ice dome. Isolated outcrops on the eastern part of Nordaustlandet and the adjacent island of Storøya, are gabbros, meta-gabbros, amphibolites and paragneisses. The rocks are considered Caledonian or older (A. Hjelle pers. comm.). At Isispynten (79°40'N 26°45'E) boulders of fossiliferous Permo-Carboniferous rocks (Fig. 5) have been observed in a moraine (A. Hjelle pers. comm.). The southernmost outcrop of sedimentary rocks in Nord-austlandet is Permo-Carboniferous grey fossiliferous limestone and chert bands overlain by Triassic shales (Sandford 1926; Thomson 1953).

In the easternmost part of Spitsbergen, Triassic rocks are exposed along the coast of Olav V Land (Orvin 1940) and on Wilhelmøya overlain by Jurassic strata (Klubov 1970; Worsley 1971).

Barentsøya and Edgeøya are covered by Triassic sediments with small outcrops of Permian limestones and chert (Lock et al. 1978; Klubov 1965). Lower Triassic rocks are fully marine shales and siltstones (>300m thick), with black phosphatic and bituminous shales in the upper part (thickness 50–100 m.) Above a possible hiatus are upper Triassic siltstones and shales (80–150 m thick) overlain by sandstones (>400 m thick) deposited as a major deltaic complex advancing from the northeast (Lock et al. 1978; Flood et al. 1971). Intrusions of sills and dykes are widespread on Barentsøya and on the western and southern part of Edgeøya and the magmatic activity probably occurred during Late Jurassic/Early Cretaceous.

The rocks on Kong Karls Land range in age from Late Triassic to Early Cretaceous and were laid down in an environment which changed from continental (porous sandstone) to fully marine (clays, shales and limestone) and back to continental (interbedded sandstones and lavas) (Smith et al. 1976; Worsley & Heintz 1977). Moderate syndepositional tectonic movements are inferred from lack of continuity of beds within the marine Kongsøya Formation Pliensbachian-Barremian). Lava flows are present within this formation and the overlying continental Kong Karls Land Formation; at least six volcanic episodes of Late Jurassic/Early Cretaceous age can be discerned (Smith et al. 1976). The rocks

on Kong Karls Land form a broad anticlinal or dome-like structure. Minor flexures and gentle folds have a N-S axial trend.

The top of the succession on the island of Hopen to the south overlaps the base of the succession on Kong Karls Land. The lithology of the three Late Triassic formations is a lowermost sequence of interbedded sandstones and shales overlain by fully marine shales followed by fluvial sandstones at the top (Smith et al. 1975). The strata are flat-lying cut by WNW-ESE high angle faults or monoclines.

Glacial history

As only limited data on the submarine geology of the Barents Sea have been available, inferences on the glacial history of the area have been drawn from raised beaches in the Svalbard archipelago, Frans Josef Land, and Novaja Zemlja as well as glacial deposits in the Pechora area to the south. Divergent conclusions have been reached regarding the extent of the Late Weichselian Barents Sea (25,000 – 10,000 years B.P.) ice cover:

- I. Non-glaciated (Boulton 1979);
- II. Limited glacial cover on the western banks and in the deep troughs (Bjørnøya and Storfjordrenna) (Matisov 1977, 1980; Elverhøi & Bomstad 1980); and
- III. Total glacial cover (Schytt et al. 1967; Grosswald 1980).

The depositional environment implied by these models differs considerably. Regional geological sampling shows widespread occurrence of till on the bank areas and in the northeastern upper reaches of Bjørnøyrenna and the appearance of pre-Holocene glaciomarine sediments below 300 meter water depth in Bjørnøyrenna. From this evidence Elverhøi & Solheim (1983) conclude that Bjørnøyrenna and probably also Storfjordrenna were calving bays for a grounded ice sheet in shallower areas during Late Weichselian time, supporting the concept of at least a partial ice cover.

Sediment distribution

Two types of data with differing penetration and resolution were used to determine the distribution of unconsolidated sediments. First, shallow

seismic reflection (sparker) measurements yielded a subbottom penetration of 50–150 msec, with a resolution of about 10 msec limited by the pulse length of the sparker source. Second, a total of 134 gravity cores (<3 meters), 11 large grab samples (1 m³), and 91 dredge hauls were recovered from 105 localities in the study area. The results of the sediment sampling were reported by Elverhøi & Solheim (1983).

Most shallow areas are devoid of unconsolidated sediments. Large boulders of pink granites and gneisses were dredged from the ridge north of Kvitøya. Southwest of the island the content of the dredge hauls changed southwards from crystalline rocks to sandstones. Sandstones also dominate in rocks recovered around Kong Karls Land and its northeast submarine extension.

A bottom of soft mud with a number of brittle stars, sea urchins and abundant tracks is evident on bottom photographs from the deeper areas. Muddy sand with pebbles occurs on the bank to the southeast of Kong Karls Land where moraine accumulations appear to be present. In the shallow areas around Kvitøya the bottom is paved by stones and boulders swept clear of finer deposits. Brittle stars and sea cucumbers are present everywhere in the area.

Although most areas contain only a thin veneer (<10–15 meter) of unconsolidated sediment, local accumulations can reach thicknesses of 30–50 meters, and in one case more than 80 meters (Figs. 3 and 4). The unconsolidated sediments may be classified into two types:

- 1) Most obvious is the acoustically transparent sediment that occurs primarily within the basins (Fig. 4, profile A). Thicknesses locally exceed 60 m and are assumed to lie in the deepest portions of the basins, although this cannot be confirmed with the limited profile coverage. In the basin north of Kong Karls Land, the transparent sediment pile laps up onto the southern basin wall, but the greatest thickness (>80 meters) appears to be along the axis of the basin. Sediment cores (stns. 84, 119 and 120 in Fig. 1) show that this sediment contains an upper unit (<140 cm) of soft, dark grey, organic-rich mud overlying mud with a downcore increase in sand and pebble content. Presumably the upper unit represents modern sediment deposited over a glacial marine

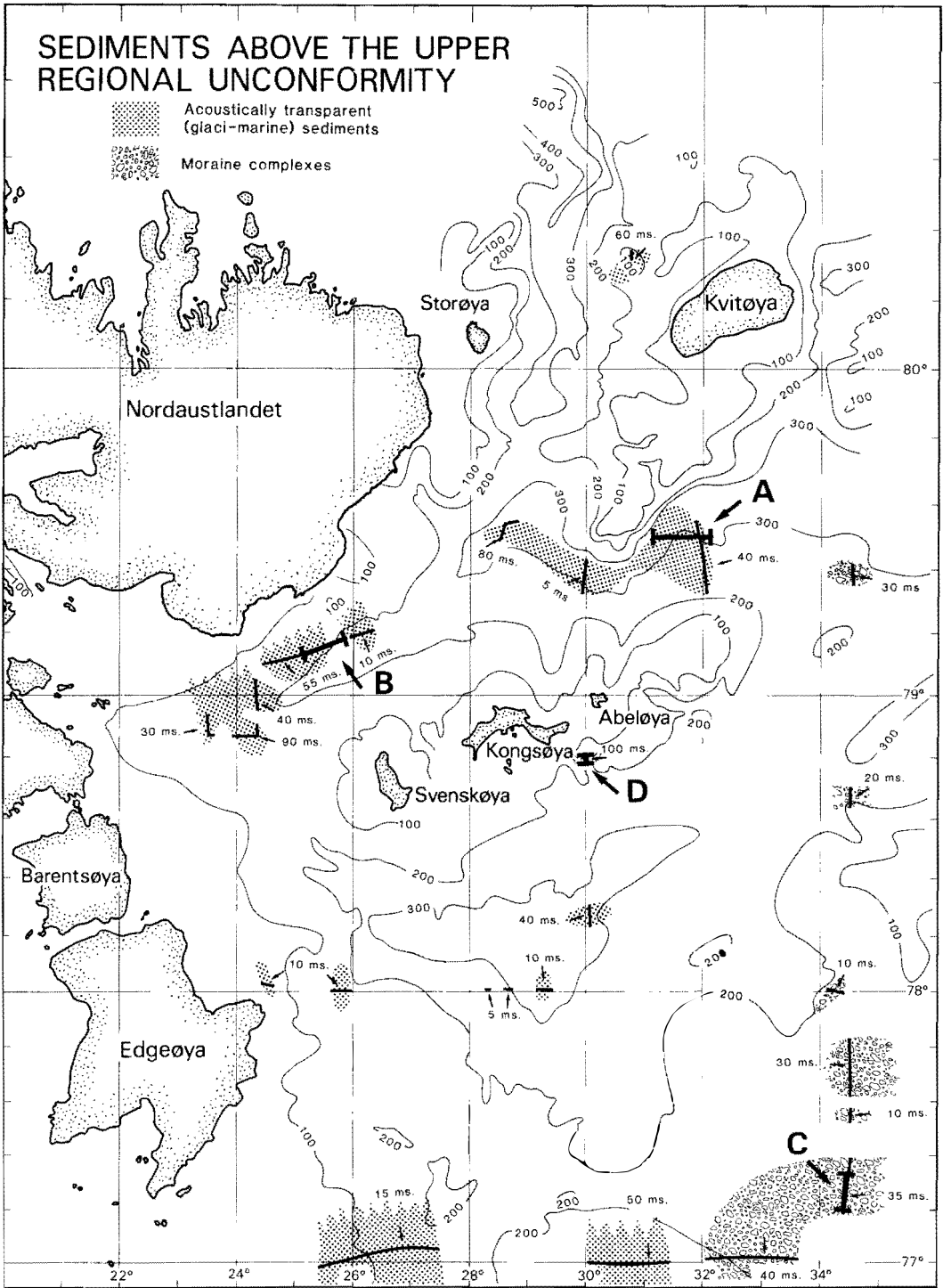


Fig.3. Distribution of sediments above the upper regional unconformity in the northern Barents Sea as derived from track coverage shown in Fig. 1. Track crossings of sediment accumulations shown by heavy lines with maximum thicknesses in milliseconds two-way travel time. Profiles A through D indicate seismic record sections shown in Fig. 4.

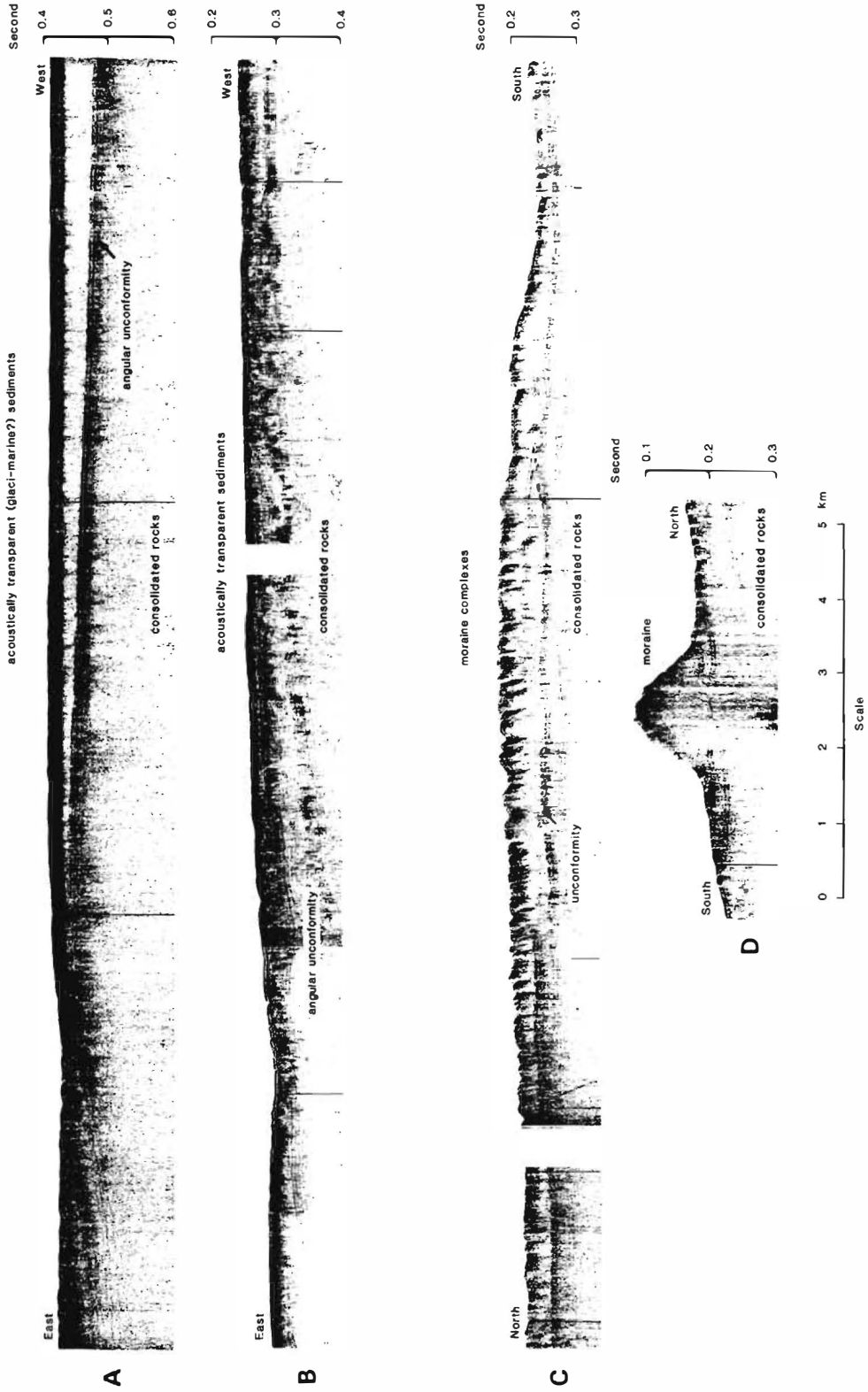


Fig. 4. Shallow seismic reflection (sparker) records representative of the two main types of unconsolidated sediments (glaci-marine sediments and moraine complexes) observed in the northern Barents Sea. Profile locations shown in Fig. 3. Vertical scale on interval of 0.1 second two-way travel time equivalent to 100 meters assuming a sound velocity of 2.0 km/s in the sediments.

(Late Weichselian) unit. In the basin south of Kong Karls Land, sediment thicknesses (max. thickness 30 m) in the central portion are localized, but the most prominent layer occurs in the depression to the south with thicknesses exceeding 35 m. The bottom sediments (stns. 49 and 50) are a thin (40 cm) unit of dark olive grey mud (modern) with an occasional drop stone overlying a gravel-rich sandy mud (glacial marine).

Acoustically transparent sediments in shallow water appear to be derived from the input of sediment-laden glacial meltwaters. South of Nordaustlandet a number of sediment lenses (max. local thickness 40 m) extend southward from the Bråsvellbreen glacier (Fig. 4, profile B). An upper 0.6 m thick unit of brownish sandy mud grades into alive grey colored sediments of similar texture below. Scattered pebbles are present throughout (stns. 67, 69 and 71). A thin draping (<12m) of acoustically transparent sediment is also found east and southeast of Edgeøya. Another occurrence is the infilling of the highly dissected ridge north of Kvitøya.

2) The other sediment type is partly acoustically transparent; local internal reflectors and uneven topography can result in diffraction patterns in the seismic records (Fig. 4, profile C and D). Gravity cores recovered from these areas were only 10 to 20 cm long due to stiff and coarse nature of the bottom sediments. Large grab samples obtained 0.7 m sections of pebble-rich sandy mud (stns. 54, 116, 133, 134, 136 and 137). This sediment type is interpreted as tills. In the seismic section it occurs only on the bank in the southeastern part of the study area with additional small accumulations southeast of Kongsøya and northward eastnortheast of Kong Karls Land (Fig. 3).

Shallow structure and geology

The lack of unconsolidated sediment cover and general exposure of underlying bed rock gave only modest sub-bottom penetration to the sparker signal. Average penetration was in the range 50 to 100 msec, only rarely exceeding 120 msec. As a result, we cannot trace individual reflectors

over longer distances. This problem is compounded by steeply dipping strata often present in the profiles – slopes greater than 3° are not uncommon – as well as the wide spacing between profiles of this reconnaissance survey. However, a general impression of the geology of the area can be gained from a study of the available sparker profiles.

Most noticeable is the basic difference in the structure north and south of Kong Karls Land (Fig. 5). To the north the strata tend to tip towards the southeast, with slopes of 1–3°. A gentle syncline is crossed at 79°30'N 33°E and a steep anticline at 79°30'N 34°30'E, which complicate the regional pattern. The transition from the Paleozoic crystalline rocks of Kvitøya and its environs to younger sedimentary deposits in the south is not apparent in the sparker data. However, crystalline rocks were dredged around Kvitøya (stns. 131, 109 and 110), while sandstones were most abundant to the south (stns. 130, 86, 113 and 114).

The ENE–WSW trending Kong Karls Land structural high (Figs. 2 and 5) appears, at least in its eastern part (30°E–32°E), to be a broad synclinal feature of the same trend as the island chain with anticlines superimposed on its southern flank (Fig. 6). On Kongsøya and Svenskøya the generally flat-lying strata has weak undulations with N–S axial trends (Smith et al. 1976). The Kong Karls Land high also appears to mark the transition to a structurally more disturbed area to the south. The dips of strata, while generally less than 3°, can reach as much as 7°. In spite of the overall complexity there is a general impression of a regional southward dip of the strata south of about 78° 40'N. Most of the faults seen in the study area, are around 77°N 34°E, again suggesting a greater degree of structural complexity to the south.

Sandstones, chert, and silicified limestone, together with crystalline rocks, are the most predominant lithologies recovered in the dredge hauls. A subordinate amount of shale was recovered, although this lithology may be under-represented due to its lesser erosional resistance or over-represented because of the greater tendency to be removed by dredging. The relative abundance of the different lithologies has been investigated by Elverhøi & Lauritzen (1984).

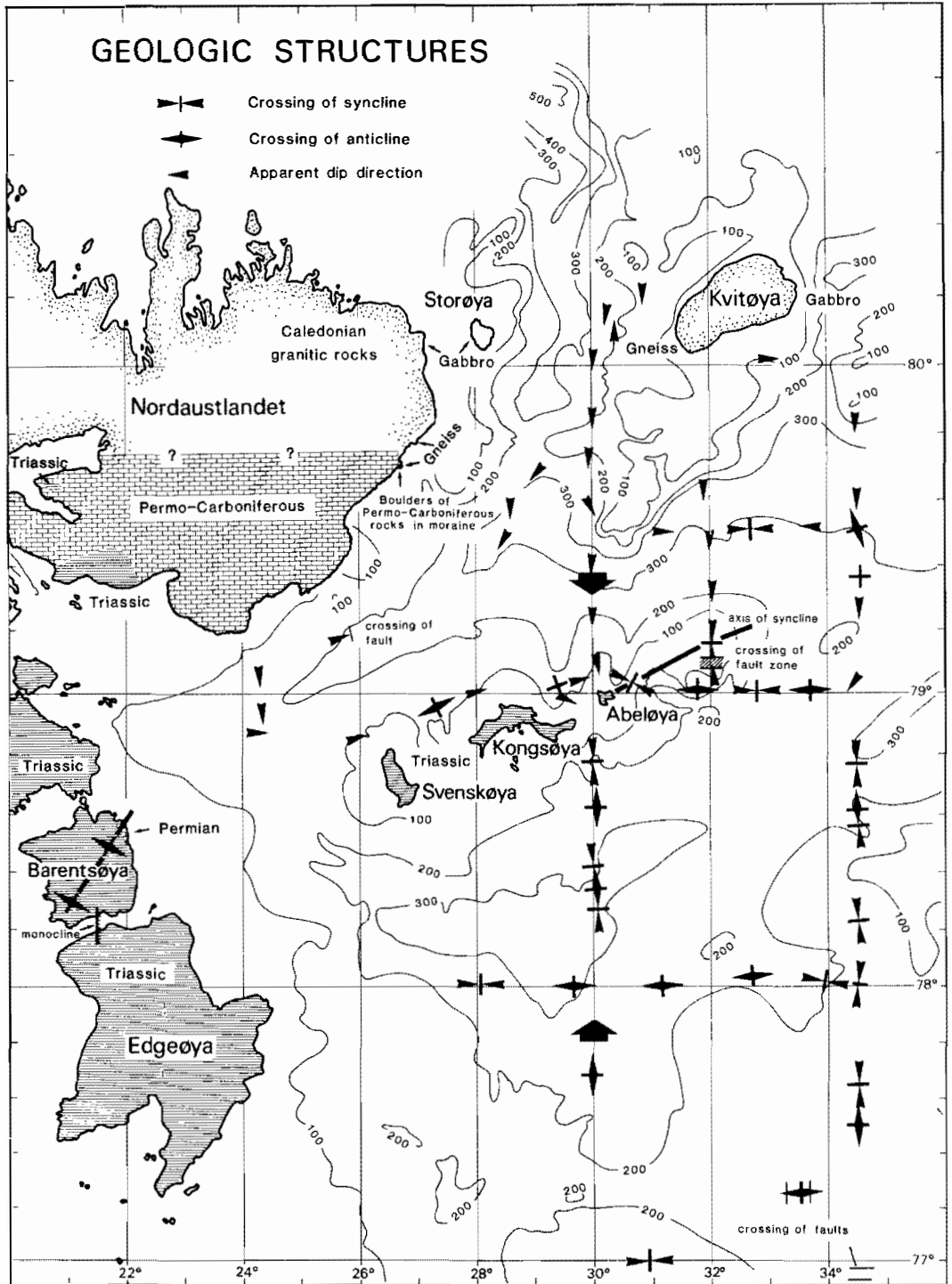


Fig 5. Shallow geological structure data from the seismic reflection (sparker) data shown in Fig. 1. The geology of Barentsøya and Edgeøya from Lock et al. (1978), of eastern Spitsbergen from Orvin (1940), of Nordaustlandet from Orvin (1940), Thomson (1953), Flood et al. (1969), and Hjelle (1978), of Storøya and Kvitøya from Hjelle (1978), and from Kong Karls Land as reported from Smith et al. (1976) and Worsley & Heintz (1977). Finds of Permo-Carboniferous boulders in moraine at Isispynnten, eastern Nordaustlandet, communicated by A. Hjelle (pers. comm.).

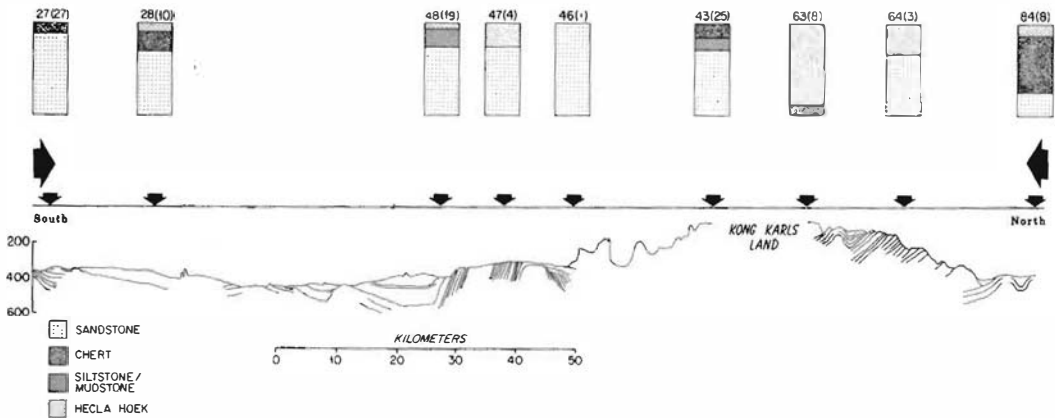


Fig. 6. Digitized shallow seismic record section along 30° East meridian from 78°N – $79^{\circ}30'\text{N}$ across Kong Karls Land structural high with lithology in dredge hauls (rock classification by Ø. Lauritzen, pers. comm.). Profile location indicated by heavy arrows in Fig. 5.

Sandstones appear in the deeper troughs east and west of Kvitøya and are dominant south to 76°N except in two areas where chert and silicified limestone fragments predominate:

1. a window extending from off-shore eastern Spitsbergen and southeastern Nordaustlandet eastwards to $79^{\circ}30'\text{N}$ 31°E ;
2. a window extending east from Edgeøya to about 30°E .

These windows crossed by the N-S profile along the 30°E meridian (Fig. 6) indicate that chert-bearing strata are probably present within the southwestern part of the ridge at $79^{\circ}30'\text{N}$ 31°E and exposed in the core of an anticline south of Kong Karls Land. In the latter case, the role of glacial transport on the distribution of rock fragments is uncertain.

A total of ten sonobuoys was shot in the nearshore area (water depths <50 meters) of the Triassic rocks on Kong Karls Land and east of the Permian outcrop on Barentsøya in an attempt to relate the seismic velocity of the sea bed to the geology of the islands. The values obtained are all in the range 2.0–2.5 km/s with an average of 2.3 km/s (Fig. 7). Some sections indicate a thin overlying layer of low velocity (1.7–1.8 km/s) surficial sediment. Triassic sandstone is the dominant lithology in the dredge hauls around Kong Karls Land and the measured seismic velocity is significantly lower than what is observed for sandstones of comparable age ($V_p=4.0$ km/s, porosity $<5\%$) on Edgeøya and in Agardhbukta

on eastern Spitsbergen by Elverhøi & Grønlie (1981) as porosities on Kong Karls Land seem to be higher (15%) (Edwards 1979). A sea floor velocity of 4.6 km/s observed northeast of Barentsøya, is comparable to velocities measured (4.8 km/s) in the chert-bearing Permian rocks outcropping on the adjacent beach on Barentsøya. Velocities of 3.4–3.8 km/s were observed in Triassic shales on Edgeøya by Elverhøi & Grønlie (1981).

Discussion

Sediment distribution and its relation to glacial history

The distribution of unconsolidated sediments in the northeastern Barents Sea has an important bearing on the controversy of a Late Weichselian ice cover in the Barents Sea. The most striking observation is the relatively small volume of unconsolidated sediment present (Fig. 3). With the exception of local accumulations of acoustically transparent sediments in the deep basins and locally around present glaciers, and moraine complexes on the bank area around $77^{\circ}30'\text{N}$ – 34°E , unconsolidated sediment is everywhere less than 15 m thick. There is insufficient seismic coverage to define the distribution of moraine complexes in relation to the overall morphology of the bank area at about $77^{\circ}30'\text{N}$ 34°E (Fig. 3). With their crests generally

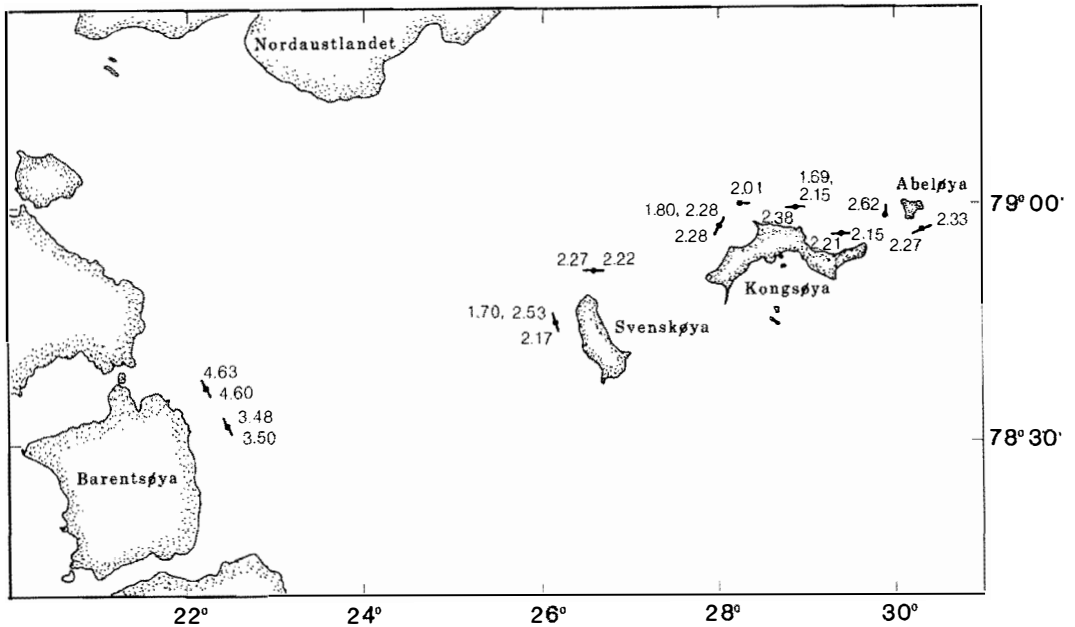


Fig. 7. Sound velocity at the sea floor in km/s measured with sonobuoys using 1 kJoule sparker as energy source.

few tens of meters shallower than the average level of the western part of the bank, the complexes may have been deposited in front of a glacier tongue extending from a local ice cap covering the shallower bank areas east of 35°E.

C^{14} dates available so far (Elverhøi & Solheim 1983) are in the range 600–8700 yrs. B.P. (stns. 106, 120, 137) from whole bivalves of *Asteris* species found at depths of 10–35 cm in the sediments and testifies to the proximity of the sites to a glacial environment well into the Holocene.

Two other important pieces of information are the general presence of firm pebbly mud (interpreted as till) in water depths less than 300 meters in the Barents Sea (Elverhøi & Solheim 1983) and 100 meters of Holocene relative uplift on Kong Karls Land decreasing northwards and westwards to 70–80 meters on Nordaustlandet, Edgeøya and Barentsøya (Salvigsen 1981, 1978; Boulton 1979). The major portion of the uplift being Early Holocene, together with the sedimentological evidence, strongly suggest the presence of a Late Weichselian ice sheet at least covering the shallower parts (present water depths less than 300 meters) with the outer parts of Bjørnøyrenna and Storfjordrenna being calving bays (Elverhøi & Solheim 1983).

If indeed a Late Weichselian ice sheet (before 8000 years B.P.) covered the shallower parts of the Barents Sea, average local sedimentation rates of 2.5–6.0 m/1000 yrs. are required to account for the 25–55 msec of sediment deposited in the basin north of Kong Karls Land (assuming, of course, that the entire section is Holocene in age). These rates seem high, particularly in light of the fact that modern non-glacial sediment cover is only about 1 m. However, a restricted depression surrounded by glacial landmasses on three sides during the Late Weichselian would trap sediments carried in suspension by glacier meltwater rivers with particularly high sediment yield during the deglaciation period. A somewhat analogue situation occurs at present, with prominent plumes of muddy water emerging in front of the Bråsvellsbreen ice stream south of Nordaustlandet. The suspended sediment sinks to the bottom within 10–20 km of the ice front, but a benthic boundary layer can be traced southward at least to Edgeøya (S. Pfirman pers. comm.).

Shallow structure and geology

The generally southward dipping sedimentary section south of Kvitøya and Nordaustlandet becomes folded and faulted along the Kong Karls Land high and in the area to the south. For lack

of more conclusive evidence, Smith et al. (1976) tentatively relate the folding of Jurassic marine Kongsøya Formation on Kong Karls Land to post-Barremian (mid-Cenozoic) movements corresponding to the west Spitsbergen Orogeny. Lava flows from at least six volcanic episodes spanning the Kimmeridgian to Barremian or later are present and syntectonic disturbances are manifested in the section. On Barentsøya and Edgeøya the Triassic rocks are only gently folded, although more intense local deformations appear to be related to post-Triassic probably latest Jurassic/earliest Cretaceous intrusions (Lock et al. 1978).

In Frans Josef Land the Triassic and Jurassic deposits form paratectonic folds and flexures (dips up to 10–15°) whose orientation is presently uncertain (Dibner 1970). The overlying lower Cretaceous strata are significantly less disturbed. Intrusion of sills (2–70 m thickness) and dykes (2–150 m thickness) took place during the lower/middle Jurassic, through the end of the lower Cretaceous (Cenomanian) with a major Aptian/Albian extrusive phase.

In view of the evidence cited above it seems tempting to relate a major part of the deformation seen in the shallow seismic records to the regional magmatic/tectonic activity culmination in the Early Cretaceous where additional disturbances induced by salt movements or block faulting at depth may have been a part.

The structural high formed by the crystalline rocks of northern Spitsbergen and Nordaustlandet, Storøya and Kvitøya forms the northern boundary of the sedimentary basins in the Barents Sea. South of this axis, strata of predominantly sandstones (?) dip south towards Kong Karls Land (Fig. 5). The presence of fossiliferous Permo-Carboniferous boulders (A. Hjelle pers. comm.) in a moraine at Isispynten, Nordaustlandet (79°41'N 26°40'E), abundant chert fragments (Permian ?) dredged from the ridge at 70°30'N 30°30'E, together with Middle Carboniferous (Moscovian) silicified limestone boulders and outcrop (?) observed on Victoriaøya (Klubov & Soloveva 1972), represent our main sources of information as to the age of the sedimentary succession of the northern-most part of the Barents Sea. On western central Nordaustlandet (Wahlenbergfjorden), the Middle Carboniferous

(Moscovian) to Triassic section rests on folded and eroded Hecla Hoek (pre-Devonian) dolomites, mudstones and quartzites with a distinct unconformity (Lauritzen 1981). It is therefore likely that the Middle Carboniferous sea transgressed a now east-west trending Spitsbergen–Kvitøya structural high and the Lower Carboniferous coal-bearing basin of Frans Josef Land farther east. Thus, the observed control on post upper-Paleozoic sedimentation exerted by the high ground on northern Spitsbergen can, to a first approximation, be extrapolated eastwards past the longitude of Kvitøya.

The Triassic to Early Cretaceous rocks on Kong Karls Land form the core of a syncline which die out towards west and east (Fig. 5). Preliminary work on palynomorphs from the dredged material in the study area indicates a southeastward younging of rocks outcropping (?) at the sea floor (T. Bjærke pers. comm.).

Smith et al. (1976) noted the remarkable similarity in the development of the rock succession on Kong Karls Land to that of Frans Josef Land. This is comparable with the observed trend of sea floor bedrock age provinces (Elverhøi & Lauritzen 1984).

The relative abundance of chert fragments found at stations along 78°N may indicate older (Permian ?) rocks exposed in a window or be a result of glacial transport. The latter is likely if the interpretation of Faleide & Gudlaugsson (1981) which place the F-reflector (top Permian at a depth of 1.6 seconds (two-way traveltime) at 78°N 28°E, is correct.

Regional variation of diagenetic effects strongly influences seismic velocities (Elverhøi & Grønlie 1981). This is clearly exemplified by velocities of 2.0–2.5 km/s observed in the nearshore area of the Triassic rocks of Kong Karls Land as compared to velocities of 3.0–4.0 km/s of the Tertiary basin of Spitsbergen (Elverhøi & Grønlie 1981) and around 4 km/s for the Mesozoic rocks on the Spitsbergen Bank (Edwards 1975). Stratigraphic inferences using seismic velocities therefore requires great caution when applied to the north-eastern Barents Sea.

Conclusion

Improved bathymetric data from the northern Barents Sea have delineated ridges (water depths 50–100 meters) extending northeast from Kong Karls Land and southwest from Kvitøya. The surrounding basins (water depth 350 meters) are linked through passage ways which are about 100 meters shallower.

Very small amounts of unconsolidated sediments are present in the northern Barents Sea. Only a thin blanket of modern and glacial marine (?) sediments covers the consolidated rocks except for local accumulations of:

1. acoustically transparent sediments in the deep basins and outside glacier streams, and
2. moraine complexes on the bank area around 77°30'N 34°E.

A Late-Weichselian ice sheet is believed to have at least partly covered the northern Barents Sea. During its waning stage a 50 m thick section of glacial marine sediments accumulated in the basin north of Kong Karls Land trapped by surrounding glaciers. Modern sedimentation has led to the accumulation of about 1 m of overlying sediment.

The western part of Kong Karls Land and its submarine prolongation lie along the axis of a syncline. The island chain marks transition between monotonously southward dipping strata to the north and more complex structures to the south.

It is likely that the situation seen on Nordaustlandet where Middle Carboniferous and younger sediments unconformably lap onto Heccla Hoek rocks (Lauritzen 1981) is generally applicable along the northern Spitsbergen–Kvitøya structural high.

Seismic velocities of 2.0–2.5 km/s in the near-shore area around Kong Karls Land are much lower than observed for rocks even in the Tertiary basin of Spitsbergen and may be related to higher porosities.

Acknowledgement

We gratefully acknowledge the cheerful cooperation of Captain G. Jakobsen, officers, and the crew aboard M/V NORVARG. Karin Andreassen, Stephanie Pfirmann, Odd Lind-Hansen, Bernt Egeland, Finn Johansen, Øyvind Lønne, Reinert Seland and Arne Vethe

provided able assistance in the field. The joint survey was part of the Norwegian Polar Research Institute's Expedition 1980 and supported by the Norwegian Petroleum Directorate. Participation of the Woods Hole Oceanographic Institution was funded by ONR Grant No. N00014-81-009.

References

- Boulton, G.S. 1979: Glacial history of the Spitsbergen archipelago and the problem of a Barents Shelf ice sheet. *Boreas* 8: 31–57.
- Dibner, V.D. 1957: The geological structure of Frans Josef Land. *Trudy nauchno issled. Inst. Geol. Arkt.* 114: 65–76 (translated from Russian).
- Dibner, V.D. 1961: Stratigraphy of the Upper Triassic and Jurassic rocks of the Barents – Kara shelf and Taimyr mountains. *Dokl. Akad. Nauk. SSSR. Geol.* 144: 1113–14 (translated from Russian).
- Dibner, V.D. 1970: Islands of the Barents Sea. Franz Josef Land and Victoria Island. In: B.V. Tkachenko & B.Ch. Egiazarov (ed) *Geology of the USSR, vol. XXVI. Islands of the Soviet Arctic. Ch. IV*: 60–108 (translated from Russian).
- Dibner, V.D. 1978: Morphostructure of the shelf of the Barents Sea. *NIIGA Trudy*, Leningrad, 221 pp.
- Dibner, V.D., Basov, V.A., Gerke, A.A., Solov'yeva M.F., Sisopatrova, G.P. & Shulgina N.I. 1970: Age of the pre-Quaternary deposits on the bottom of the Barents Sea. *Oceanology* 10: 520–529.
- Edwards, M.B. 1979: Sandstone in Lower Cretaceous Helvetiafjellet Formation, Svalbard: bearing on the reservoir potential of the Barents Shelf. *Am. Ass. of Petrol Geol. Bull.* 63: 2193–2203.
- Edwards, M.B. 1979: Sandstone in Lower Cretaceous Helvetiabank, NW Barents Shelf. *Norges Geol. Unders.* 316: 205–217.
- Eggvin, J. 1963: *Bathymetric chart of the Norwegian Sea and adjacent areas*. Fiskeridirektoratets Havforskningsinstitutt, Bergen.
- Elverhøy, A. & Bomstad, K. 1980. *Preliminary results on Late Weichselian glacial and glacial marine sedimentation in the western, central Barents Sea*. Norsk Polarinstitutt, unpublished report, 29 pp.
- Elverhøy, A. & Grønlie, G. 1981: Diagenetic and Sedimentologic Explanation for High Seismic Velocity and Low Porosity in Mesozoic-Tertiary Sediments, Svalbard Region. *Am. Ass. of Petrol Geol. Bull.* 65: 145–153.
- Elverhøy, A. & Lauritzen, Ø. 1984: Bedrock geology of the northern Barents Sea (west of 35°E) as inferred from the overlying Quaternary deposits. *Nor. Polarinst. Skr.* 180: 5–16 (this volume).
- Elverhøy, A. & Solheim, A. 1983: The Barents Sea ice sheet – a sedimentological discussion. *Polar Research 1 (1) n.s.*: 23–42.
- Falck, J.I. & Gudlaugson, S., 1981: *Geology of the western Barents Sea: A regional study based on marine geophysical data*. Thesis. Univ. of Oslo, 160 pp.
- Flood, B., Gee, D.G., Hjelle, A., Siggerud, T. & Winsnes, T.S. 1969: The geology of Nordaustlandet, northern and central parts. *Norsk Polarinst. Skr.* 146: 1–141.
- Grosswald, M.G. 1980: Late Weichselian Ice Sheet of Northern Eurasia. *Quaternary Research* 13: 1–32.
- Hjelle, A. 1978: An Outline of the Pre-Carboniferous Geology of Nordaustlandet. *Polarforschung* 48: 62–77.

- Horn, G. 1932: Some geological results of the Norwegian Expedition to Frans Josef Land 1930. *Norsk Geol. Tidsskr.* XI: 482-489.
- Klenova, M.V. 1960: *Geologija Barenova morja (Geology of the Barents Sea)* Izdatel'stvo Akademii nauk SSSR. (Translated from Russian) 355 pp.
- Klubov, B.A. 1965. Concerning the occurrence of Permian rocks on Barentsøya (Spitsbergen archipelago). *Dokl. Akad. Nauk SSR 162(3)*: 629-631 (translated from Russian).
- Klubov, B.A. 1970: Triassic and Jurassic deposits of Wilhelmøya. In: V.N. Sokolov (ed.) *Geology of Spitsbergen*. National Lending Library of Science and Technology. Boston Spa., Yorkshire, England. 2:182-192.
- Klubov, B.A. & Soloveva, N.N. 1972: On the characterization of the Carboniferous deposits of Victoria Island (translated from Russian). *Doklady Akademii Nauk SSSR, from 203*. No. 1, 4 pp.
- Kristoffersen, Y. & Elverhøi, A. 1980: Maringeologiske og geofysiske undersøkelser. Svalbard ekspedisjonen 1980. *Norsk Polarinstittutt Rapport Nr. 4/80*.
- Lauritzen, Ø. 1981: The Carboniferous and Permian stratigraphy of the Wahlenbergfjorden area. Nordaustlandet, Svalbard. *Norsk Polarinstittutt Skr. Nr. 176*: 23-44.
- Lock, B.E., Pickton, C.A.G., Smith, D.G., Batten, D.J. & Harland, W.B. 1978: The Geology of Edgeøya and Barentsøya, Svalbard. *Norsk Polarinst. Skr. Nr. 168*: 1-63. Oslo.
- Matisov, G.C. 1977. Bottom geomorphology and the problem of Pleistocene glaciation of the Barents Sea shelf (in Russian). *Geomorfologija 2*: 91-98. Moscow.
- Matisov, G.C. 1980: Geomorphological indications of the impact of the Scandinavian, Novaja Zemlja, and the Spitsbergen ice cover upon the surface of the bottom of the Barents Sea. *●keanologija 4*: 669-680 (translated from Russian).
- Nansen, F. 1904: The bathymetrical features of the North Polar Seas. *The Norwegian North Polar Exhibition 1893-1896, Scientific Results IV*.
- Orvin, A.K. 1940: Outline of the geological history of Spitsbergen. *Skr. om Svalbard og Ishavet Nr. 78*: 1-57.
- Pirozhnikov, L.P. 1958: Upper Jurassic of the Frans Josef Land Archipelago. *Doklady Akademii Nauk SSSR 122*: 462-464.
- Salvigsen, O. 1978: Holocene emergence and finds of pumice, whalebones, and driftwood at Svartknausflya, Nordaustlandet. *Norsk Polarinstittutt Årbok 1977*: 217-228.
- Salvigsen, O. 1981: Radiocarbon dated raised beaches in Kong Karls Land, Svalbard, and their consequences for the glacial history of the Barents Sea area. *Geogr. Ann. 63*: 283-291.
- Sandford, K.S. 1926: The geology of Nord-East Land (Spitsbergen). *Quat. Journ. Geol. Soc. Land. 82*: 615-665.
- Schytt, V., Hoppe G., Blake Jr. W. & Grosswald, M.G. 1967: The extent of the Würm glaciation in the European Arctic. *Naturgeografiska Institutionen vid Stockholms Universitet Meddelanden Nr. A20*: 207-216.
- Smith D.G., Harland, W.B. & Hughes, N.F. 1975: Geology of Hopen, Svalbard. *Geol. Mag. 112*: 1-112.
- Smith, D.G., Harland, W.B., Hughes, N.F. & Pickton, C.A.G. 1976: The geology of Kong Karls Land, Svalbard. *Geol. Mag. 113*: 193-304.
- Thompson, H.R. 1953: Geology and Geomorphology in Southern Nordaustlandet, Spitsbergen. *Proc. Geologists' Assoc. 64(4)*: 293-311.
- Worsley, D. 1971: The Wilhelmøya Formation - a new lithostratigraphical unit from the Mesozoic of eastern Svalbard. *Norsk Polarinstittutt Årbok 1971*: 7-16. Oslo 1973.
- Worsley, D. & Heintz, N. 1977: The stratigraphical significance of a marine vertebrate fauna of Ractian age, Kong Karls Land. *Norsk Polarinstittutt Årbok 1976*: 69-82. Oslo 1977.

Compilation of seismic velocity measurements along the margins of the Norwegian – Greenland Sea

Myhre, Annik M. 1984: Compilation of seismic velocity measurements along the margins of the Norwegian-Greenland Sea. *Nor. Polarinst. Skr. 180*: 41–61. ISBN 82-90307-26-6.

Refraction and wide-angle reflection measurements collected during the last 20 years on the margins of the Norwegian-Greenland Sea have been analysed in terms of regional variations in the seismic velocities both laterally and vertically. As a first-order approximation a linear increase of velocity with depth is representative for the main part of the sedimentary section. The data from the uppermost sediments are more scattered but indicate a .5–.8 km thick zone in which the velocity increases non-linearly with depth. The velocity distribution clearly reflects the main geological provinces along the margin. Of particular importance is the observation that the western Barents Sea margin can be divided in two separate regions based on the velocity-depth functions. South of Bjørnøya the Cenozoic sedimentary wedge exhibits an unusually low velocity gradient, $.3s^{-1}$. Velocity gradients in this range are generally observed in the world's major deltas. North of Bjørnøya the velocity gradient attains a value of $.7s^{-1}$. This study also indicates that variations in refractor velocities from the same interface may be caused by former overburden. The limited number of measurements on the East-Greenland margin and the Jan Mayen Ridge suggests a similar velocity stratification as observed on the conjugate parts of the Norwegian margin.

Annik M. Myhre, Department of Geology, University of Oslo, Blindern, Oslo 3, Norway. Received April 1983 (revised January 1984).

Introduction

During the last decade a large number of seismic refraction and wide-angle reflection profiles have been recorded in the Norwegian-Greenland Sea and adjacent areas. Most of these profiles have been obtained as a part of exploratory regional studies.

The objective of this study is to compile and analyse the existing data in order to establish regionally characteristic features in the velocity distribution, both laterally and vertically. The profiles on oceanic crust have earlier been described by Myhre & Eldholm (1981). This work is therefore restricted to profiles on the continental margins and the Jan Mayen micro-continent. The continent-ocean boundaries of Talwani & Eldholm (1977) have been applied.

Data and data presentation

This study is based on a compilation of all published refraction and wide-angle reflection profiles including a small number of still unpublished data. We have not reanalysed any of the profiles but relied solely on the published information. The profiles have been edited and

stored on a computer file which allows simple retrieval and display of the data. A total of approximately 600 profiles are presently available. The various data sources are listed in Table 1; Fig. 1 shows the distribution of the profiles. It is evident that the coverage of the eastern margin is quite extensive whereas only a few measurements exist off Greenland.

Except for the very few profiles measured before 1970, the majority are recorded by the sonobuoy method as unreversed profiles (Le Pichon et al. 1968). The data have been almost exclusively reduced by the slope-intercept method (Ewing et al. 1939) resulting in a seismic section consisting of layers with constant velocities. Many of the later surveys, however, have also made use of the wide-angle hyperbolas. The resulting interval velocities have been integrated in the final solutions used here.

The velocity distributions are illustrated by seismic structure sections, histograms, velocity-depth curves and isopach maps. The isopach maps show the thickness in kilometers between the sea floor and a given refractor.

The seismic structure is shown here in dip sections on the margin, and profiles on either side have been projected onto the sections. The

Table 1. *List of data sources used in this study*

<i>Source</i>		<i>Area:</i>
Ewing & Ewing	1959	Regional
Houtz, Ewing & Le Pichon	1968	SW Barents Sea and Lofoten Basin
Eldholm & Nysæther	1969	Lofoten-Vesterålen margin
Eldholm	1970	Møre and Nordland margin
Eldholm & Ewing	1971	SW Barents Sea
Hinz & Moe	1971	Norway Basin
Sundvor	1971	SW Barents Sea
Sundvor & Sellevoll	1971	Lofoten margin
Talwani & Eldholm	1972	Norwegian margin (60-70° N)
Eldholm & Windisch	1974	Regional
Renard & Malod	1974	Barents Sea
Sundvor	1974	S Barents Sea
Sundvor, Sellevoll & Haugland	1974	Møre and Nordland margins
Sundvor, Eldholm, Haugland, Sellevoll & Bruland	1975	Norwegian margin and Barents Sea
Sundvor & Eldholm	1976	NW Barents Sea
Eldholm & Talwani	1977	Barents Sea
Houtz & Windisch	1977	W Barents Sea
Sundvor, Eldholm, Gidskehaug & Myhre	1977	Svalbard margin
Hinz & Schlüter	1978	Barents Sea
Garde	1978	Jan Mayen Ridge
Eldholm, Sundvor & Myhre	1979	Lofoten margin
Sundvor, Gidskehaug, Myhre & Eldholm	1979	Jan Mayen Ridge
Lamont-Doherty Geol. Observatory	unpubl.	Regional

correlation between single profiles is based on approximate similar velocities and depths in adjacent profiles. The scatter in velocity values makes the correlation difficult in many cases. However, a systematic analysis using profiles both along and to the side of the section may improve the reliability of the correlation. One may obtain estimates of the variation of the refractor velocities by computing average velocities and standard deviations for correlated refractors. If there is a continuous velocity increase with depth the slope-intercept solution normally yields a multi-layer model with small velocity contrasts which might cause difficulties in the refractor correlation.

A velocity interval of .2 km/s have been used in the histograms. This interval appears to distinguish between refractors of regional character. We caution, however, that the number of measurements tends to decrease with depth, a fact which should be kept in mind when evaluating the absolute numbers of velocities.

Two kinds of velocity-depth curves, standard and relative, have been used. The standard curve

shows depth from the sea floor plotted against the velocity. Data from all profiles in a given region are plotted and a representative velocity-depth curve is computed by fitting a higher order polynomial by the least square method to the data set. In many areas there is a relatively rapid increase in velocity with depth and a large apparent scatter between the single measurements in the upper .5 km of sediments. On the other hand, the deeper part of the section normally exhibits a much more systematic velocity-depth relationship. To remove the effect of the uppermost sediments we have constructed a velocity-depth curve for each profile assuming a linear velocity increase between the individual refractors. Then the upper .5 km has been removed and all the velocity-depth curves shifted to the origin. In this relative velocity-depth diagram the maximum and minimum velocity gradients have been marked by straight lines. This kind of presentation often reflects regional differences quite well.

The term «low-velocity sediments» has been used by some authors to describe the upper

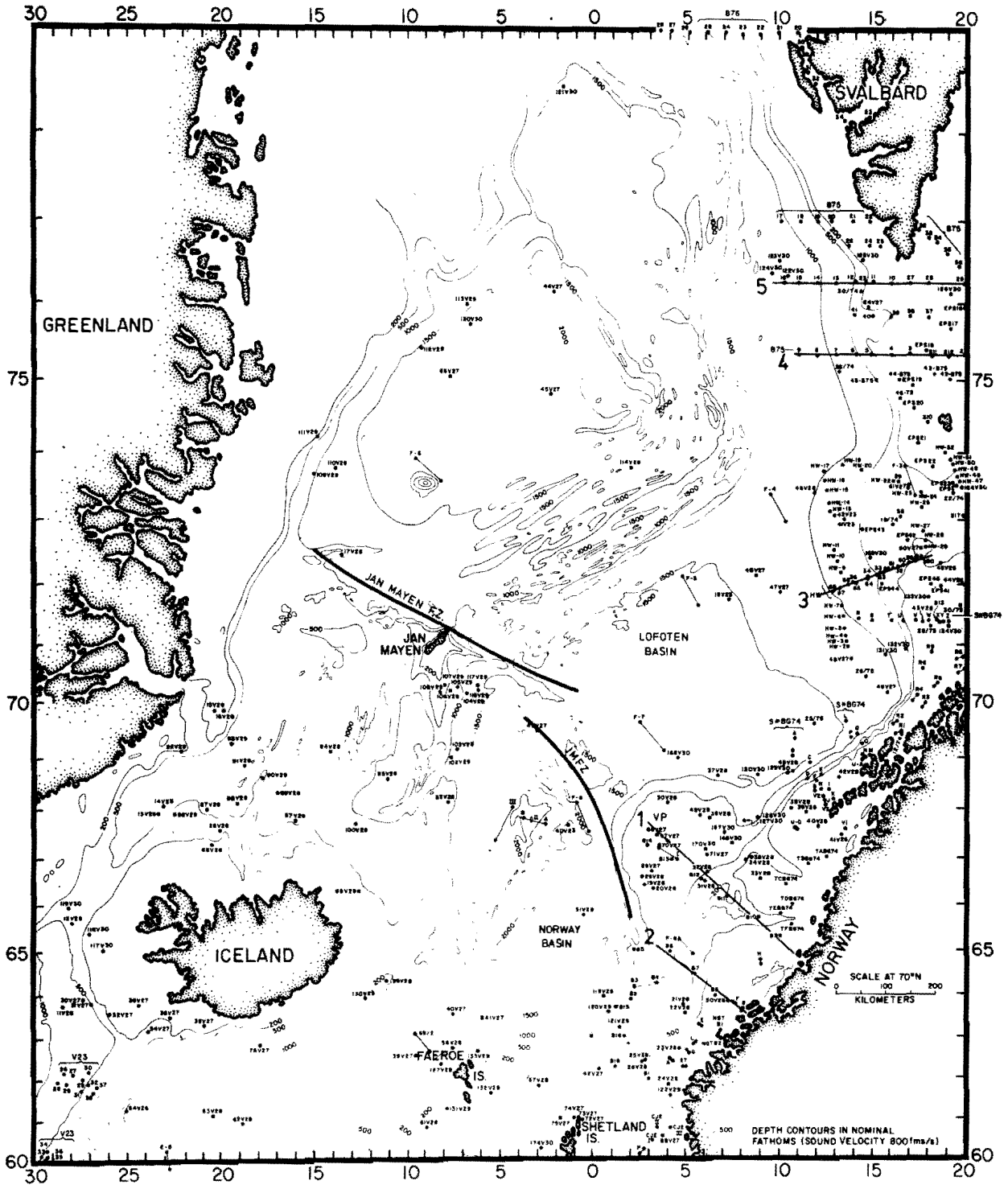


Fig. 1. Locations of profiles and seismic structure sections (1-5). Base map from Talwani & Eldholm (1977). Vøring Plateau denoted VP.

sedimentary sequence of velocity less than 2.5 km/sec representing unconsolidated and semi-consolidated sediments of Cenozoic age (Talwani & Eldholm 1972). Here, a similar definition is used but without inferences with respect to the age of the sediments.

In the following discussion the margins are divided into regional geological provinces. The division is guided both by the seismic velocities and available geologic information. In the Barents Sea the 19° E longitude marks the eastern limit for the study area between Norway and Bjørnøya. Farther north the eastern boundary follows a straight line from Bjørnøya to the southern tip of Spitsbergen (Sørkapp). 80° N demarcates the study area to the north while the shallow transverse Greenland–Iceland–Faeroe Ridge forms the southern limit.

The Norwegian margin 62–70° N

The margin off Norway between 62–70° N is divided into:

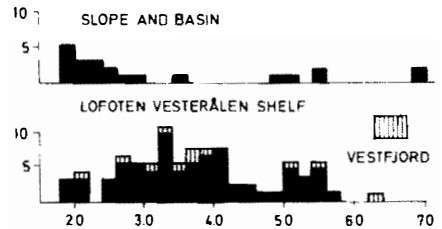
1. Lofoten–Vesterålen 67–70° N
2. Nordland–Vøring Plateau 64–68° N
3. Møre 62–65° N

There are no distinct geological boundaries between these regions but differences in sediment thickness, velocity distribution and the distribution of ridges and basins have made this division natural. The Lofoten–Vesterålen margin is quite narrow with a very steep continental slope. It is also different from the adjacent shelves as there is little or no low-velocity sediments. The two southern areas lie on either side of the landward continuation of the Jan Mayen Fracture Zone. The Nordland margin includes the Vøring Plateau at a depth of about 1500 m, whereas the slope off Møre plunges gently into the Norway Basin (Fig. 1). Rønnevik et al. (1975) have shown that the shelf off Møre is a natural extension of the North Sea Basin. The southern boundary, at 62° N, has been chosen because of limited refraction data south of this latitude.

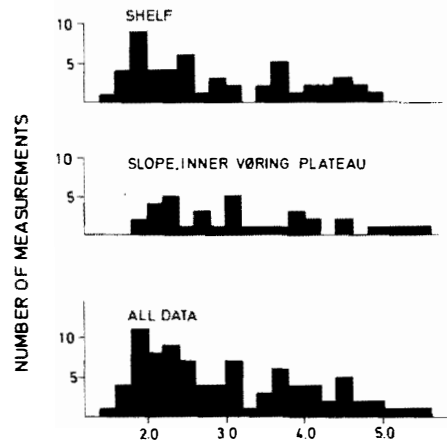
Lofoten–Vesterålen

The most significant observation is the absence of low-velocity sediments at the sea floor on the main shelf. However, a narrow wedge of low-

A LOFOTEN-VESTERÅLEN



B NORDLAND-VØRING PLATEAU



C MØRE

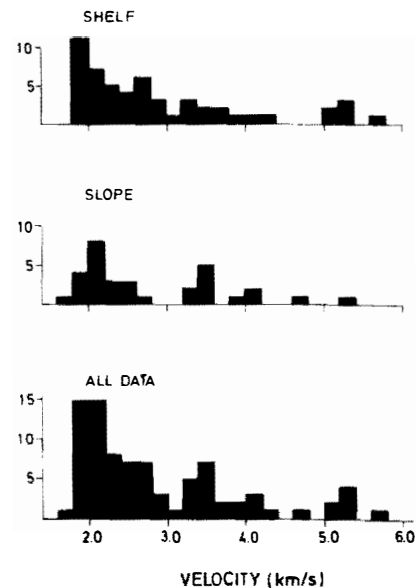


Fig. 2. Histograms of seismic refraction velocities 62–70° N.

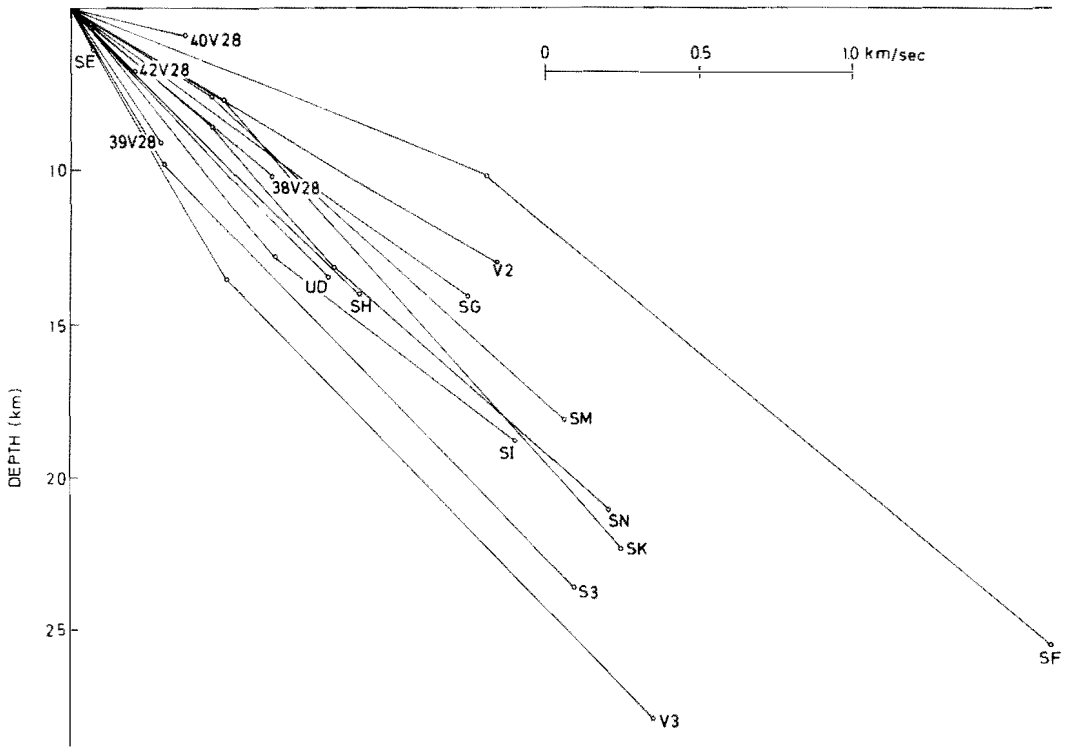


Fig. 3. Relative velocity-depth diagram for individual profiles on the Lofoten-Vesterålen margin. (Eldholm et al. 1979).

velocity sediments exists on the very outermost part of the shelf. The histograms (Fig. 2A) show quite clearly the difference between the shelf and slope. Regional refractors with average velocities of 2.8, 3.3, and 5.3 km/s have been identified (Table 2). The 5.3 km/s refractor is defined as acoustic basement and interpreted to represent crystalline rocks (Sundvor 1971; Eldholm et al. 1979).

The vertical velocity distribution is illustrated in Fig. 3. Although the velocity gradient varies somewhat between profiles, the individual profiles generally exhibit a first order velocity increase with depth. A velocity gradient of 1.0 s^{-1} appears representative for the area.

The 3.9 km/s refractor velocity has also been plotted as a function of overburden (Fig. 4) revealing a probable linear increase with depth of burial. The individual refractor values have been split into two groups (I and II), which yield similar velocity gradients. Line II represents velocities on the Røst High (RH in Fig. 5). By shifting line II down about 1.5 km, it forms a natural continuation of line I. If the sedimenta-

tion and subsidence had been similar over most of the shelf one would expect similar velocity-depth curves. Thus, the deviation of the line II may be explained if Røst High has been buried by approximately an additional 1.5 km of the sediments which later on have been eroded without changing the elastic rock parameters which were established by the former overburden.

There is no evidence that this part of the margin is structurally separated from the margin

Table 2. Average velocities, standard deviations and number of measurements (N), 62–70° N. Velocities in km/s.

A: Lofoten-Vesterålen shelf						
Ave. vel		2.8	3.3	3.9	5.3	
St. dev.		.11	.15	.17	.23	
N		10	17	21	18	
B: Nordland margin						
Ave. vel.	1.9	2.2	2.7	3.4	4.2	5.2
St. dev.	.09	.12	.16	.28	.27	.28
N	16	19	16	20	16	6
C: Møre margin						
Ave. vel.	1.9	2.2	2.6	3.4	4.1	5.2
St. dev.	.09	.10	.15	.17	.28	.20
N	17	16	17	15	7	7

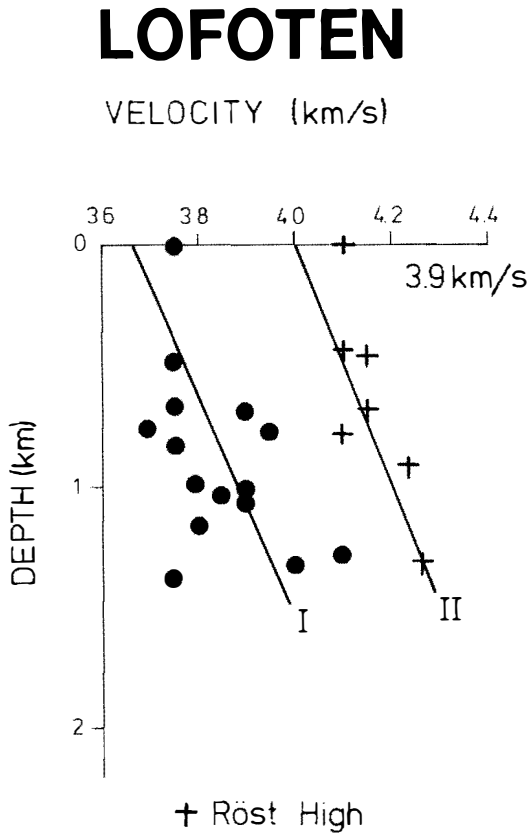


Fig. 4. Velocity increase as a function of overburden for the 3.9 km/s regional refractor on the Lofoten-Vesterålen shelf.

on either side. Rather, it appears that the high-velocity sequence dips below gradually thickening low-velocity sediments both to the north and south (Fig. 5). The velocities in Vestfjorden are similar to those on the Lofoten shelf. Vestfjorden forms a southward plunging basin opening up onto the Nordland margin (Jørgensen & Navrestad 1979).

The two regional sedimentary refractors, 3.3 and 3.9 km/s, are observed in the entire Lofoten-Vesterålen region. In general, these refractors follow the basement topography, thus forming the characteristic system of subsurface ridges and small basins off Lofoten. This structural pattern (Fig. 5) is also reflected in the seismic reflection data. It also appears that the basins and ridges at this margin are fault controlled, forming a system of horsts and grabens (Eldholm et al. 1979; Jørgensen & Navrestad 1979).

At about 68.8° N, 13.5° E, Lien (1976) reported a local basement outcrop at the sea floor. This outcrop appears to be a continuation of the Røst High basement ridge. A sonobuoy, 26/77, recorded in the vicinity of the outcrop reveals 1.1 km of sediments with velocity 4.5 km/s above an acoustic basement with velocity 5.5 km/s. At a depth of 1.1 km below basement a 6.3 km/s refractor was recorded. This is a velocity which could reflect intrabasement ultrabasic rocks. Gravity data indicate that the ridge at the outer shelf may be a belt of rocks similar to the high density intrabasement belt underlying the Lofoten-Vesterålen Islands. These belts may for long periods have subsided relatively less than the surrounding areas (Talwani & Eldholm 1972).

Nordland-Vøring Plateau

The average refractor velocities in Table 2 differ little from values calculated separately on the shelf and the slope, including the inner Vøring Plateau. The predominance of velocities in the low-velocity interval (Fig. 2B) is to a large part caused by poor penetration in many profiles, particularly those recorded during the early surveys. Fig. 6 shows a seismic structure section across the margin. The simplified relative velocity-depth diagram (Fig. 7) reveals that this region may be divided into a northern and southern province. The average velocity gradient is lower to the south, which we believe reflects a gradual increase in layer thickness towards the south.

The thickness of the low-velocity layer is variable but increases towards the outer shelf where an average thickness of 1.2 km is reached. A similar thickness exists on the slope and the inner Vøring Plateau. The sequence is composed of refractors of average velocities 1.9 and 2.2 km/s. On the northern shelf the 2.2 km/s sequence outcrops at the sea floor dipping below the 1.9 km/s layer towards the south and west. The 2.7 km/s refractor is not observed on the shelf in the north but forms a regional refractor elsewhere. This is probably related to differences in elevation during deposition. The 3.4 and 4.2 km/s refractors are determined from a large number of measurements. However, the high standard deviations (Table 2B) may suggest that this model is too simplistic. Possibly, each of these two refractors should be treated as originating from two

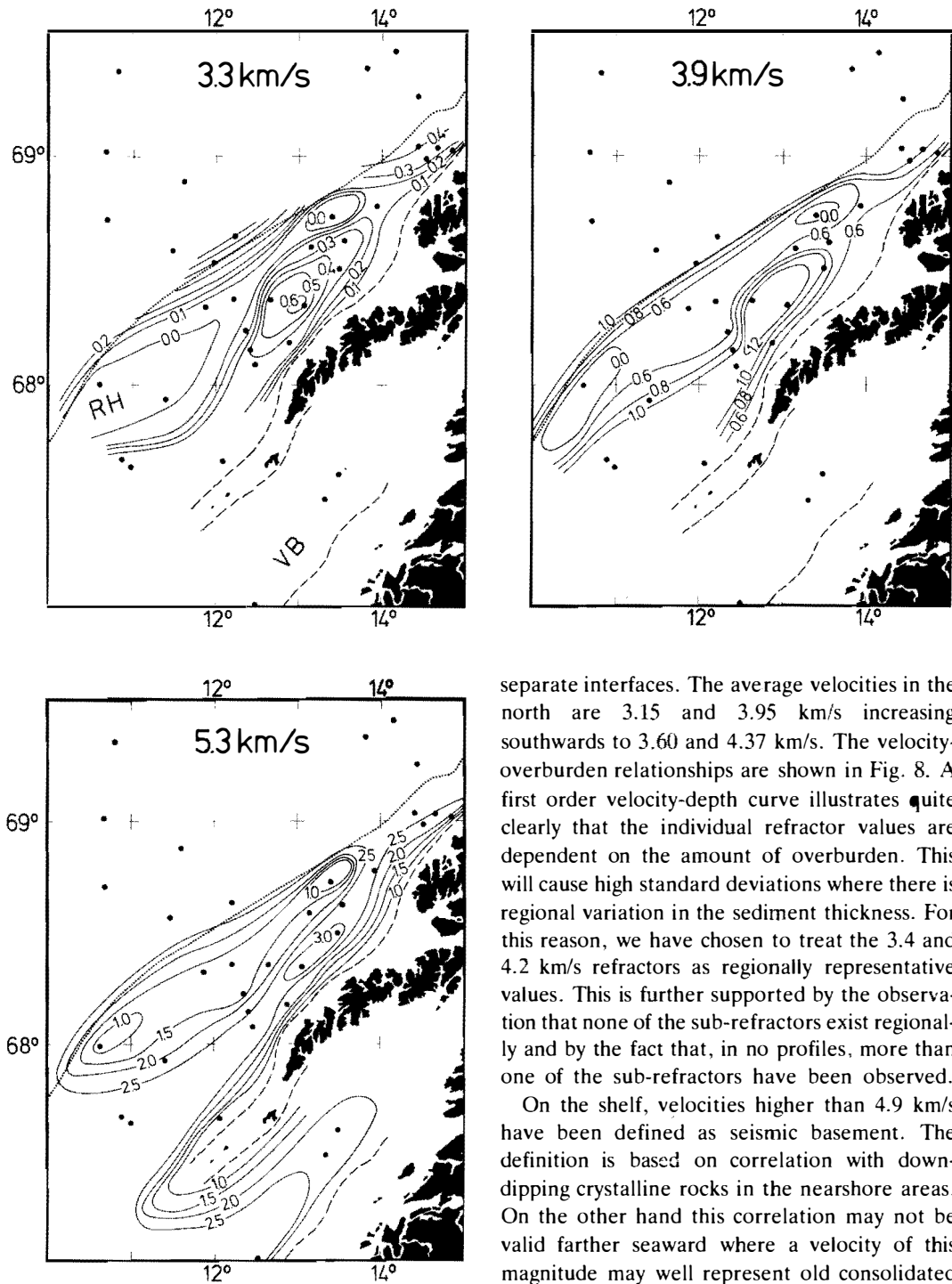


Fig. 5. Isopach maps showing thickness between the sea floor and regional refractors off Lofoten-Vesterålen. Røst High is denoted RH and the Vestfjorden Basin VB.

separate interfaces. The average velocities in the north are 3.15 and 3.95 km/s increasing southwards to 3.60 and 4.37 km/s. The velocity-overburden relationships are shown in Fig. 8. A first order velocity-depth curve illustrates quite clearly that the individual refractor values are dependent on the amount of overburden. This will cause high standard deviations where there is regional variation in the sediment thickness. For this reason, we have chosen to treat the 3.4 and 4.2 km/s refractors as regionally representative values. This is further supported by the observation that none of the sub-refractors exist regionally and by the fact that, in no profiles, more than one of the sub-refractors have been observed.

On the shelf, velocities higher than 4.9 km/s have been defined as seismic basement. The definition is based on correlation with down-dipping crystalline rocks in the nearshore areas. On the other hand this correlation may not be valid farther seaward where a velocity of this magnitude may well represent old consolidated sediments of various kinds. This may be the case, for example, at the inner Vøring Plateau, where there are large differences between the deepest high velocity refractor and magnetic depth estimates (Åm 1970; Talwani & Eldholm 1972).

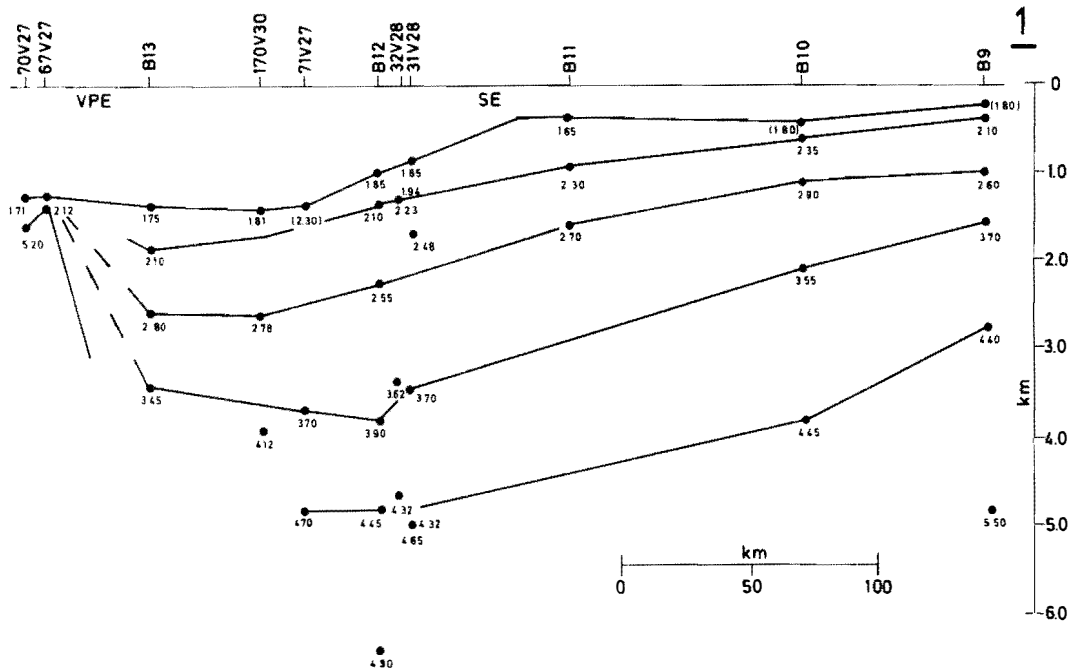


Fig. 6. Seismic structure section across the Nordland margin. VPE refer to Vøring Plateau Escarpment. Location in Fig. 1.

A system of ridges and basins has been mapped on the Nordland shelf (Rønnevik & Navrestad 1977). Unfortunately, most refraction profiles were recorded prior to the mapping of these features and the distribution of our data does not allow a discussion of these features in terms of regional refractors.

Møre

The data are irregularly distributed within this area particularly in the transitional region between the Møre and the Nordland margins (Fig. 1). There is an apparent velocity difference between the shelf and slope (Fig. 2C). No velocities exist in the intervals 2.8–3.2, 3.6–3.8 4.2–4.6 and 4.8–5.2 km/s on the slope, whereas velocities between 4.4–5.0 km/s are absent on the shelf. On the other hand, the average velocities and standard deviations calculated for the correlated refractors are similar on the shelf and slope. (Table 2C and Fig. 9).

Most profiles show a linear velocity-depth relationship (Fig. 7). The velocity gradient is higher on the shelf than on the slope, reflecting an increase in layer thickness. However, the significant differences in the velocity gradients

shown in Fig. 7 indicate a relatively large variation in the refractor velocities as a function of depth. It has not been possible to observe a relationship between the regional 3.1 and 4.1 km/s refractors and the overburden.

Also in this region there are considerable discrepancies between the assumed seismic basement and magnetic depth estimates (Åm 1970).

Age correlation

The North Sea sediment basin may be considered as continuing northwards along the present margins off Norway and Greenland. Tertiary sediments in the North Sea normally exhibit velocities of less than 2.25 km/s (Hornibroek 1967; Wyrobek 1969). From an analysis of both seismic reflection and refraction data Talwani & Eldholm (1972) suggested that velocities below 2.5 km/s represent Cenozoic sediments. It is quite possible, however, that their base Tertiary reflector originates at the top of or within the Paleocene sequence. The North Sea Mesozoic velocities are generally lower than 4.0 km/s (Wyrobek 1969) a relationship which may be extended northwards along the margin. An analogy with the North Sea leads us tentatively to suggest that the 2.6–2.7

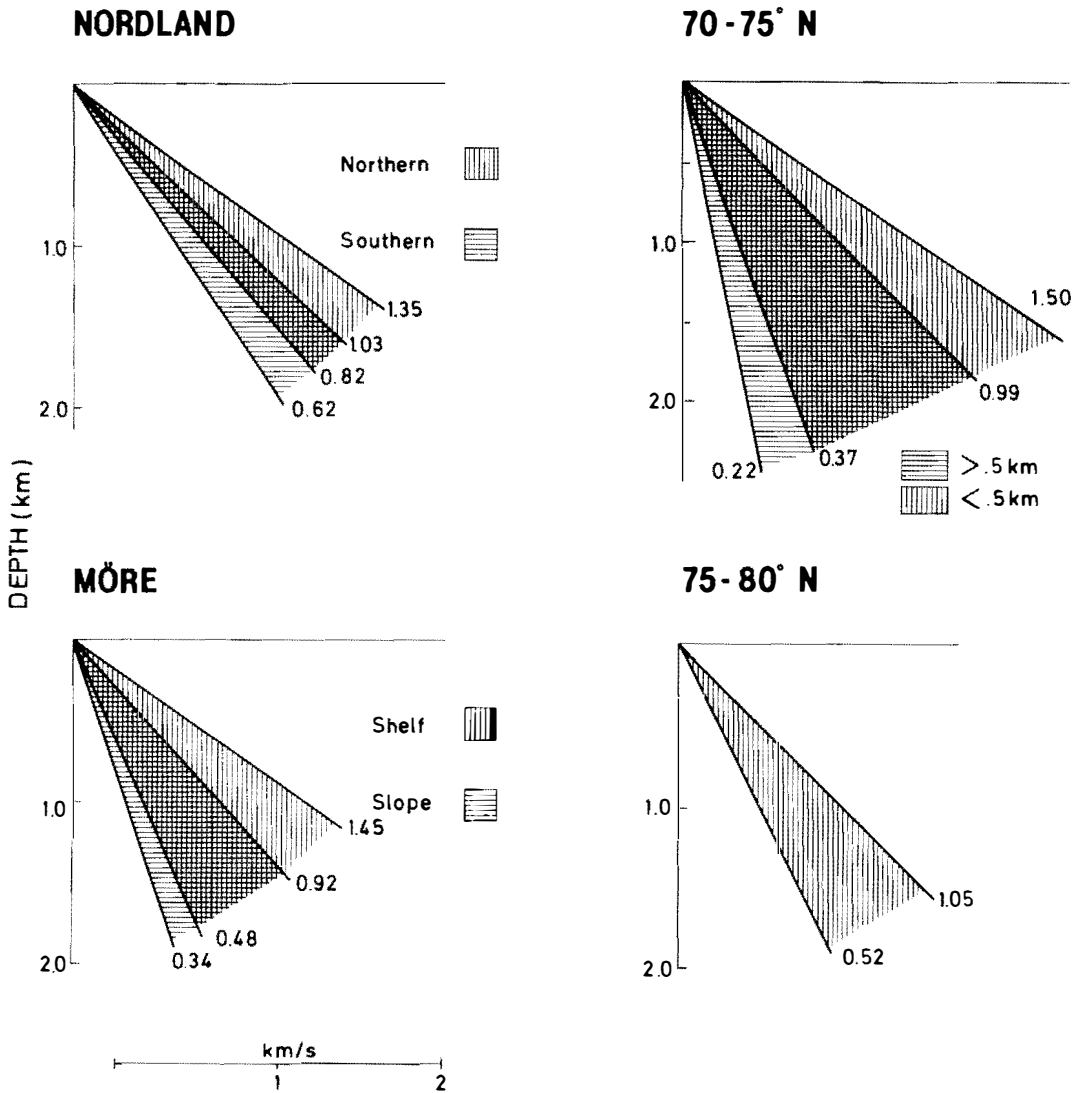


Fig. 7. Simplified relative velocity-depth diagrams for various areas of the margin. Maximum and minimum velocity gradients are indicated.

km/s refraction off Nordland and Møre are associated with Cretaceous sediments. The velocities higher than 4.0 km/s might represent Paleozoic as well as Mesozoic deposits. The difference in depth to magnetic and seismic basement is most likely attributed to high velocities in non-magnetic Paleozoic sediments. For example, the Devonian sandstones exposed onshore (Holtedahl 1960) may be found locally along the adjacent margin. The margin off Lofoten-Vesterålen differs from the other regions by the absence of low-velocity sediments and a small total sediment thickness. This area, which

has been above sea level in the Upper Cretaceous and Tertiary, appears to have been relatively elevated for long periods. Thus, the small layer thicknesses may reflect different depositional and erosional regimes also prior to the Cenozoic.

The margin from 70–80° N

The seismic velocities in the Barents Sea have been studied as a part of regional investigations by Eldholm & Ewing (1971), Sundvor (1974), Renard & Malod (1974), Sundvor et al. (1975), Sundvor & Elholm (1976), Eldholm & Talwani

NORDLAND

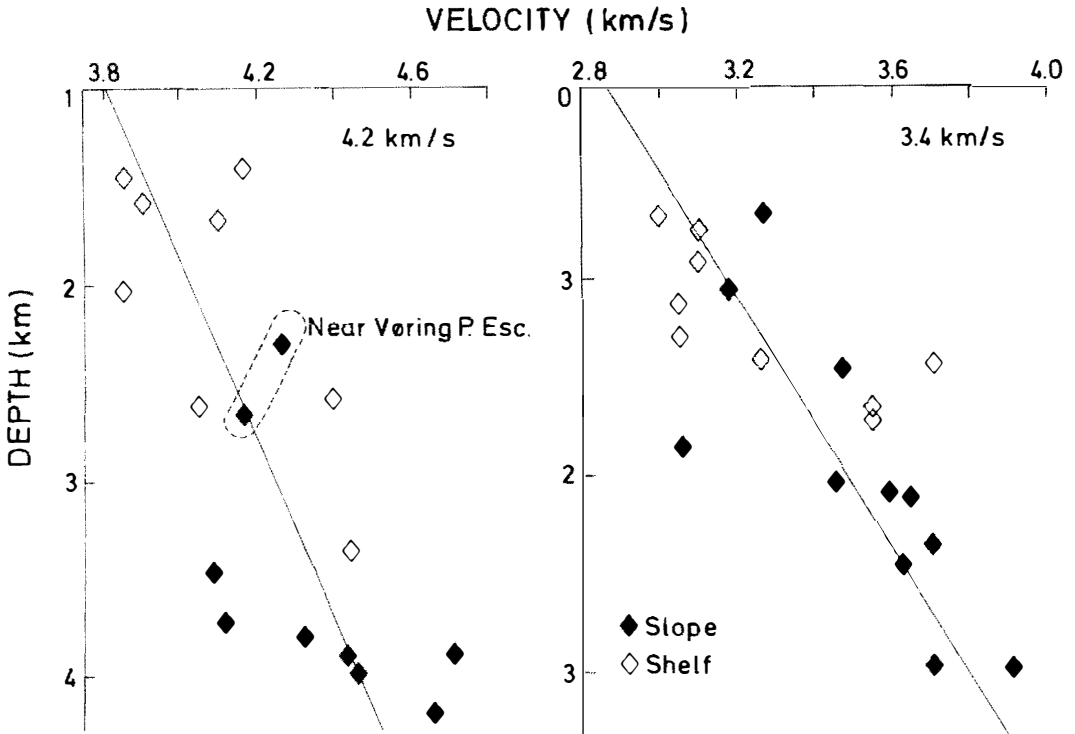


Fig. 8. Velocity increase as a function of overburden for the 3.4 and 4.2 km/s regional refractors on the Nordland margin.

(1977), Houtz & Windisch (1977) and Hinz & Schlüter (1978). Here, we only discuss the westernmost part of the Barents Sea and the western Svalbard margin. In the Barents Sea, the area of study approximately coincides with the eastern limit of the Tertiary sedimentary wedge (Eldholm & Ewing 1971). A detailed study of the seismic velocities and multichannel seismic profiles in the western Barents Sea is presented by Faleide & Gudlaugsson (1981).

The large number of measurements and differences in the geology have made it convenient to separate this margin at about 75° N.

70–75° N

There is little difference between average velocities on the shelf and slope (Table 3). Neither systematic regional lateral variations nor typical changes due to overburden have been observed in the refractor velocities. The relative abund-

Table 3. Average velocities, standard deviation and number of measurements (N), 70–80° N. Velocities in km/s.

75–80° N							
<i>All data</i>							
Ave. vel.	1.9	2.2	2.7	3.2	3.7	4.4	5.5
St. dev.	.11	.09	.15	.12	.19	.18	.24
N	23	28	34	15	25	17	11
70–75° N							
<i>Shelf</i>							
Ave. vel.	2.0	2.3	2.7	3.4	4.2	5.2	
St. dev.	.10	.10	.17	.20	.26	.28	
N	19	27	30	27	19	10	
<i>Slope</i>							
Ave. vel.	1.9	2.3	2.6	3.3			
St. dev.	.15	.09	.14	.22			
N	29	37	27	11			
<i>All data</i>							
Ave. vel.	1.9	2.3	2.7	3.4			
St. dev.	.14	.10	.16	.20			
N	48	64	57	38			

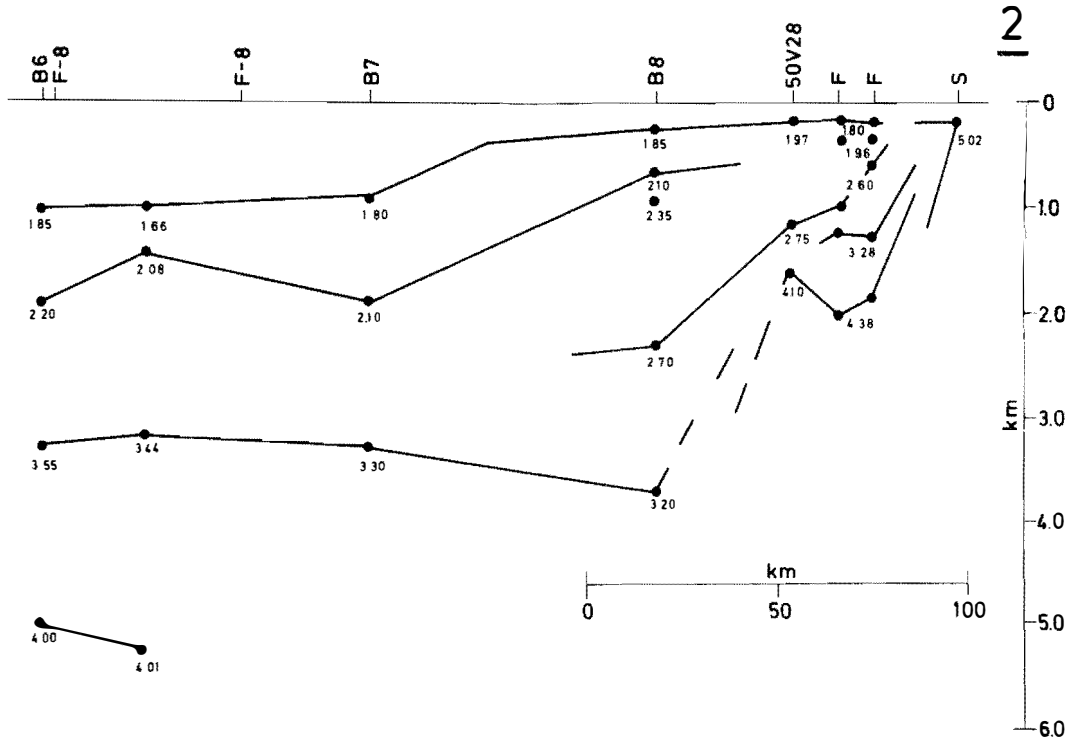


Fig. 9. Seismic structure section across the Møre margin. Location in Fig. 1.

ance of higher velocities on the shelf (Fig. 10) is attributed to the eastward thinning of the Cenozoic low-velocity sequence (Eldholm & Ewing 1971).

The velocities have been grouped with respect to the water depth. The velocity-depth distributions, however, did not reveal considerable differences (Table 4). The measurements from the entire area are also shown in Fig. 7, revealing large differences between maximum and minimum velocity gradients. The change in gradients is related to the considerable increase in the refractor depth westward across the margin. The velocity-depth relationship on the slope is shown

in Fig. 11 where first and second order velocity-depth functions have been fitted to the data-points. Similar computations have been made for the four water depth zonations (Table 4). For water depths greater than 1.5 km a first order velocity-depth function represents the data. In general, there appears to be a high velocity gradient in the uppermost (.6-.8 km) sediments, whereas a much more linear increase with depth occurs deeper in the section (Fig. 11). Based on a few profiles only, Eldholm & Ewing (1971) found that the second order polynomial $V = V_0 + .86z + .15z^2$ represented the upper 1.5 km of sediment. Although the curve fitted to all data

Table 4. First order velocity-depth functions with respect to water-depth, 70-75° N. This analysis included 33 velocity values not used by Houtz & Windisch (1977).

Water depth (km)	Number of measurements	$V = V_0 + kz$	Correlation coeff.
.5-1.0	20	$V = 2.10 + .26z$.77
1.0-1.5	24	$V = 2.06 + .20z$.74
1.5-2.0	46	$V = 1.87 + .34z$.91
2.0-2.5	18	$V = 1.77 + .37z$.92
.5-2.5	108	$V = 1.95 + .30z$.83

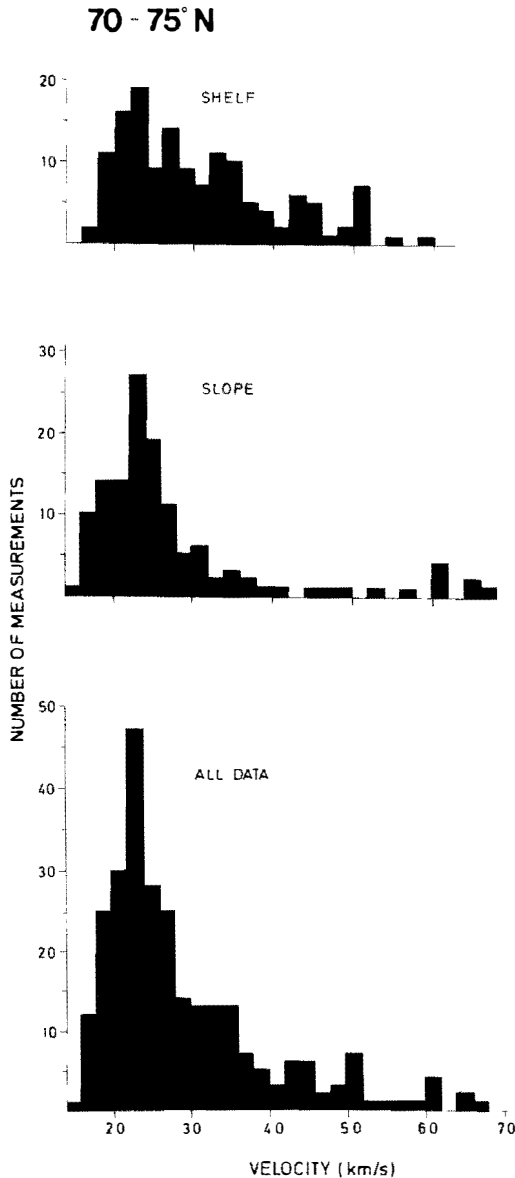


Fig. 10. Histograms of seismic refraction velocities 70–75° N.

is not entirely satisfactory, the very low-velocity gradient, $.30\text{s}^{-1}$ (Table 4), clearly indicates major differences with respect to other parts of the Norwegian margin between 62 and 80° N.

The seismic refraction section of Houtz & Windisch (1977) (Fig. 12) reveals the general features discussed above. The 5.2 and 5.4 km/s refractors in profiles 59 and 60 (Fig. 12) are the only possible continental basement velocities. Talwani & Eldholm (1977) proposed that the

Senja Fracture Zone demarcates the continent-ocean boundary. The fracture zone is located just east of profile 63 in Fig. 12. The section does not yield conclusive evidence of the change in crustal nature but profiles 33 and 62, recorded close to the fracture zone, are the only ones where velocities higher than 2.7 km/s are missing. Possibly the absence of deeper layers is related to an irregular basement relief and complex structures associated with the deeply buried fracture zone.

Houtz & Windisch (1977) studied the area to the south and southwest for Bjørnøya and divided it into several sub-regions, based on differences in velocity-depth functions. They computed velocity gradients using only their own data. The gradients have normally been expressed with respect to one-way reflection time. The area between the Lofoten Basin and the shelf edge yields a gradient of $.93\text{ km/s}^2$, which is indeed low also compared with deposits in deep oceans where the gradients generally lie in the range $1.5\text{--}2.5\text{ km/s}^2$. On the other hand, similarly low values have been observed in the Amazon Cone (1.3 km/s^2), Gulf of Mexico ($.97\text{ km/s}^2$), and the Niger delta (1.26 km/s^2). Consequently, Houtz & Windisch (1977) interpret the sediments on the slope as being composed of rapidly deposited deltaic sequences.

75–80° N

The most prominent geological feature is the north-northwest trending Hornsund Fault Zone at the central shelf (Fig. 13). The fault zone was first mapped by Sundvor & Eldholm (1976) and its nature and location more detailedly described by Myhre et al. (1982) and Myhre (1984) who suggest that it is closely related to the continent-ocean boundary. The existence and the nature of the fault zone have made it natural to treat the data on either side separately. We note, however, that only a limited number of profiles have been recorded between the fault zone and the coastline.

There are no differences in average refractor velocities on either side of the fault zone despite a pronounced difference in level between the layers. On the other hand, the low-velocity sediments are bounded eastward by the fault zone with only a veneer or local occurrences on

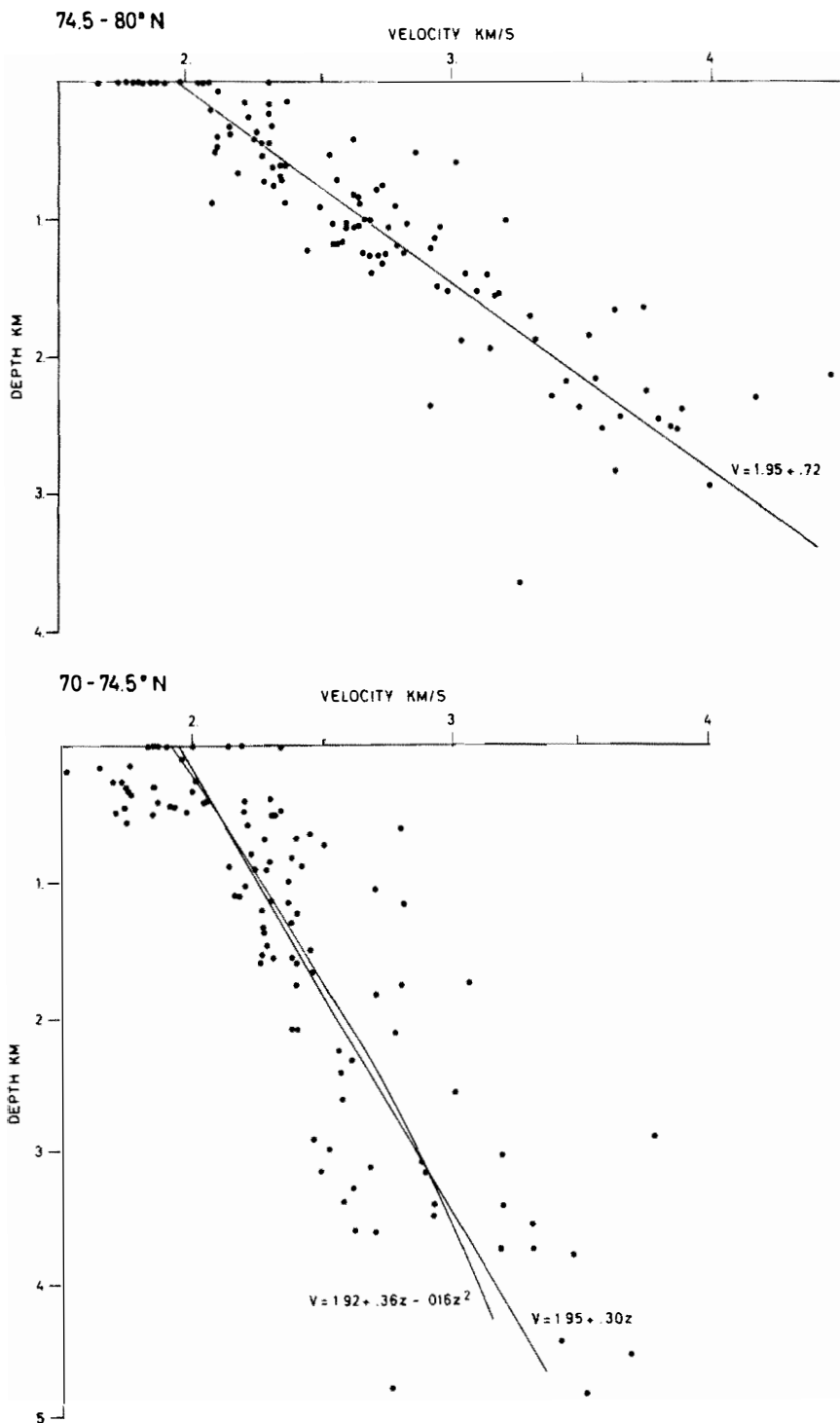


Fig. 11. Velocity-depth diagrams 70-80° N. The diagram south of 74.5° N refers to water depths of more than 500 m, whereas the northern diagram is for profiles west of the Hornsund Fault Zone.

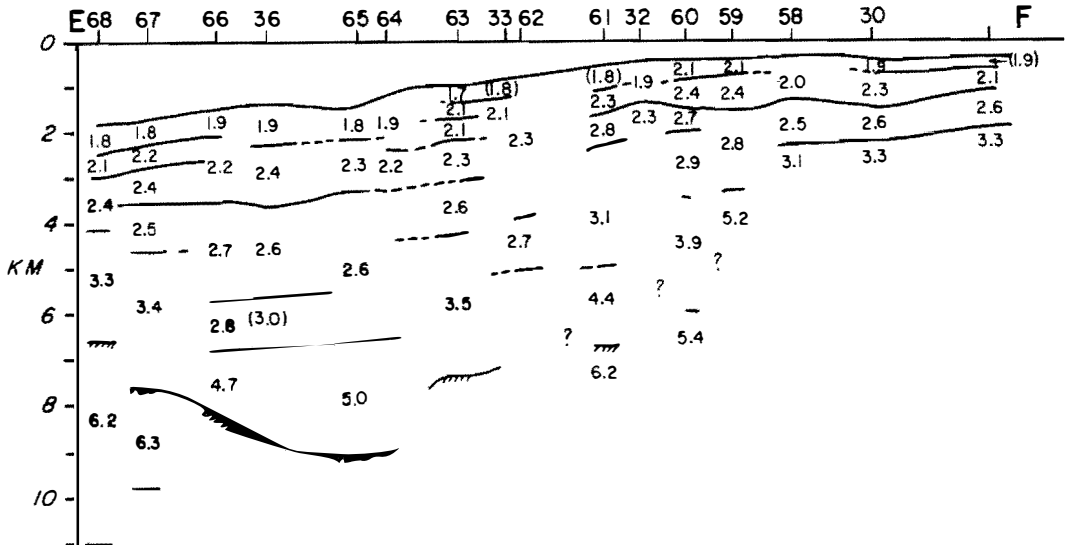


Fig. 12. Seismic structure section across the southwestern Barents Sea margin (Houtz & Windisch 1977). Location in Fig. 1.

top of the high sea floor velocities, 3.7–4.4 km/s, on the landward side. Typical features of the velocity distribution are illustrated in Figs. 14, 15 and Table 3. In some profiles on the continental slope it has been difficult to decide if the 4.+ km/s velocities could represent oceanic crust or consolidated sediments. The average velocities 4.4 and 5.5 km/s in Table 3 are based on profiles without this problem.

The velocities on the landward side of the Hornsund Fault Zone are indeed similar to those on the Svalbard Platform (Faleide & Gudlaugsson 1981). This observation suggests that the Hornsund Fault Zone demarcates the wes-

tern boundary of the Svalbard Platform between Bjørnøya and Svalbard (Fig. 13).

In order to determine the influence of the Svalbard islands on the margin sedimentation and the regional margin velocity distribution we have studied the areas north and south of Sørkapp (76.5° N) separately. The histograms (Fig. 14) and the velocity-depth functions are quite similar (Table 5). Both areas yield a linear velocity increase with depth and first order regression calculations show reliable correlations. These similarities reveal that the entire margin west of the fault zone may be considered as one region in terms of seismic velocities. This

Table 5. Velocity-depth functions, 75–80° N. *N* – number of measurements.

Area	N	$V = V_0 + kz$	Correlation coeff.
<i>West of Hornsund Fault Zone</i>			
South of Sørkapp	74	$V = 1.94 + .72z$.94
North of Sørkapp	41	$V = 1.98 + .71z$.94
75–80° N	115	$V = 1.95 + .72z$.95
<i>West of shelf edge:</i>			
South of Sørkapp	38	$V = 1.90 + .73z$.95
North of Sørkapp	22	$V = 1.87 + .85z$.93
75–80° N	60	$V = 1.91 + .74z$.94

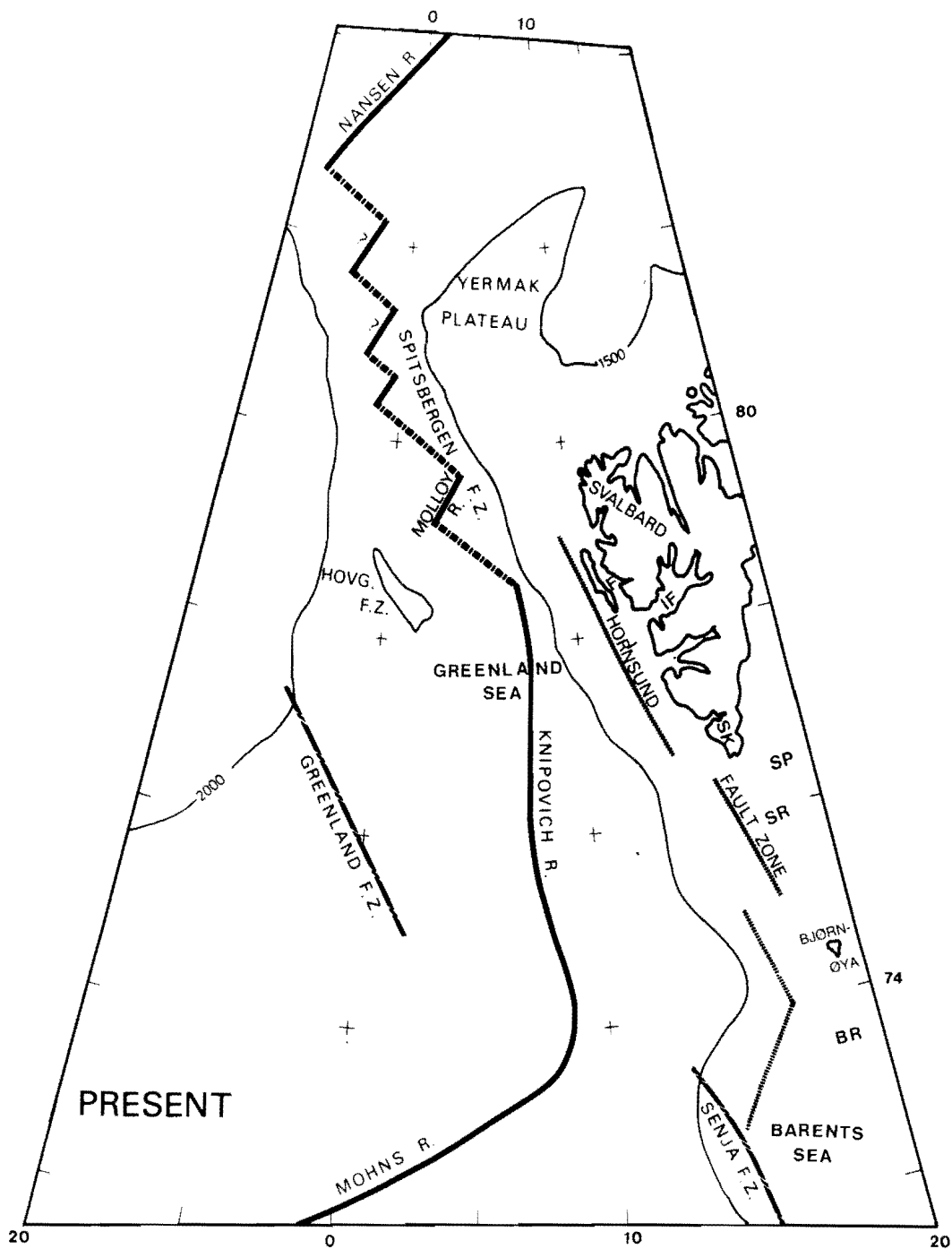


Fig. 13. Location of the Hornsund Fault Zone and the rifted margin structure connecting it to the Senja Fracture Zone. (Myhre et al. 1982). HOVG. F.Z.—Hovgaard Fracture Zone, F—Forlandsundet, IF—Isfjorden, SK—Sørkapp, SP—Svalbard Platform, SR—Storfjordrenna and BR—Brønnøyrenna.

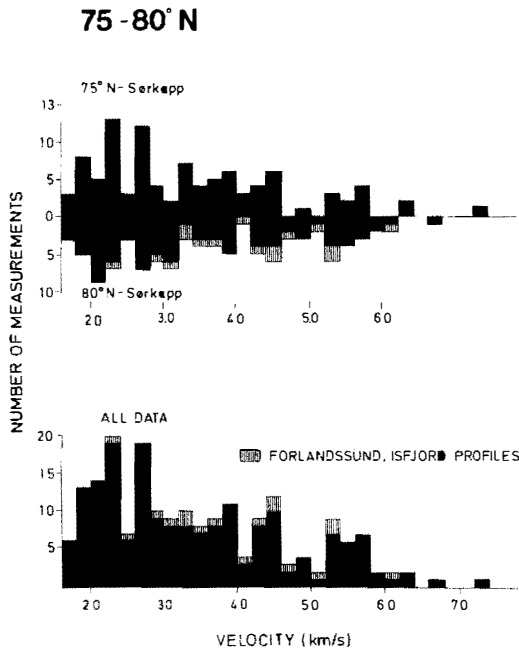


Fig. 14. Histograms of seismic refraction velocities 75–80° N.

suggests that the mode of deposition from Svalbard and the Svalbard Platform may have been regionally uniform prior to the Quaternary. There is no expression of the shelf edge in the velocity distribution (Table 5) indicating that it is only a morphological boundary. In terms of velocities the inner shelf west of Svalbard appears to be an extension of the Svalbard Platform. The sections in Fig. 15 clearly reveal the existence of the Hornsund Fault Zone but refraction data alone do not distinguish between a major single fault, a system of downfaulted blocks or a sharp flexure.

The 3.2 and 3.7 km/s refractors observed south of 75° N do not exist as regional refractors north of Bjørnøya. Particularly, the 3.2 km/s is only found locally off the southwestern part of Spitsbergen.

It has been suggested that the main part of the Barents Sea and Svalbard was emerged during the Cenozoic and that two large drainage systems carried terrigenous deposits into the young ocean. These systems are defined by the submarine channels Bjørnøyrenna and Storfjordrenna located to the south and north of Bjørnøya, respectively. Although major deltas have been built out

in both areas the present data indicate that less sediments have been deposited to the west of Storfjordrenna than west of Bjørnøyrenna. It is also suggested that the difference in velocity gradients to the north and south of Bjørnøya reflects a different regional mode of deposition.

The ocean-continent boundary north of the Senja Fracture Zone has not been conclusively established in earlier work. Sundvor & Eldholm (1979) proposed the Hornsund Fault Zone and the eastern escarpment of the Knipovich Ridge as the extreme locations of the boundary. In an analysis of the sedimentary and basement velocities in the oceanic areas including only profiles on well defined oceanic crust, Myhre & Eldholm (1981) found a high velocity gradient also in the sediments overlying oceanic crust in the eastern Greenland Sea. The gradient, $.71s^{-1}$, is identical to that on the adjacent margin, but twice as high as the average gradient in the main basins of the Norwegian-Greenland Sea. Later investigations based on multichannel seismic data suggests, however, that oceanic crust extends all the way to, or close to, the Hornsund Fault Zone (Myhre et al. 1982). Thus, the similarity in the velocity-depth gradients is not surprising.

Age relationship

There is little offshore information relating seismic velocity with sedimentary lithology and ages. Lower Cretaceous and Upper Jurassic sediments at Andøya (69° N) exhibit a velocity increase from 2.5–3.1 km/s near the Cretaceous-Jurassic boundary (Dalland et al. 1973). Eocambrian sediments in northern Norway yield velocities in the range 4.9–5.8 km/s (Eldholm & Talwani 1977), whereas Sundvor (1971) interprets the 5.2 km/s refractor to represent a continuation of the Caledonian basement.

The youngest rocks at Bjørnøya which is a part of the Svalbard Platform, are of Triassic age (Worsley & Edwards 1976) and the youngest sediments of Svalbard are probably of Eocene age (Kellogg 1975). The Svalbard Platform has most likely been a positive area for a long time judged by the absence of unconsolidated sediments and the high sea floor velocities. Edwards (1975) suggests that the bottom deposits at the Svalbard Platform have mainly been derived from local sources. Comparing sandstone sam-

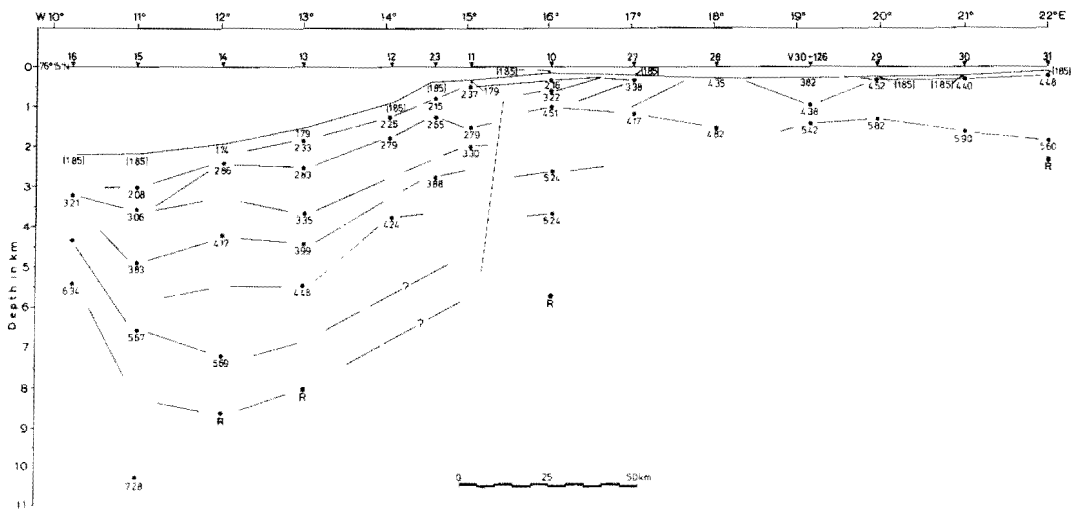
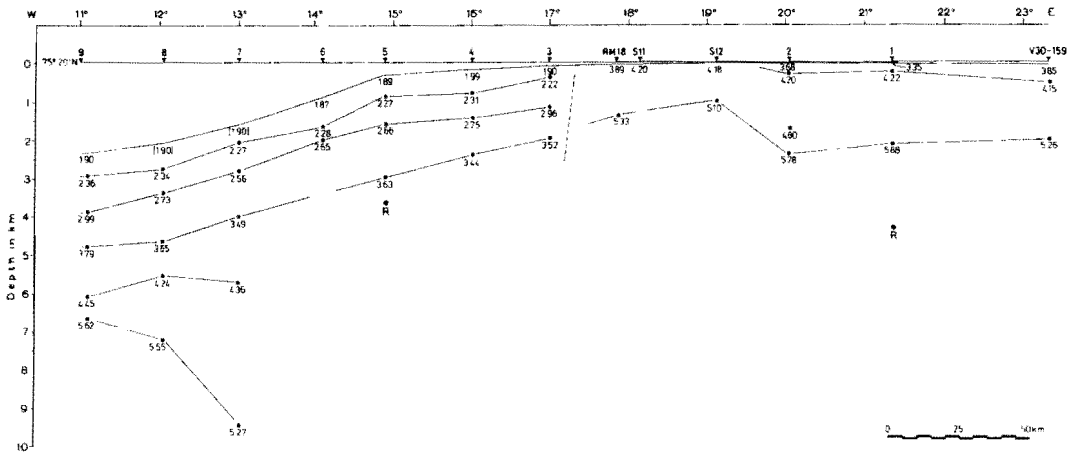


Fig. 15. Seismic structure sections across the Svalbard margin (Sundvor & Eldholm 1976). Locations in Fig. 1.

ples with various Mesozoic beds in Svalbard he proposes correlation with Triassic, Jurassic and Cretaceous formations.

Bjærke (1979) attempted to correlate ages and bottom samples in the Barents Sea and suggested that the 3.1 km/s refractor represents the upper part of the Lower Cretaceous which is absent on the Svalbard Platform. The 4.3 km/s refractor is correlated with formations in Svalbard of Upper Triassic-Lower Jurassic age. Moreover, this refractor outcrops at the sea floor a short distance away from the island of Hopen (76°30' N, 25° E) (Eldholm & Talwani 1977) which is composed of

Triassic rocks (Flood et al. 1971). Faleide & Gudlaugsson (1981), on the other hand, pointed out that there is no one-to-one correspondence between bottom samples and subcropping pre-Cenozoic sediments.

According to Myhre et al. (1982) the entire sedimentary sequence west of the Hornsund Fault Zone is of post-Middle Eocene age south of 77° N and post-Middle Oligocene further north. It is therefore possible that the high velocities in the lower part of the sequence is mainly a function of overburden in a local basin with an extremely rapid sedimentation and subsidence.

The velocities measured in the Early Tertiary and Mesozoic sediments in Svalbard are much higher, normally above 4.0 km/s (Grønlie 1978), than in the margin sediments west of the Svalbard Platform. This could possibly reflect an increased thermal gradient associated with the opening of the Greenland Sea. On the other hand, it is more likely related to former deep burial noting that Manum & Throndsen (1978) have shown that the present outcrop of Tertiary rocks in Svalbard has previously been buried at a depth of at least 1.7 km.

South of Bjørnøya the velocities lower than 2.5 km/s exist only along the western margin of the Barents shelf. The low-velocity section which is of a prograded nature (Rønnevik & Motland 1979) represents material derived from an emerged Barents shelf since the Early Eocene. The continuity of pre-Tertiary layers below the wedge suggests that the sequence of Mesozoic and Paleozoic sediments dated in the Barents Sea extends beneath the continental slope towards the Senja Fracture Zone (Rønnevik & Motland 1979; Faleide & Gudlaugsson 1981).

The margin off East-Greenland and the Jan Mayen ridge microcontinent

In general little geophysical data exist on the East-Greenland margin north of 70° N. The available data were reviewed by Johnson et al. (1975). The paucity of data is mainly caused by difficult ice conditions although systematic surveying has been carried out during the last few years. Closely spaced aeromagnetic data have been published by Larsen (1980), and Hinz & Schlüter (1980) presented some multichannel reflection lines south of Jan Mayen Fracture Zone. A program of exploration on the continental shelf has been initiated by the Geological Survey of Greenland but few results have yet been made available.

Before spreading began, an epicontinental sea with connections to the North Sea and the Barents Sea existed between Norway and Greenland. This region has been a regional depocenter from the Late Paleozoic to the opening of the Norwegian Sea in the Late Paleocene.

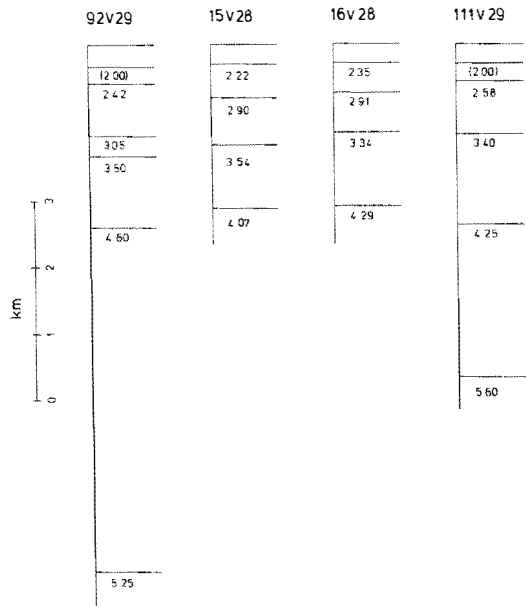


Fig. 16. Seismic refraction profiles on the Greenland continental shelf.

The refraction profiles are few and scattered along the margin. Only four profiles have been published landwards of the shelf edge (Figs. 1 and 16). Therefore, a systematic division into geological provinces is not yet warranted. In view of the pre-opening continuity of the sedimentary sequences the average velocities are compared with those from the conjugate Møre and Nordland margins (Table 6).

The average refractor velocities are slightly higher than those off Norway. We believe that this difference is real for the two upper refractors. These layers are also thinner on the Greenland side which may partly reflect stronger glacial erosion. In an interpretation of sediment type and age the same inferences are made as off Norway south of 70° N noting that a series of Mesozoic sediments exists onshore in East-Greenland (Birkelund 1976; Surlyk 1977).

Analysis of geophysical data and plate tectonic reconstructions imply that the flat-topped aseismic Jan Mayen Ridge is a continental fragment which was broken off the East-Greenland margin 20–25 my ago (Johnson & Heezen 1967; Eldholm & Talwani 1977; Garde 1978; Gairaud et al. 1978; Myhre et al. in press). The velocity stratification (Table 6) is again quite similar to those on the East-Greenland and

Table 6. Average velocities for the regions discussed in the text. Velocities in parentheses refer to the shelf only.

Area	Average velocities (km/s)						
Møre	1.9	2.2	2.6	3.4		4.1	5.2
Nordland	1.9	2.2	2.7	3.4		4.2	5.2
Lofoten–Vesterålen			2.8	3.3	3.9		5.3
70–75° N	1.9	2.3	2.7	3.4		(4.2)	(5.2)
75–80° N	1.9	2.2	2.7	3.2	3.7	4.4	5.5
East-Greenland	2.0	2.4	3.0	3.5		4.3	5.4
Jan Mayen Ridge	1.9	2.2	2.7	3.1		4.0	5.6

Norwegian margins, but we refer to Myhre et al. (in press) for a comprehensive discussion of the velocities.

Summary

The average regional refraction velocities have been compiled in Table 6. Keeping in mind the limitations of the refraction method and the variable profile density in the various provinces, the table reveals typical similarities in the velocity stratification as well as some significant differences. The correspondence in lateral and vertical distribution may be interpreted in terms of regional similarities in the sedimentation and evolution of the marginal areas. The Lofoten–Vesterålen area has acted as a positive province for long periods of time and was probably emerged during the Tertiary. A similar mode of evolution is inferred for the Svalbard Platform although post-Triassic sediments appear to exist only locally. The margin south of Bjørnøya consists of a huge prograded sedimentary wedge exhibiting an extremely small velocity gradient. We believe that this is caused to a large extent by build up of deltaic sequences of terrigenous material eroded and transported from an emerged Barents shelf.

It is characteristic for most of the areas that a linear velocity increase with depth appears to reflect the vertical velocity distribution except for the uppermost .5–.8 km of sediments. Here, the velocity increases more rapidly with depth and a second order velocity-depth curve may be representative. Moreover, there is a slight decrease in the sea floor velocities seaward from the shelf towards the ocean basins.

The 3.9 and 3.4–4.2 km/s regional refractors at the Lofoten and Nordland margins, respectively,

show a clear relationship with overburden. It is indeed important to be aware of this effect both when correlating seismic refraction velocities and in a discussion of the relative vertical movements within these areas.

The assumption that the Cenozoic sediments generally have velocities below 2.5 km/s seems to be valid except in areas of very thick sequences where the velocities may increase considerably, predominantly due to overburden.

A 5+ km/s velocity has often been used to define crystalline basement rocks. Although this relationship may be valid in places, comparisons with other measurements, particularly magnetic depth estimates and multichannel reflection data, indicate that velocities in this range often originate from consolidated sediments.

The overall analysis points toward sequences of Mesozoic and Upper Paleozoic sediments along most of the margins. The velocity information is consistent with the idea of a regional basin between Norway and Greenland prior to the opening of the Norwegian–Greenland Sea and with the idea of a continental origin of the Jan Mayen Ridge.

A study of this kind obviously contains uncertainties due to the quality of the different data bases, reduced by many investigators. Furthermore, the relationship between seismic velocities, varying lithology, physical properties, and age is in no way simple. This study indicates, however, that when combined with other geophysical information, systematic analyses of lateral and vertical changes in the refraction velocities may yield significant information about the regional geology.

References

- Birkelund, T. 1976: Geology of East Greenland: a review. *Norw. Petrol. Soc. Offshore North Sea 1976*, Stavanger. 23 pp.
- Bjørkcc, T. 1979: Geology of the Barents Sea shelf: Evidence from palynological studies of drift material. *Norw. Petrol. Soc. NSS- 17*, 15 pp.
- Dalland, A., Hansen, R. & Sellevoll, M. 1973: Geologiske og geofysiske undersøkelser av jura-kritt feltet på Andøya utført av Universitetet i Bergen 1969-1971. Forclopig meddelelse. In Sellevoll, M.A. & Sundvor, E. (eds.) *Tekn. rapp. nr. 7*. Jordskjelvstasjonen, Univ. i Bergen, 35 pp.
- Edwards, M.B. 1975: Gravel fraction on the Spitsbergen Bank, NW Barents Shelf. *Norges Geol. Unders. 316*: 205-218.
- Eldholm, O. 1970: Seismic refraction measurements on the Norwegian continental shelf between 62° and 65° N. *Norsk geol. Tidsskr. 50*: 215-229.
- Eldholm, O. & Ewing, J. 1971: Marine geophysical survey in the southwestern Barents Sea. *J. Geophys. Res. 76*: 3832-3841.
- Eldholm, O. & Nysæther, E. 1969: Seismiske undersøkelser på den norske kontinentalsokkel. *Tekn. Rapp. 2C Jordskjelvstasjonen*. Univ. i Bergen, 17 pp.
- Eldholm, O. & Talwani, M. 1977: Sediment distribution and structural framework of the Barents Sea. *Geol. Soc. Am. Bull. 88*: 1015-1029.
- Eldholm, O. & Windisch, C.C. 1974: Sediment distribution in the Norwegian-Greenland Sea. *Geol. Soc. Am. Bull. 85*: 1661-1676.
- Eldholm, O., Sundvor, E. & Myhre, A.M. 1979: Continental margin off Lofoten-Vesterålen. *Mar. Geophys. Res. 4*: 3-35.
- Ewing, J. & Ewing, M. 1959: Seismic refraction measurements in the Atlantic Ocean Basins, in the Mediterranean Sea, on the Mid-Atlantic Ridge and in the Norwegian Sea. *Geol. Soc. Am. Bull. 70*: 291-318.
- Ewing, M., Wollard, G.P. & Vine, A.C. 1939: Investigations in the emergent and submerged Atlantic Coastal Plain (Part III: Barnegat Bay, New Jersey Section). *Geol. Soc. Am. Bull. 50*: 257-296.
- Falchide, J.I. & Gudlaugsson, S.T. 1981: *Geology of the Western Barents Sea*. Cand. real. thesis, Univ. Oslo. 160 pp.
- Flood, B., Nagy, J. & Winsnes, T.S. 1971: The Triassic succession on Barentsøya, Edgeøya and Hopen (Svalbard). *Norsk Polarinst. Medd. 100*. 20 pp.
- Gairaud, H., Jacquart, G., Aubertin, F. & Beuzart, P. 1978: The Jan Mayen Ridge synthesis of geological knowledge and new data. *Oceanologica Acta. 1*: 335-358.
- Gardé, S.S. 1978: *Zur geologischen Entwicklung des Jan Mayen Rücken nach geophysikalischen Daten*. Dissertation, Univ. Clausthal, 74 pp.
- Grønlic, G. 1978: Preliminary results of seismic velocity measurements in Spitsbergen 1977. *Norsk Polarinst. Årbok 1977*: 229-236.
- Hinz, K. & Moe, A. 1971: Crustal Structure in the Norwegian Sea. *Nature Phys. Sci. 232*: 187-190.
- Hinz, K. & Schlüter, H.U. 1978: The geological structure of the western Barents Sea. *Mar. Geol. 26*: 199-230.
- Hinz, K. & Schlüter, H.U. 1980: Continental margin off East Greenland. *Proc. Tenth World Petrol. Congr. 2*: 405-418.
- Holtedahl, O. 1960: Devonian. Including Downtonian in the Hitra district etc. Pp. 285-297 in Holtedahl, (ed.) *Geology of Norway*.
- Hornabroek, J.T. 1967: Seismic interpretation problems in the North Sea with special references to the discovery well 48/6-1. *Seventh World Petrol. Congr. Proc. 2*: 837-856.
- Houtz, R.E., Ewing, J. & Le Pichon, X. 1968: Velocity of deep-sea sediments from sonobuoy data. *J. Geophys. Res. 73*: 2615-2641.
- Houtz, R.E. & Windisch, C. 1977: Barents Sea continental margin sonobuoy data. *Geol. Soc. Am. Bull. 88*: 1030-1036.
- Johnson, G.L. & Heezen, B.C. 1967: Morphology and evolution of the Norwegian-Greenland Sea. *Deep-Sea Res. 14*: 755-771.
- Johnson, G.L., McMillan, N.J. & Egloff, J. 1975: East Greenland continental margin. In Yorath, C.J., Parker, E.R. & Glass, D.J. (eds): *Canada's Continental Margin and Offshore Petr. Explor. Can. Soc. Petrol. Geol. Mem. 4*: 205-224.
- Jørgensen, F. & Navrestad, T. 1979: Main structural elements and sedimentary succession on the shelf outside Nordland (Norway). *Norw. Petrol. Soc. NSS-11*, 20 pp.
- Kellogg, H.E. 1975: Tertiary stratigraphy and tectonism in Svalbard and continental drift. *Am. Assoc. Pet. Geol. Bull. 59*: 465-485.
- Larsen, H.C. 1980: Geological perspectives of the East Greenland continental margin. *Bull. geol. Soc. Denmark 29*: 77-101.
- Le Pichon, X., Ewing, J. & Houtz, R.E. 1968: Deep Sea sediment velocity determination made while reflection profiling. *J. Geophys. Res. 73*: 2597-2614.
- Lien, R. 1976: Ingeniørgeologisk kartlegging på kontinentalsokkelen utenfor Lofoten-Vesterålen. *IKU, Rept. 78*, 36 pp.
- Manum, S.B. & Thronsen, T. 1978: Rank of coal and dispersed organic matter and its geological bearing in the Spitsbergen Tertiary. *Norsk Polarinst. Årbok 1977*: 159-177.
- Myhre, A.M. 1984: *The Western Svalbard continental margin (74-80° N)*. In Dr. Scint. thesis, Univ. of Oslo.
- Myhre, A.M. & Eldholm, O. 1981: Sedimentary and crustal velocities in the Norwegian-Greenland Sea. *J. Geophys. Res. 86*: 5012-5022.
- Myhre, A.M., Eldholm, O. & Sundvor, E. 1982: The margin between Senja and Spitsbergen Fracture Zones: Implication from plate tectonics. *Tectonophysics. 89*: 33-50.
- Myhre, A.M., Eldholm, O. & Sundvor, E. in press: The Jan Mayen Ridge: Present Status. *Polar Research*.
- Renard, V. & Malod, J. 1974: Structure of the Barents Sea from seismic refraction. *Earth Planet. Sci. Lett. 24*: 33-47.
- Rønnevik, H.C., Bergsaker, E.L., Moe, A., Øvrebø, O., Navrestad, T. & Stangenes, J. 1975: The geology of the Norwegian continental shelf. *Petr. and cont. shelf of NW Europe. V.1 Geology, Appl. Sci. Publ.*: 117-129.
- Rønnevik, H.C. & Navrestad, T. 1977: Geology of the Norwegian shelf between 62° N and 69° N. *Geo. Journ. 1*: 33-46.
- Rønnevik, H.C. & Motland, K. 1979: Geology of the Barents Sea. *Norw. Petrol. Soc. NSS-15*, 34 pp.
- Sundvor, E. 1971: Seismic refraction measurements on the Norwegian continental shelf between Andøya and Fugløy-banken. *Mar. Geophys. Res. 1*: 303-313.
- Sundvor, E. 1974: Seismic refraction and reflection measurements in the southern Barents Sea. *Marine Geology, 16*: 255-273.
- Sundvor, E. & Eldholm, O. 1976: Marine geophysical survey on the continental margin from Bjørnøya to Hornsund, Spitsbergen. *Univ. Bergen, Seism. Obs. Sci. Rept. 3*, 28pp.
- Sundvor, E. & Eldholm, O. 1979: The western and northern margin off Svalbard. *Tectonophysics. 59*: 239-250.
- Sundvor, E. & Sellevoll, M.A. 1971: Seismiske undersøkelser av den norske kontinentalsokkel. Lofoten-Bjørnøya (68-75° N). *Univ. Bergen, Seism. Obs., Tekn. Rapp. 5*, 31 pp.
- Sundvor, E., Sellevoll, M.A. & Haugland, K. 1975: Seismic measurements on the Norwegian continental margin. *Univ. Bergen, Seism. Obs., Sci. Rept. 1*, 34 pp.
- Sundvor, E., Eldholm, O., Gidskchaug, A. & Myhre, A.M. 1977: Marine geophysical survey on the western and northern continental margin off Svalbard. *Univ. Bergen, Seism. Obs., Sci. Rept. 4*, 35 pp.

- Sundvor, E., Gidskehaug, A., Myhre, A.M. & Eldholm, O. 1979: Marine geophysical survey on the northern Jan Mayen Ridge. *Univ. Bergen, Seism. Obs. Sci. Rept.* 6. 18pp.
- Sundvor, E., Eldholm, O., Haugland, K., Sellevoll, M.A. & Bruland, L. 1975: Seismic measurements on the Norwegian continental margin. *Univ. Bergen, Seism. Obs. Sci. Rept.* 2, 30 pp.
- Surlyk, F. 1977: Mesozoic faulting in East Greenland. *Geol. Mijnbouw*, 56: 311–329.
- Talwani, M. & Eldholm, O. 1972: The continental margin off Norway: A geophysical study. *Geol. Soc. Am. Bull.* 83: 3575–3608.
- Talwani, M. & Eldholm, O. 1977: Evolution of the Norwegian-Greenland Sea. *Geol. Soc. Am. Bull.* 88: 969–999.
- Worsley, D. & Edwards, M.B. 1976: The Upper Palaeozoic succession of Bjørnøya, *Norsk Polarinst. Årbok*. 1974: 17–34.
- Wyrobek, S.M. 1969: General appraisal of velocities of the Permian basin of northern Europe, including the North Sea. *J. Inst. Petrol. London*, 55: 1–13.
- Åm, K. 1970: Aeromagnetic investigations on the continental shelf of Norway, Stad-Lofoten (62°–69° N). *Norges Geol. Unders.* 266: 49–61.

Free-air gravity anomaly maps of the Greenland Sea and the Barents Sea

Faleide, J.I., Gudlaugsson, S.T., Johansen, B., Myhre, A.M. & Eldholm, O.: Free-air gravity anomaly maps of the Greenland Sea and the Barents Sea. *Nor. Polarinst. Skr. 180* 63–67. ISBN 82-90307-26-6.

Two new free-air gravity anomaly maps of the Greenland Sea and the western Barents Sea have been constructed using all the available data. A careful analysis of the data has resulted in level adjustments of some surveys. Both maps have been contoured at 10 mGal intervals. The anomaly pattern reflects a first-order relationship to main structural features. Particularly important is the observation that anomaly belts occur near the predicted continent-ocean transition along the margin off the western Barents Sea and Svalbard. Furthermore, the anomaly field in the western Barents Sea is closely related to the subsurface geology.

Jan I. Faleide, Steinar T. Gudlaugsson, Annik M. Myhre, and Olav Eldholm, Department of Geology, University of Oslo, Blindern, Oslo 3, Norway; Bård Johansen, Norsk Hydro A/S, Harstad, Norway. Received April 1983 (revised December 1983).

Introduction

Recent studies of the Barents and Greenland Seas have demonstrated important relationships between the gravity field and main structural features (Rønnevik 1981; Faleide & Gudlaugsson 1981; Myhre et al. 1982). Therefore, we have constructed new regional free-air gravity anomaly maps for the Greenland Sea and the Barents Sea (Fig. 1).

The detailed interpretation of the maps will be presented as parts of separate studies dealing with the plate tectonic evolution of the Greenland Sea, the western margin off Svalbard (Myh-

re 1984), and the regional geology of the western Barents Sea (Faleide et al. in press). Here, we present the maps and brief descriptions of the data base, map construction, and main features of the gravity field. Large scale copies at a scale of 1'' per degree longitude may be requested from the authors.

Some gravity maps both of regional and local coverage have been published earlier (Table 1). The two regional maps presented here include a large amount of new measurements and the various surveys have been carefully evaluated in terms of data quality and level adjustments. The maps are contoured at intervals of 10 mGal.

Table 1. *Earlier gravity maps.*

<i>Reference</i>		<i>Anomaly type</i>	<i>Contour int.</i>	<i>Area</i>
Renard & Malod	1974	Free-air	10	Western Barents Sea
Talwani & Grønlie	1976	»	25	Norw.–Greenland Sea
Syrstad et al.	1976	Bouguer	2	Tromsøflaket (70–72° N, 17–22° E)
Eldholm & Talwani	1977	Free-air	10	Western Barents Sea
Talwani & Eldholm	1977	»	10	Mohn/Knipovich ridges
Gjerstad	1977	»	5	Norw. coastal region (14–30° E)
Gjerstad	1977	»	10	Southern Barents Sea
Eldholm & Myhre	1977	»	10	Hovgaard F.Z.
Cochran & Talwani	1978	» 1x 2° res.	10	Norw.–Greenland Sea
Cochran & Talwani	1978	» 5x10° res.	10	Norw.–Greenland Sea
Sobczak	1978	Free-air	20	Arctic, north of 60° N
Sobczak	1978	Residual	20	Arctic, north of 60° N
Rønnevik	1981	Bouguer	10	Western Barents Sea
Grønlie & Talwani	1982	Isostatic	10	Senja F.Z.
Grønlie & Talwani	1982	Free-air	10	Svalbard margin
Rønnevik	1984	Bouguer	5	Western Barents Sea

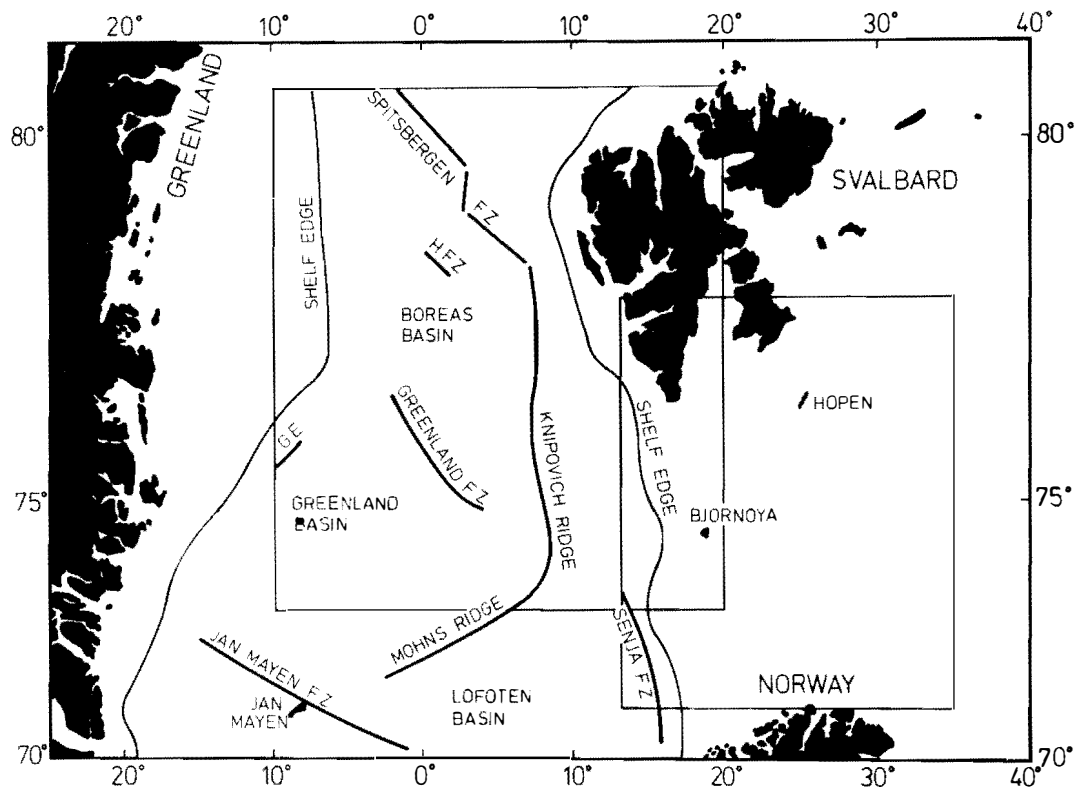


Fig. 1. Index map.

The Greenland Sea map (Fig. 2, enclosed in pocket) covers the area between the Greenland-Senja and Spitsbergen fracture zones, roughly outlined by 73–80.5° N, 10° W–20° E. The Barents Sea map (Fig. 3, enclosed in pocket) is limited by 71–78° N, 13–35° E. The maps overlap in the region between 73–78° N, 13–20° E. This relatively large overlap is made because the structural evolution of this region is closely related to both the geology of the Barents Sea and the plate tectonic evolution of the Greenland Sea.

The Greenland Sea is characterized by low amplitude magnetic anomalies. Few magnetic lineations have been mapped and no reliable identifications exist, but several studies indicate that the detailed plate tectonic history includes ridge jumps and corresponding adjustments in the plate boundary (Talwani & Eldholm 1977; Vogt et al. 1981; Myhre et al. 1982). In identifying basement lineations, basement escarpments and areas of different elevation which may be critical to develop evolutionary models, a de-

tailed analysis of the gravity anomaly map may prove useful.

Analysis of multichannel seismic reflection and refraction measurements, gravity and magnetic data have contributed to an understanding of the regional geology of the western Barents Sea (Eldholm & Talwani 1977; Rønnevik 1981; Faleide & Gudlaugsson 1981; Rønnevik et al. 1982; Rønnevik 1984; Faleide et al. in press). This includes the distribution and layering of sediments, definition of geological provinces and regional structural features, and identification of tectonic phases and gross lithology. Thick series of Late Paleozoic, Mesozoic and Cenozoic sediments cover a basement of probably Caledonian origin. Faleide et al. (in press) demonstrated that the main features of the free-air gravity field reveal a first-order correlation with the subsurface structures. This observation has been used to postulate structural elements based on gravity data in areas of scarce multichannel seismic reflection coverage.

Map construction

The data base is shown in Table 2. Gravity values are referred to European datum and the international gravity formula (1930). Gravity data collected during the drift of the ice-island «Arlis» along the Greenland continental shelf (Ostenson & Pew 1968) have not been included because of the large distances to the nearest ship's track.

All available gravity anomalies were annotated on a Mercator map and contoured at 10 mGal. In the Greenland Sea the bathymetry has been used as a guideline for contouring where there was limited data. Structural information from multi-channel seismic data has guided the contouring in some parts of the Barents Sea.

At some track intersections significant differences in values were noticed. Therefore, all intersecting lines were given a careful evaluation. This exercise established that some of the surveys were more consistent than others. In particular:

Barents Sea map –

- Vema 3010 and 3011, CH 14, BAR 78, and the part of the TOPOCOM data off Norway show rather good consistency. The differences are in most cases less than 5 mGal.
- The TOPOCOM data have internal differences of less than 3 mGal. The measurements north of Bjørnøya appear to have navigational errors and are also systematically 3 mGal higher than the other data.
- Vema 2304 and 2803 have values that are systematically too high, 8 mGal and 10 mGal, respectively.
- Parts of Vema 2704 and CH 13 show large unsystematic differences with the other tracks.
- The point measurements (Table 2) are consistent with the continuous measurements.

Greenland Sea map –

- Vema 2803 is systematically too high by 10 mGal.
- Vema 2304 shows large unsystematic variations, normally 5–15 mGal higher than intersecting lines.
- Along the other tracks the differences at intersections are normally less than 5 mGal.

Table 2. Data used in construction of the free-air anomaly maps.

<i>Institution</i>	<i>Year</i>	<i>Cruise</i>
<i>Underway measurements</i>		
Lamont-Doherty Geological Observatory	1966	Vema 23
	1969	Vema 27
	1970	Vema 28
	1972	Vema 29
	1973	Vema 30
Institut Francais du Pétrole	1978	BAR 78
U.S. Topographical Command	1970	TOPOCOM
CNEXO	1970	Nestlante II
Norwegian Petroleum Directorate	1977	
<i>Point measurements</i>		
Norwegian geograph. Survey ¹	1958	
French Hydrogr. Serv. ²	1965–68	

¹ Bakkelid (1959), ² Anonymous (1970).

After corrections had been made for the systematic differences, the maps were manually contoured with a 10 mGal contour interval, with less weight given to the data considered of low quality.

The data coverage is in general quite satisfactory, however, the western Greenland Sea and northern Barents Sea are poorly covered due to the ice conditions. The gravity maps are considered to have an accuracy which varies with the data coverage; in areas of good data control it is probably better than 5 mGal.

Main features of the maps

Greenland Sea (Fig. 2, enclosed in pocket)

A well defined belt of gravity anomalies reflects the northern part of the Mohs Ridge and the transition to the Knipovich Ridge. The continuity of this belt indicates that no transform fault presently offsets the ridge axis. The Knipovich Ridge rift valley appears to be continuous striking north-northwest between 74 and 76° N. The axial trend changes to due north at about 77° N. Between 76 and 77° N there is an area characterized by several positive gravity anomalies forming a northwest-southeast lineament.

The most prominent anomaly to the west of the ridge is associated with the Greenland Fracture Zone. West of 2° E the fracture zone has a well defined linear northwest-southeast trend. This

positive gravity anomaly with a maximum of 117 mGal is associated with a basement ridge (Eldholm & Windisch 1974). Close to the mid-oceanic ridge, no obvious lineaments in the gravity field outline the fracture zone. However, several positive gravity anomalies in this area indicate a more easterly azimuth for this part of the fracture zone. This change is probably related to the reorganisation of relative plate motion at about 36 my (Talwani & Eldholm 1977).

The gravity field shows different levels on either side of the Greenland Fracture Zone. The regional level of the free-air anomalies in the Boreas Basin to the northeast is about 50 mGal, gently decreasing towards the north. Southwest of the Greenland Fracture Zone the level is much lower, with average values around 0 mGal and a minimum of -15 mGal. This reflects the different crustal age and basement elevation across the fracture zone. The bathymetry, for example, shows a regional difference of approximately 500–700 m. Similarly, the free-air gravity field shows a regional increase towards the Knipovich Ridge.

The decrease of the free-air anomalies towards the Hovgaard Fracture Zone appears to be partly associated with an increasing depth to oceanic basement. Two pronounced gravity maxima coincide with the Hovgaard Fracture Zone and in general reflect the bathymetry of the segmented submarine ridge.

The maximum anomaly is 173 mGal over the eastern ridge segment, whereas the maximum value over the western ridge is 131 mGal. These prominent anomalies are surrounded by minima which indicate a significant degree of local compensation. The 42 mGal difference in maximum values between the two ridge segments does not appear to be any simple topographic effect because the eastern segment is even deeper than the western segment. It may be attributed to an important difference in the densities of the underlying rocks (Eldholm & Myhre 1977). Possibly, it reflects a different crustal nature of the two ridge blocks (Myhre et al. 1982).

Due to the permanent ice cover only the southeasternmost part of the Spitsbergen Fracture Zone has been surveyed. This area is characterized by a northwesterly trend in the anomaly pattern.

Between the Knipovich Ridge axial province and the Svalbard margin the gravity field is subdued. Seismic reflection and refraction data indicate a thick sediment cover extending from the continental shelf to the eastern axial ridge mountains.

Continental margin (Figs. 2 and 3)

A prominent positive anomaly belt centered at the outer continental shelf is the main feature of the field from Bjørnøya to 77.5° N. The anomaly belt continues north of 77.5° N, however, its character changes pronouncedly. Here, the anomaly maximum is more closely associated with the shelf edge and may therefore largely be caused by edge effects. South of 77.5° N only a small part of the anomaly appears to reflect a contribution by edge effects. On the other hand, recent work indicates a relationship with structures and basement highs at or near the continent-ocean boundary (Myhre et al. 1982).

A well defined positive anomaly, maximum 106 mGal, on the lower continental slope between 71–74° N has been defined as the Senja Fracture Zone by Talwani & Eldholm (1977). By making isostatic corrections they demonstrated that the positive anomaly does not arise from edge effects. More recently, basement relief has been observed in two multichannel seismic reflection profiles crossing the margin at about 72 and 73° N (Faleide et al. in press).

A northeasterly trending positive anomaly southwest of Bjørnøya links the main north-northwest trending anomalies at the margin. Together these anomaly belts show a systematic relationship with the continent-ocean boundary which is proposed to consist of the Senja Fracture Zone in the south and the Hornsund Fault Zone in the north connected by a rifted margin segment southwest of Bjørnøya (Myhre 1984).

Barents Sea (Fig. 3)

In the Barents Sea south of 74° N the field changes character at about 23° E. To the east the gravity field is relatively smooth with values typically ranging from -10 to +20 mGal. The regional trend is northeasterly and the anomalies reveal a first order correlation with the subsurface structures (Faleide et al. in press). In the southeast, there are some local poorly defined

negative anomalies between 72 and 73° N. These anomalies, which are better defined in the Bouguer gravity map of Rønnevik (1981) are associated with salt deposits in the Nordkapp Basin.

West of 23° E the field is more accentuated, the largest amplitudes and steepest gradients occur in the southwest and are associated with two north-south trending anomalies. Also here there is an obvious correspondence with subsurface structures, the positive contours reflecting structural highs and the negative ones defining basins.

North of 74° N, a system of generally positive anomalies is associated with the Svalbard Platform.

Acknowledgements

We are indebted to the Norwegian Petroleum Directorate and Institut Français du Pétrole (on behalf of CEPM) for making available gravity data along the tracks of selected multichannel seismic profiles.

References

- Anonymous 1970: Anomalies de la Pesanteur en mer de Norvège. Resultates de mesure effectuées à bord du «Paul Goffeny» 1965-1968. *Cahiers Oceanog.* 22: 503-514
- Bakkeliid, S. 1959: Gravity Observations in a submarine along the Norwegian coast. *Geol. publ., no. 11, Norw. Geogr. Survey, Oslo.* 30 pp.
- Cochran, R.R. & Talwani, M. 1978: Gravity anomalies, regional elevation, and the deep structure of the North Atlantic. *J. Geophys. Res.* 83: 4907-4924.
- Eldholm, O. & Myhre, A. M. 1977: Hovgaard Fracture Zone. *Nor. Polarinst. Årbok* 1976: 195-208.
- Eldholm, O. & Talwani, M. 1977: Sediment distribution and structural framework of the Barents Sea. *Geol. Soc. Am. Bull.* 88: 1015-1029.
- Eldholm, O. & Windisch, C. 1974: Sediment distribution in the Norwegian-Greenland Sea. *Geol. Soc. Am. Bull.* 85: 1661-1676.
- Falcide, J.I. & Gudlaugsson, S.T. 1981: *Geology of the western Barents Sea - a regional study based on marine geophysical data.* Cand. real. thesis, Univ. of Oslo. 160 pp.
- Falcide, J.I., Gudlaugsson, S.T. & Jacquart, G. in press: Evolution of the western Barents Sea. *Marine Petrol. Geol.*
- Gjerstad, H. 1977: *Maringeofysisk undersøkelse av det sørvestre Barentshav.* Cand. real. thesis, Univ. of Oslo, 150 pp.
- Grønlie, G. & Talwani, M. 1982: The free-air gravity field of the Norwegian-Greenland Sea and adjacent areas. *Earth Evol. Ser.* 2: 79-103.
- Myhre, A.M. 1984: *The Western Svalbard continental margin (74-80° N)*, in Dr. Scient. thesis, Univ. of Oslo. 201 pp.
- Myhre, A.M., Eldholm, O. & Sundvør, E. 1982: The margin between Senja and Spitsbergen fracture zones: Implication from plate tectonics. *Tectonophysics* 89: 1-32.
- Ostenso, N.A. & Pew, J.A. 1968: Sub-bottom seismic profile off the east coast of Greenland. Pp 345-363 in Sater, J.E. (Coord.) *Arctic Drifting Stations.*
- Renard, V. & Malod, J. 1974: Structure of the Barents Sea from seismic refraction. *Earth Planet. Sci. Lett.* 24: 33-47.
- Rønnevik, H.C. 1981: Geology of the Barents Sea. Pp. 395-406 in Illing, L.V. & Hobson, G.D. (eds.) *Petroleum Geology of the Continental Shelf of North-West Europe.* Inst. Petrol. London.
- Rønnevik, H.C. 1984: Structures and basins in the western Barents Sea. *Norwegian Petrol. Soc., NEMS* 83.
- Rønnevik, H.C., Beskow, B. & Jacobsen, H.P. 1982: Structural and stratigraphic evolution of the Barents Sea. *Can. Soc. Petroleum Geologists Mem.* 8: 431-440.
- Sobczak, L.W. 1978: Gravity from 60° N to the North Pole. *Publ. Earth Phys. Branch, Ottawa.* 45: 67-74.
- Syrstad, E., Navrestad, T. & Bergseth, S. 1976: Gravity modelling offshore Troms, northern Norway. *Offshore North Sea 1976, Norw. Petrol. Soc.*, 24 pp.
- Talwani, M. & Eldholm, O. 1977: Evolution of the Norwegian-Greenland Sea. *Geol. Soc. Am. Bull.* 88: 969-999.
- Talwani, M. & Grønlie, G. 1976: Free-air gravity field of the Norwegian-Greenland Seas. *Geol. Soc. Am. Map and Chart Ser. MC-15.*
- Vogt, P.R., Perry, R.K., Feden, R.H., Fleming, H.S. & Cherkis, N.Z. 1981: The Greenland-Norwegian Sea and Iceland environment: Geology and geophysics. Pp. 493-598 in Nairn, A.E.M. & Churkin, M. (eds.) *The Arctic Ocean.* Plenum Press, New York & London.

Fig. 2. Free-air gravity anomaly map of the Greenland Sea. Bathymetry from Talwani and Grønlie (1976).

Fig. 3. Free-air gravity anomaly map of the Barents Sea. Bathymetry from Falcide and Gudlaugsson (1981).

A.S JOHN GRIEG